This is to certify that the

thesis entitled

Joining of Ceramic Materials Using Spin-on Interlayer

presented by

Jong-Gi Lee

has been accepted towards fulfillment
of the requirements for

Master's degree in Materials Science and Engineering

Eldon D. Case
Major professor

Date Oct. 19, 2000

O-7639

JOINING OF CER

i

Dep

JOINING OF CERAMIC MATERIALS USING SPIN-ON INTERLAYER

By

Jong-Gi Lee

A THESIS

Submitted to

Michigan State University

in partial fulfillment of the requirements

for the degree of

MASTER OF SCIENCE

Department of Materials Science and Mechanics

2000

JOINING OF CERAM

Using various spin-o

amics including alumina

alumina-zirconia composites

including silicon carbide and

microwave heating or conve

10 minutes to 60 minutes

the temperature 700 C ar

transformed into an amorph

bond layers with thickness r

Prior to joining, not

were cut into selected spec

composites, partially stabil

Mo$_2$^{TM}. Microscopic in

interactions had changed by

ABSTRACT

JOINING OF CERAMIC MATERIALS USING SPIN-ON INTERLAYER

By

Jong-Gi Lee

Using various spin-on materials with submicron initial coating thickness, oxide ceramics including alumina, partially stabilized zirconia, fully stabilized zirconia, alumina-zirconia composites, hydroxyapatite, and MaCor™ and non-oxide ceramics including silicon carbide and magnesium fluoride have been joined using either microwave heating or conventional heating with applied low external pressure for a range of 40 minutes to 60 minutes. Non-oxide ceramics including MgF_2 and SiC were joined at a low temperature (700°C and 900°C) using ceramic precusor spin-on interlays transformed into an amorphous ceramic upon heating. SEM micrographs showed smooth bond layers with thickness ranging from ~0 to 10 microns.

Prior to joining, notches about 400 microns in depth and 350 microns in width were cut into selected specimens using a low speed diamond saw for alumina-zirconia composites, partially stabilized zirconia, fully stabilized zirconia, hydroxyapatite, and MaCor™. Microscopic investigation of the joined specimens showed that the notch dimensions had changed by less than 3 % on average.

Table of Contents

List of Tables

List of Figures

Ceramic materials h

application and protectio

produced from powders, t

component. The brittle na

components. Over the last

difficulty of processing cer

processing technique to for

area of ceramic joining is t

various shapes of ceramics

joining techniques that red

energy costs. In terms of th

utilized as the main heatin

INTRODUCTION

Ceramic materials have many attractive properties in terms of high temperature application and protection against chemical attack. Ceramic materials are typically produced from powders, thus, a subsequent sintering process is required to form a dense component. The brittle nature of ceramics leads to difficulties in obtaining net-shape components. Over the last decade, many researchers have attempted to reduce the difficulty of processing ceramic materials. For this reason, joining has been studied as a processing technique to form a desired shape without additional processing. The main idea of ceramic joining is to produce a complex shape from simpler subcomponents using various shapes of ceramics such as bars, discs, tubes, and rods. There are many ceramic joining techniques that reduce processing difficulty, save processing time, and reduce energy costs. In terms of the joining processing techniques, microwave energy has been utilized as the main heating source in this thesis.

Goal of This Study

In this thesis, a pos
various spin-on interlaye
ceramics including alum
fully stabilized zirconia. M
MgF_2 and SiC were joine
were applied for a range o
conventional heating.

1.1 Classification of Cera

In the last two decad
techniques. Ceramic mate
essential for processing ce
important to form the desi

Ceramic/ceramic joi
metal brazes, glass powde
without a bond agent. M
energy to join ceramic cer

1.2 Joining Techniques U

It is difficult to form
components. Interface m
been widely used by man

Goal of This Study

In this thesis, a possible ceramic/ceramic joining technique was proposed using various spin-on interlayers to join oxide and non-oxide ceramic materials. Oxide ceramics including alumina, alumina-zirconia composites, partially stabilized zirconia, fully stabilized zirconia, MaCor™ and hydroxyapatite, and non-oxide ceramics including MgF_2 and SiC were joined to produce a smooth and thin bond layer. Low external loads were applied for a range of 40 minutes to 60 minutes via either microwave heating or conventional heating.

1.1 Classification of Ceramic Joining

In the last two decades, many researchers have developed various ceramic joining techniques. Ceramic materials are mainly produced in a powder form, thus, sintering is essential for processing ceramic materials. The ceramics joining process is very important to form the desired various shapes from simpler components.

Ceramic/ceramic joining techniques are classified as using bonding agents including metal brazes, glass powder, slurry, or spin-on materials. Diffusion bonding is performed without a bond agent. Microwave joining is another joining technique using microwave energy to join ceramic/ceramic materials as a heating method.

1.2 Joining Techniques Using Interface

It is difficult to form ceramics into complex shapes without making simpler sub-components. Interface materials, which act as "glue" to join ceramic materials, have been widely used by many researchers [1-18]. Various types of interfaces have been sed in ceramic ceramic

aterials [7, 12, 14], gl

aterials [19, 20]

First, brazing (liqu

ining process, since a l

mpared to the tempera

echanical properties bet

sadvantages of using br

Expansion) results in ther

ckel filler braze was use

ckel and Si_3N_4 (Nickel

sidual stresses around t

etween metal braze and

onding temperature [2].

eramic ceramic material

oxides within the bon

roduce a hole or channe

ould induce a thermal m

operties [16, 23].

The brazing is per

ubstrates and then heatin

braze filler metal alloy

bstrate material and me

used in ceramic/ceramic joining such as metal brazes [1, 4, 8, 10, 11, 16-18], glass materials [7, 12, 14], glass slurry [2, 3, 5, 6, 9, 13], glass powder [15], or spin-on materials [19, 20].

First, brazing (liquid-solid state joining) technique is currently the most typical joining process, since a lower temperature (melting temperature of brazes) is required compared to the temperatures required by other joining techniques. However, different mechanical properties between the substrate and interface are one of the considerable disadvantages of using brazes as an interface. A different CTE (Coefficient of Thermal Expansion) results in thermal stress between the substrate and bond-layer. For example, nickel filler braze was used in joining of ZrO_2 with Si_3N_4. The different CTE between nickel and Si_3N_4 (Nickel: 13.6 x$10^{-6}K^{-1}$ and Si_3N_4: 3 x$10^{-6}K^{-1}$) induced the highest residual stresses around the Ni-Si_3N_4 interface [1]. Thus, thermal expansion differences between metal braze and ceramic substrate induced thermal stress upon cooling from the bonding temperature [2]. The brazing technique has disadvantages for joining ceramic/ceramic materials; (1) high costs, since a large-scale vacuum furnace is needed, (2) oxides within the bond-layer can be a problem during heating, (3) it is difficult to produce a hole or channel during brazing, and (4) the bond-layer is much thicker and could induce a thermal mismatch through the interface causing poor mechanical properties [16, 23].

The brazing is performed by filling braze filler metal between two ceramic substrates and then heating to the melting temperature with or without external pressure. A braze filler metal alloy is chosen depending upon wettability (Figure 1) between the substrate material and metal braze. Additional components can improve the wettability

9]. Many researches ha

substrate material and by

[16,17], and Ti-Sn alloy

behavior. Also, adding a

metal [10,11].

For brazing, contact

wettability. Wettability is

the contact angle between

theory of wetting has been

γ

where γ_{SL} is the interfacial

between solid and vapour

is the contact angle.

When γ_{SL} is larger th

spreading occurs (Figure 1

angle $\theta < 90°$), the solid s

in contact with a solid red

that wetting and spread

Equation 1) can also be w

γ

where γ_{LV} is the interfacial

solid and γ_{L} is the surface

[4]. Many researches have developed brazes depending upon the wettability between substrate material and braze filler metal such as Ag-Cu alloy brazes [4, 18], aluminum [16,17], and Ti-Sn alloy braze [10] since bond strength improves with improved wetting behavior. Also, adding a third element can reduce the melting temperature of braze filler metal [10, 11].

For brazing, contact angle and interfacial energy states are directly connected with wettability. Wettability has been evaluated from the sessile drop technique [21,22] where the contact angle between liquid and solid phase is measured (Figure 1). A spreading theory of wetting has been developed by Harkins [21].

$$\gamma_{SL} = \gamma_{SV} - \gamma_{LV}\cos\theta \qquad (1)$$

where γ_{SL} is the interfacial energy between solid and liquid, γ_{SV} is the interfacial energy between solid and vapour, γ_{LV} is the interfacial energy between liquid and vapour, and θ is the contact angle.

When γ_{SL} is larger than γ_{SV} the value of the contact angle θ is greater than 90°, no spreading occurs (Figure 1(b)). On the other hand, "when γ_{SL} is lower than γ_{SV} (contact angle $\theta < 90^{\circ}$), the solid surface will be covered by liquid (Figure 1(c))" [21], since liquid in contact with a solid reduces the surface energy of the solid [21, 22]. Thus, in order to obtain wetting and spreading, the following equation applies:

$$\gamma_{SL} < \gamma_{SV} - \gamma_{LV}\cos\theta \qquad (2)$$

Equation (1) can also be written for the case of brazing a metal to a ceramic

$$\gamma_{c} = \gamma_{m}\cos\theta + \gamma_{cm} \qquad (3)$$

where γ_{cm} is the interfacial energy between ceramic and metal, γ_{m} is the surface energy of metal, and γ_{c} is the surface energy of the ceramic.

If the interfacial er
liquid will not spread fr
and the contact angle w
θ is smaller than 90° and
surface.

Using a glass powd
The bond agent is selecte
substrate materials. After
and then are transformed
the brazing technique is li
Brazing can be used in hi
due to high temperature er
advantages over using me
material is generally assum
properties, and melting ch
For example, sialon was j
Y_2O_3-SiO_2-Al_2O_3-Si_3N_4 s
reduced differences in CT
MAS filler (MgO (99%, 0
been calcined to produce

If the interfacial energy γ_{cm} is larger than the ceramic surface energy γ_c, then the liquid will not spread freely or flow into capillary gaps. In this case $\cos\theta$ will be negative and the contact angle will be greater than 90°. On the other hand, when the contact angle θ is smaller than 90° and γ_{cm} is smaller than γ_c, then wetting is possible on the ceramic surface.

Using a glass powder or slurry are other techniques for ceramic/ceramic joining. The bond agent is selected upon the basis of having nearly the same properties of the substrate materials. After heating at a desirable temperature, interface materials pyrolize and then are transformed into amorphous ceramics. For high temperature applications, the brazing technique is limited due to using low melting temperature metal brazes. Brazing can be used in high temperature applications using glass ceramic as a bond agent due to high temperature endurance of the bond agent. Using glass ceramic has certain advantages over using metal brazes since (1) chemical compatibility with substrate material is generally assured and (2) some physical properties such as viscosity, flow properties, and melting characteristics of glasses can be controlled over a wide range [3]. For example, sialon was joined using a Y-sialon slurry [2] and Si_3N_4 was joined using a Y_2O_3-SiO_2-Al_2O_3-Si_3N_4 slurry [5]. Using a glass powder or slurry as a bonding agent reduced differences in CTE and elastic modulus at higher temperatures [2, 5]. Also, a MAS filler (MgO (99%, 0.5 μm), Al_2O_3 (99.99%, 0.2 μm), SiO_2 (99.9%, 0.8 μm)) has been calcined to produce a slurry with almost the same CTE as SiC substrate [12].

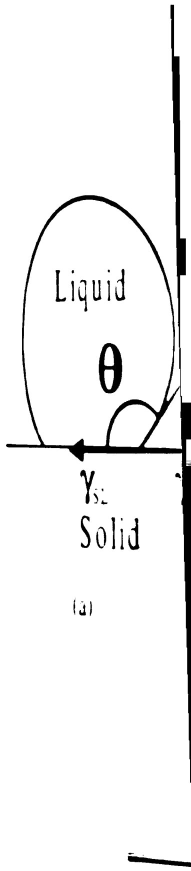

Figure 1. Schematic illus
the contact angle and inter
wetting [21].

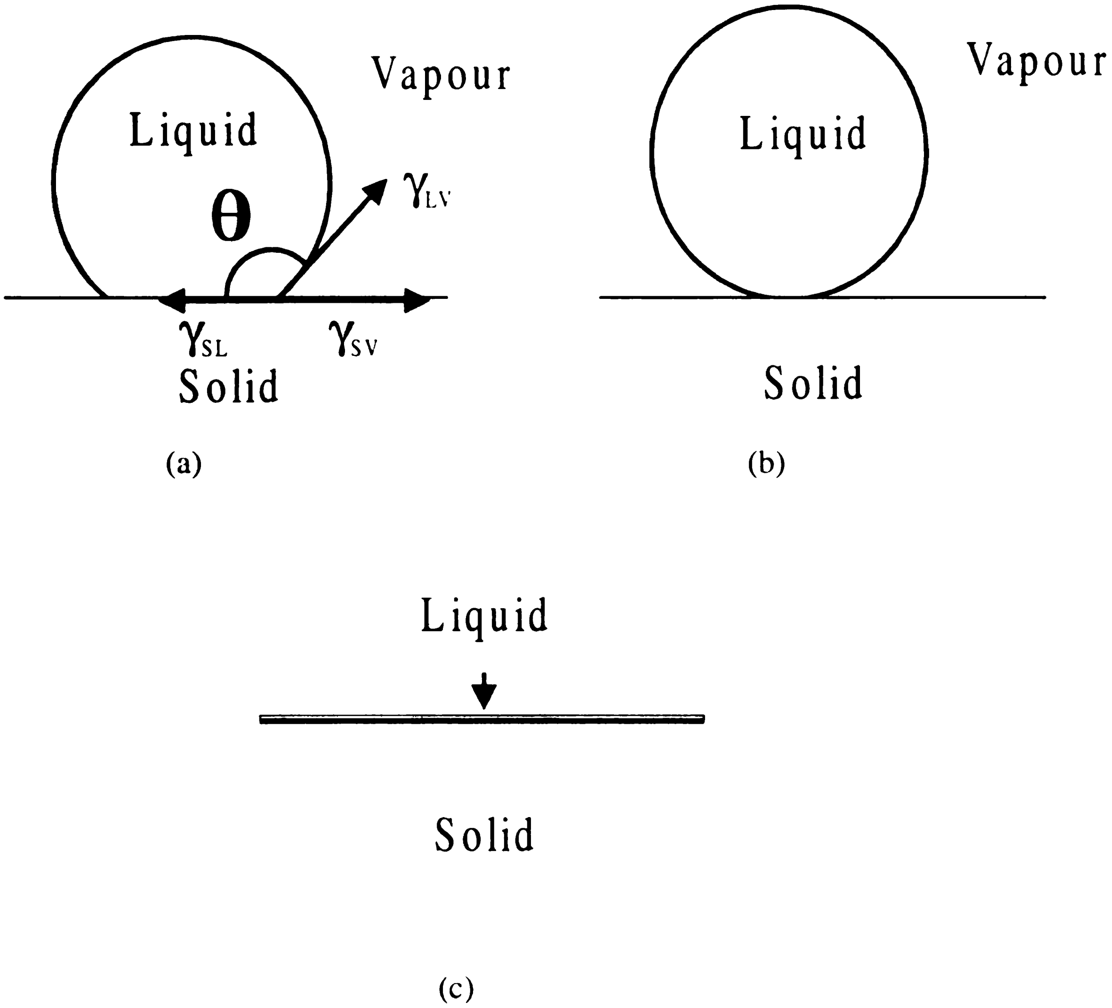

Figure 1. Schematic illustration of sessile drop formation: (a) principle of wetting, where the contact angle and interfacial energy are noted, (b) non-wetting drop, and (c) complete wetting [21].

1.3 Joining Techniques

Another ceramic
state bonding technique
are the main factors for
are depend on the visco
diffused between interfa

High temperature a
at least 60 % of the subs
example of a diffusion b
RBSC (reaction-bonded
interface was softened by
interface [24].

Joining of dissimilar
energy and no bonding ag
X 5 mm X 25 mm were jo
applied pressure of 0.03 –
which was about 60 % of
MgO specimen bending st
observed after heating at 1
diffusion of Al^{3+} and Mg^{2+}
after joining. A crack ran
phase during the three poin
MPa.

1.3 Joining Techniques Without Using a Bond Agent

Another ceramic/ceramic joining technique is diffusion bonding which is a solid state bonding technique. A bonding agent is not applied in this case. Heat and pressure are the main factors for using diffusion bonding. The mechanism of diffusion bonding can depend on the viscous flow of the glassy grain-boundary phase, which can be diffused between interface [24].

High temperature and pressure are required to join ceramic/ceramic materials since at least 60 % of the substrate melting temperature is needed for significant diffusion. An example of a diffusion bonding mechanism is shown in Figure 2. The substrate was RBSC (reaction-bonded silicon carbide). As pressure and temperature were applied, the interface was softened by the glassy phase due to free silicon migration across the interface [24].

Joining of dissimilar ceramics was reported by Sato et al. [26] using microwave energy and no bonding agents. Alumina and magnesia rods with the dimension of 5 mm X 5 mm X 25 mm were joined for temperature ranges of 1577°C to 1877°C using an applied pressure of 0.03 – 0.5 MPa for 2-10 minutes. The 90 MPa of joint strength, which was about 60 % of the MgO bending strength (150 MPa) and 70 % for that of MgO specimen bending strength (130 MPa) heat treated at 1877°C for 4 minutes, was observed after heating at 1877°C for 4 minutes under 5 MPa applied pressure. Due to diffusion of Al^{3+} and Mg^{2+} across the joining plane, $MgAl_2O_4$ formed at the interface after joining. A crack ran along the interface between the $MgAl_2O_4$ phase and the MgO phase during the three point bend test due to lower bending strength than alumina (340 MPa).

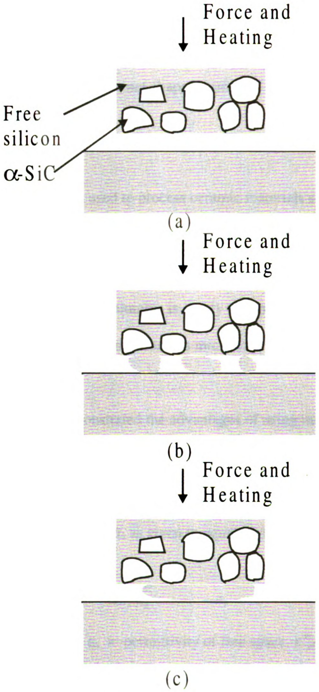

Figure 2. A schematic illustrating diffusion bonding of free silicon onto a butting surface. (a) Migration of free silicon onto surface of the RBSC, (b) As force (pressure) is applied, the silicon spreads across the RBSC surface, (c) Free silicon forms a continuous interlayer [24].

Applied pressures

Si_3N_4 joint due to the h

in height after heating

difference is not ideal a

1.4 Microwave Joining

Microwave energy

materials absorb microw

inside (Figure 3 (a)). C

Figure 3 (b)). At room te

however, above roughly 1

heating from the inside

Many researchers ha

ceramic processing. A ke

processing is the loss tang

factor to the relative diele

$$\tan\delta = \frac{\varepsilon}{\varepsilon}$$

where ε'' = dielectric los

dielectric loss factor, σ =

and displacement current

Applied pressures (20 MPa and 21 MPa) induced a large creep deformation in the Si_3N_4 joint due to the high pressure [27, 29]. The specimen dimension changed about 1 % in height after heating at 1500°C with applied 21 MPa for 1 hour. More than a 1 % difference is not ideal accuracy to form net-shape joining [27].

1.4 Microwave Joining

Microwave energy has been used to process ceramic materials since ceramic materials absorb microwave energy and heating can be generated from the inside to the outside (Figure 3 (a)). Conventional heating is generated from the outside to the inside (Figure 3 (b)). At room temperature, alumina is nearly transparent to microwave energy, however, above roughly 1000°C, alumina absorbs microwave energy (Figure 4) and starts heating from the inside.

Many researchers have demonstrated the advantages of using microwave energy in ceramic processing. A key consideration when using microwave energy in ceramic processing is the loss tangent (tan δ), defined as the ratio of the effective relative loss factor to the relative dielectric constant, as given in equation (4) [31].

$$\tan\delta = \frac{\varepsilon''_{eff}}{\varepsilon'_r} = \frac{\varepsilon''}{\varepsilon'_r} + \frac{\sigma}{\varpi\varepsilon'_r\varepsilon_o} \qquad (4)$$

where ε'' = dielectric loss factor, ε_o = permittivity of free space, ε''_{eff} = effective relative dielectric loss factor, σ = total effective conductivity caused by conduction and displacement currents, ω = frequency ($2\pi f$), and ε'_r = relative dielectric constant.

Figure 3. Patterns of he
from Sutton [31] and Le

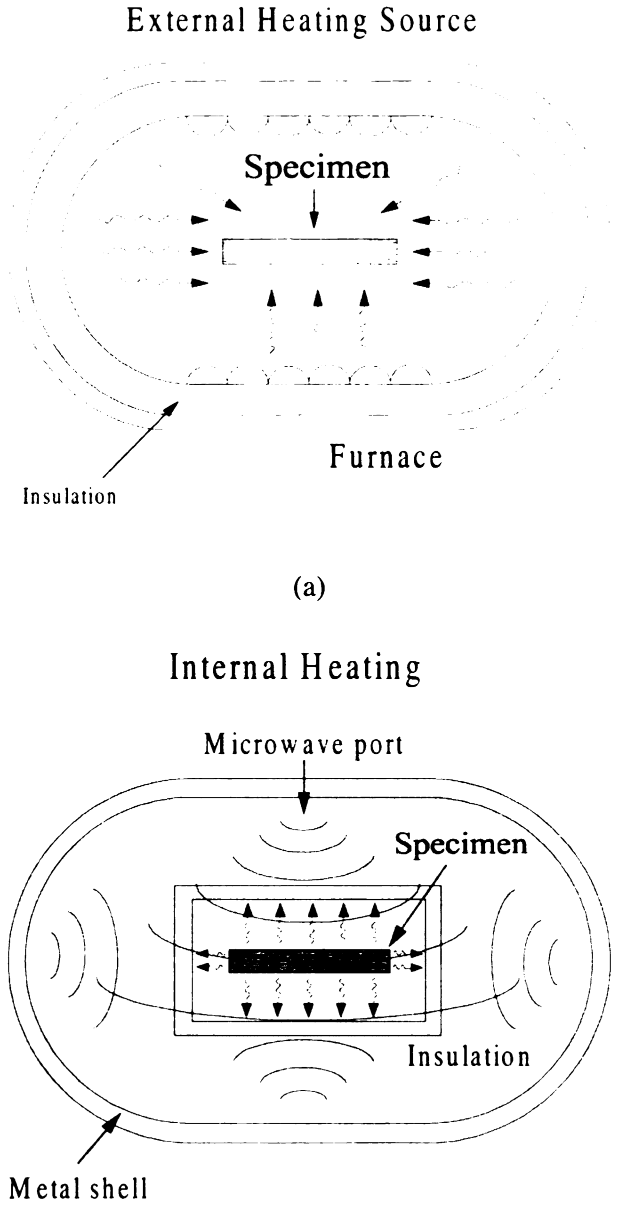

(a)

(b)

Figure 3. Patterns of heating in (a) conventional furnace and (b) microwave (adapted from Sutton [31] and Lee [48]).

Figure 4. Interaction of m
[illegible] [31] and Lee [48],

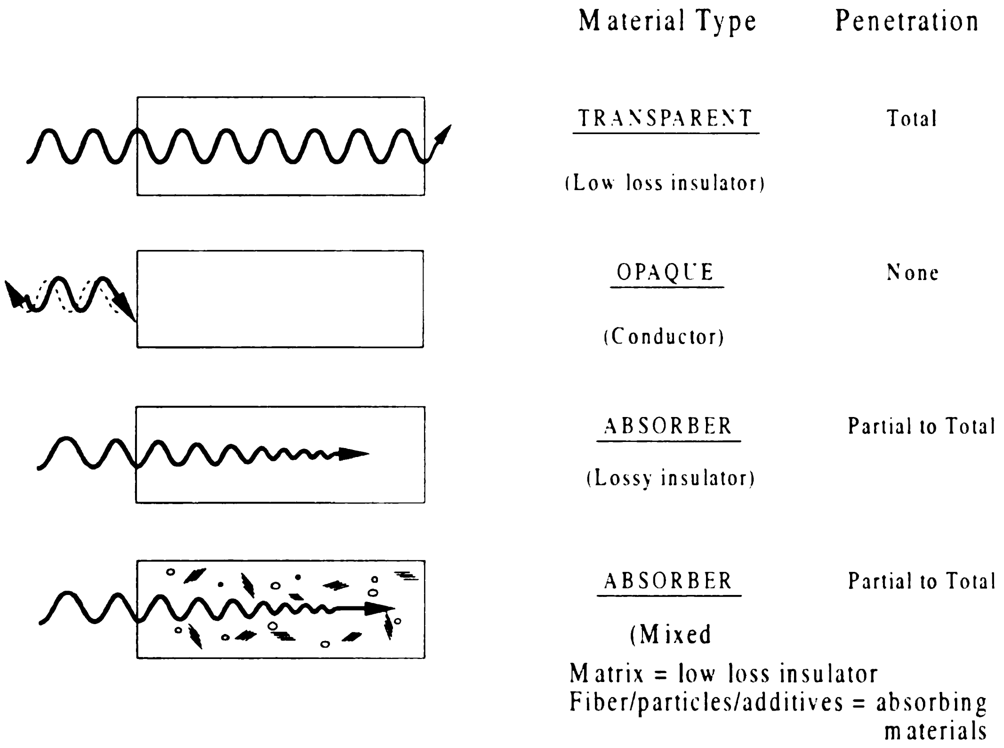

Figure 4. Interaction of microwaves with materials at ambient temperature (adopted from Sutton [31] and Lee [48]).

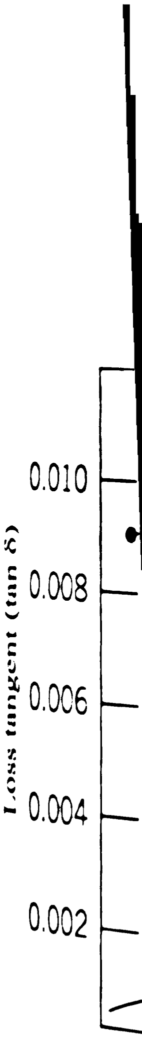

Figure 5. Loss tangent

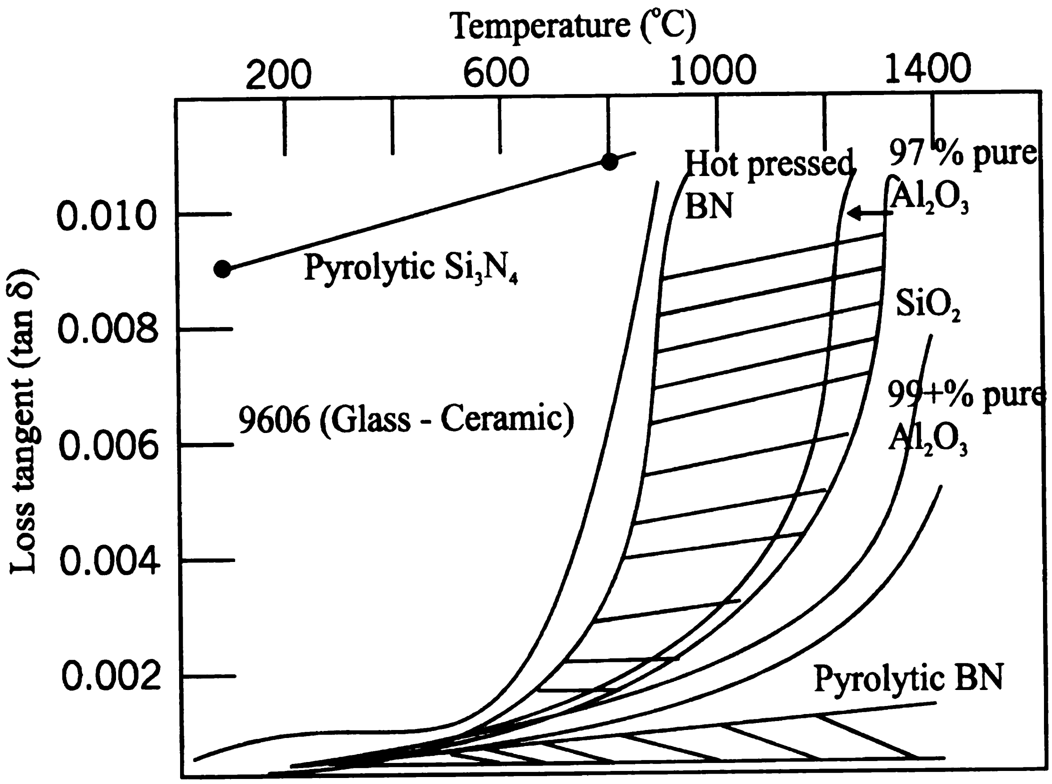

Figure 5. Loss tangent (8 to 10 GHz) versus temperature [31].

Ceramic mater
temperature rises above
rapidly, resulting in a g
leads to more effective
oscillating at a frequenc
ranging from 1 mm to 1
industrial applications of

In general, the loss
and the temperature ha
more rapidly with the ad
alumina tan δ was less
Figure 5[31, 32].

The potential adva
possible since less energ
generated within the m
improved since heating
required to join ceramic
to reach a same temperat

Clark and Sutton [3
effective when the ceram
certain phases that soften
in Figure 4, ceramic mate
temperature increases.

Ceramic materials are transparent to microwave radiation. However, as the temperature rises above a certain temperature (critical temperature, T_{crit}), tan δ rises rapidly, resulting in a greater absorption of the microwave energy by the materials, which leads to more effective heating. Generally, microwaves are electromagnetic waves oscillating at a frequency between 0.3 and 300 GHz which correspond to wavelengths ranging from 1 mm to 1m. Magnetrons (microwave power supplies) commonly used in industrial applications operate at 2.45 GHz [32].

In general, the loss tangent (tan δ) initially rises slowly with increasing temperature until the temperature has reached a critical temperature (T_{crit}). The loss tangent rises more rapidly with the addition of compositional additives and impurites. Thus, 99% pure alumina tan δ was less susceptable to heating than that of 92% or 97% pure alumina (Figure 5)[31, 32].

The potential advantages of using microwave energy are; (1) a cost reduction is possible since less energy is required, (2) uniform heating is possible since heating is generated within the material, (3) a material's microstructure and properties can be improved since heating is more efficient within ceramic material, and (4) less time is required to join ceramic materials using microwave energy since less energy is required to reach a same temperature compared to conventional joining technique [31, 32, 33].

Clark and Sutton [31] described the microwave joining process as "joining is most effective when the ceramic sufficiently absorbs microwaves and the grain boundaries contain phases that soften and 'glue' the surfaces of adjacent materials". As mentioned in Figure 4, ceramic materials can absorb microwave energy efficiently as the temperature increases.

Alumina specime
gent at temperatures a
using a single mode re
joining was done by lo
assumed more efficient

Binner et al. [19]
99.7 alumina. The join
layer when heated at the
comparison, alumina join
the width of the specimen
sparsely distributed. Hi
inability to heat the mate

Selective and fast
[18]. For alumina/zircon
minutes since the materi
phase. During microwa
phase. The reduction of

Microwaves have
joined silicon carbid
SiC (RBSC) tube specim
cm and a length of 2.54
1465 C, 1515 C, and 15
rectangular multimode c

Alumina specimens with purity of 92 % to96 % were joined without a bonding agent at temperatures above 1750°C with 0.6 MPa applied pressure for 3 minutes in air using a single mode rectangular microwave cavity [33]. The most successful microwave joining was done by lower purity alumina, indicating that the microwave energy was absorbed more efficiently for lower purity alumina.

Binner et al. [19] investigated microwave joining via diffusion bonding of 94 % and 85 % alumina. The joined specimens showed the almost invisible layer (very thin bond layer) when heated at the highest temperature (1600°C) and pressure (0.25 MPa). In comparison, alumina joined at 1400°C alumina clearly showed a visible bond layer across the width of the specimen and regions of contact between the opposing faces were sparsely distributed. High purity alumina 99.8 % was not successfully joined due to the inability to heat the material to a sufficiently high temperature.

Selective and fast heating using microwave energy suggested by Aravindan et al. [13]. For alumina/zirconia composites, temperature could reach at 1000°C within 2 minutes since the material absorbed microwave energy very quickly via the amorphous phase. During microwave joining zirconia transformed from tetragonal to the monoclinic phase. The reduction of hardness at the interface was due to Al-Zr inter-diffusion [13].

Microwaves have been used for other various joining techniques. Katz et al. [34, 35] joined silicon carbide using three different microwave methods: (1) Reaction bonded SiC (RBSC) tube specimens with an outer diameter of 3.5 cm, an inner diameter of 2.54 cm, and a length of 2.54 cm were joined with temperatures range of 1410°C, 1420°C, 1465°C, 1515°C, and 1565°C using an applied load of 0.23 MPa in a 2.45 GHz rectangular multimode cavity. No adhesive was used between the specimens, making is an example of mi

bonding, which requi

successfully done with

joined SiC SiC specim

base material in the 4 p

composites disks, 2.54

Cusin-1 ABA™ active

approximately 900 C fo

mode (TE microwave

thin layer of braze alloy

matrix. However, the m

reinforced SiC/SiC com

joined using a polymer p

added to SiC powder to

together by hand [34]. T

and then the microwave

was then heated in a mi

was observed througho

no mechanical testing w

Many researche

selective heating of par

microwave absorption

this an example of microwave diffusion bonding. Compared to conventional diffusion bonding, which requires 2000°C and a long time (1 hour), SiC/SiC joining was successfully done within 5 minutes at temperature between 1420°C and 1515°C. The joined SiC/SiC specimens showed equal or greater fracture toughness than that of the base material in the 4 point bend test. (2) Continuous fiber-reinforced SiC/SiC composites disks, 2.54 cm in diameter and approximately 0.32 cm thick, were joined with Cusin-1 ABA™ active brazing alloy (2.54 cm diameter and about 0.005 cm thick) at approximately 900°C for 30 minutes in 95% N_2 and 25% H_2 atmosphere using a single mode (TE_{103}) microwave cavity. The specimens showed a homogenous metallic interlayer of braze alloy that wet the ceramic composites and spread into pores in the SiC matrix. However, the mechanical behavior was not reported. (3) Continuous fiber-reinforced SiC/SiC composites plates of dimension 1.27 cm X 1.27 cm X 0.0.32 cm were joined using a polymer precursor (allyhydridropolycarbosilane (AHPCS) which was added to SiC powder to form a slurry). Prior to joining, the specimens were squeezed together by hand [34]. The refractory insulator was heated to 1000°C for one to 1.5 hours and then the microwave cavity was evacuated to $6X10^{-3}$ psi with argon. The specimen was then heated in a microwave cavity at 1100°C for 30 minutes. Occasional porosity was observed throughout the interface. However, the interface was invisible and smooth but mechanical testing was not reported [34].

Many researchers have used microwave power as a heating source due to its selective heating of particular materials since each ceramic material has different microwave absorption ability. Microwave energy offers the potential of a new ceramic/ceramic joint

materials and fast heat

ceramic/ceramic joining processes because of absorption characteristics in ceramic materials and fast heating ability.

2 EXPERIMENTA

2.1 Materials Used in

Commercial p

partially stabilized zirc

specimens for this thes

used in this thesis.

Hydroxyapatite (

reconstruction of damag

bioactive glasses due to

over hydroxyapatite, hyd

hydroxyapatite is classif

attached by chemical bo

Two kinds of zirc

% Y_2O_3 zirconia) and (2

MaCor™, a fluro

SiO_2-Al_2O_3-MgO-K_2O-

include (1) excellent phy

resistivity, (4) non-poro

shapes and precision par

electrical or thermal ins

as in electrical and op

mica platelets in the mic

2 EXPERIMENTAL PROCEDURE

2.1 Materials Used in This Thesis

Commercial powders of alumina (Table 1), fully stabilized zirconia (Table 3), partially stabilized zirconia (Table 3), and hyroxyapitite (Table 2) were used to fabricate specimens for this thesis. As-received MaCor^{TM} (Table 4) and MgF_2 (Table 5) were also used in this thesis.

Hydroxyapatite (HAP) is a known bio-ceramic used for replacement, repair, or reconstruction of damaged human bodies. Hydroxyapatite and HAP composites are good bioactive glasses due to their resemblance to human bone. When human blood flows over hydroxyapatite, hydroxyapatite acts like human bone. Polycrystalline hydroxyapatite is classified in bio-ceramics as bioactive fixation meaning that it can be attached by chemical bonding directly to bone [36].

Two kinds of zirconia powder were used: (1) partially stabilized zirconia (3 mol % Y_2O_3 zirconia) and (2) fully stabilized zirconia (8 mol % Y_2O_3 zirconia).

MaCor^{TM}, a flurophlogopite mica platelet reinforced glass ceramic in the system SiO_2-Al_2O_3-MgO-K_2O-F was also used for this thesis. The properties of MaCor ^{TM} include (1) excellent physical properties, (2) high dielectric strength, (3) good electrical resistivity, (4) non-porous and non-shrinking, and (5) machinable into complicated shapes and precision parts using ordinary metal working tools. MaCor^{TM} is used as an electrical or thermal insulator, for structural components, in semi-conductor processing, and in electrical and opto-electronic equipment in industrial fields. Randomly oriented mica platelets in the microstructure of MaCor^{TM} are the key to its machinability [43].

Table 1. Alumina (TM
coefficient [38], and Y

Gr
Lo
Cryst
Surfac
Average s
Pu
Imp
Green d
Fired density after hea hea
Thermal expansion c 1000
Young's m
Thermal co

Table 2. Hydroxyapatite
coefficient [41]

Description
Specific analysis or pro
Spectrographic analysis
Thermal expansion coe 25 C - 400 C 400 C - 800 C

Table 1. Alumina (TM-DAR, Taimi Co, Japan) powder information. Purity [37], thermal coefficient [38], and Young's moduli and thermal conductivity[39]

Grade	TM-DAR
Lot No	2831
Crystal form	α
Surface area	13.6 m^2/g
Average surface size	0.21 μm
Purity	99.99 %
Impurity	Na (3 ppm), K (1 ppm), Fe (6 ppm), Ca (1ppm), Mg (1 ppm), and Si (6 ppm)
Green density	2.32 g/cm^3
Fired density after heating at 1350°C for 1 hour	3.96 g/cm^3
Thermal expansion coefficient (25°C-1000°C)	8.8 X 10^{-6} K^{-1}
Young's moduli	390 GPa
Thermal conductive	30.0-35.0 W/m·°C

Table 2. Hydroxyapatite powder material information [40] and thermal expansion coefficient [41]

Description	Calcium hydroxylapatite $Ca10(OH)_2(PO_4)_6$, Powder, 99 %		
Specific analysis or property	Test for	Found	Theoretical
	Ca	37.28 %	37.00 %
Spectrographic analysis	Element	Result (wt %)	
	Al	< 0.01	
	Cr	< 0.01	
	Fe	< 0.01	
	Mg	0.08	
	Mn	< 0.01	
	Na	< 0.01	
	Si	0.08	
	Sr	< 0.01	
Thermal expansion coefficient			
25°C - 400°C	14.5 X $10^{-6}$$K^{-1}$		
400°C – 800°C	15.5 X $10^{-6}$$K^{-1}$		

Table 3. Material inf

Materials
Y_2O_3 (mol %)
Y_2O_3 (wt %)
Al_2O_3 (wt %)
SiO_2 (wt %)
Fe_2O_3 (wt %)
Na_2O (wt %)
Specific surface Are
Density (g/cm^3)
Bending Strength R
Fracture Toughness R (MPa m$^{0.5}$)
Hardness (HV 10)
Mean Particle diamete

Table 4 Information of
ratio [56])

Temperature Lim
Dielectric Cons
Dielectric Stren
DC Volume Res
Thermal Condu
Thermal expans 25-300 C 25-600 C 25-800 C
Density
Modulus of Elas
Porosity
Poisson's Ratio

Table 3. Material information of two kinds of zirconia [42]

Materials	TZ-3 YS (Partially stabilized)	TZ-8 YS (Fully stabilized)
Y_2O_3 (mol %)	3 %	8 %
Y_2O_3 (wt %)	5.15 ± 0.20	13.3 ± 0.60
Al_2O_3 (wt %)	≤ 0.1	≤ 0.1
SiO_2 (wt %)	≤ 0.02	≤ 0.02
FeO_2 (wt %)	≤ 0.01	≤ 0.01
Na_2O (wt %)	≤ 0.04	0.12
Specific surface Area (m^2/g)	7 ± 2	7 ± 2
Density (g/cm^3)	6.05	5.90
Bending Strength R.T. (MPa)	1200	300
Fracture Toughness R.T. (MPa $m^{0.5}$)	5.0	1.5
Hardness (HV 10)	1250	1250
Mean Particle diameter (μm)	0.59	0.54

Table 4 Information of MaCor™ [43] (Thermal expansion coefficient and Poisson's ratio [56])

Temperature Limit	1000° C
Dielectric Constant	1Khz at 25° C 6.03
Dielectric Strength	40KV/mm
DC Volume Resistivity	at 25° C >1016 ohm-cm
Thermal Conductivity	at 25° C 1.46 W/m° C
Thermal expansion coefficient 25-300°C 25-600°C 25-800°C	 9.3 /K x 10^6 11.4/K x 10^6 12.6/K x 10^6
Density	2.52 g/cm^3
Modulus of Elasticity	at 25° C 64 GPa
Porosity	0
Poisson's Ratio	0.29

Table 5. Material inf

Formula
Other na
Thermal Conductiv
High wavelength d<6mm
High wavelength d<6mm
Strength (FaEL.FA
Density (g c
Melting point
Hardness (Knoop
Thermal expansion
Specific heat capacity 1)
H2O Solubility
Refractive Ind n at 5μm

Table 6. The spin-on ma

Material
ZrO_2, MaCor™ and Al_2O_3·ZrO_2 composi
Al_2O_3 (AKP 30)
SiC
MgF_2

Table 5. Material information of MgF_2 [44].

Formula	MgF_2
Other name	Itran I, sellaite
Thermal Conduct'y mW/cm· K	~150
High wavelength limit, μ d<6mm	8
High wavelength limit, μ d<6mm	6.5
Strength (FaEL,FAEL) MPa	49
Density (g/cm3)	3.18
Melting point (°C)	1255
Hardness (Knoop) kgf/mm^2	415 (575)
Thermal expansion coefficient	11
Specific heat capacity (J kg-1 K-1)	920
H2O Solubility wt.%	0.0076
Refractive Index n at 5μm	1.34

Table 6. The spin-on materials used for ceramic/ceramic joining.

Material	Spin-on Material	Spin-rate	Curing
ZrO_2, MaCor™ and $Al_2O_3ZrO_2$ composites	Silica film	3000 rpm	Yes
Al_2O_3 (AKP 30)	Sodium alginate	3000 rpm	Yes
SiC	Blackglas™	3000 rpm	No
MgF_2	Sodium silicate	3000 rpm	No

MgF$_2$ (Irtran I

with a mean grain siz

MgF$_2$ transmits infra

In this thesis, th

amorphous silica-film

sodium alginate.

The silica-film

has impurity levels less

President information.

densified by annealing

Blackglas^{TM} (2

SiC. After spinning at 3

cured. Blackglas^{TM} is p

transforms it into relat

mixed with catalyst w

a fiber matrix in CMC

Sodium algin

is a glass powder ma

per 3 grams of sodiu

of alginate are utilize

properties. *Sodium al*

ceramics, pharmaceutic

MgF_2 (Itran I, Eastman Kodak Company) is a hot pressed polycrystalline material with a mean grain size of approximately 2.8μm determined by line intercept method. MgF_2 transmits infrared ration over the wavelength range of 1.5 μm to 9 μm (Table 5).

In this thesis, the following four materials were used as interlayer materials, (1) an amorphous silica-film, (2) an amorphous Blackglas^{TM}, (3) sodium silicate, and (4) sodium alginate.

The silica-film^{TM}(Emulsitone Company, Whippany, NJ) used as spin-on material has impurity levels less than one part per million of metallic ions from Emulsitone President information. The silica film is an alcohol based liquid material and can be densified by annealing at 200°C for 20 minutes.

Blackglas^{TM} (2vol %) mixed with a catalyst (98 vol %) was utilized for joining of SiC. After spinning at 3000 rpm with Blackglas^{TM}, the coated SiC specimen was not cured. Blackglas^{TM} is preceramic polymer and pyrolizing it the 800-1000°C range transforms it into relatively high yielding in system of Si-O-C ceramics. Blackglas^{TM} mixed with catalyst was heated and then formed into ceramics. Blackglas^{TM} was used for a fiber matrix in CMC's (ceramic matrix composites) [45].

Sodium alginate (Alginic Acid Sodium Salt, Sigma Chemical Co, St. Louis, MO) is a glass powder material. Alginic acid is water soluble, thus, adding 100 ml of water per 3 grams of sodium alginate controlled the viscosity of glass powder. The properties of alginate are utilized in the thickening, stabilizing, gel-forming, and film-forming properties. Sodium alginate is used for application in textiles, welding electrodes, ceramics, pharmaceuticals, cosmetics, etc [47].

Sodium silicate

on interlayer to join

combination of almo

viscosity. Sodium s

concrete [46].

2.2 Cold Pressing Ce

Commercial pow

composite, and HAP

The mass of the pow

Mettler Instrument C

powder compacts we

approximately 32 M

simultaneously using

2.3 Preparation of

Refractory

Two types of cylind

in diameter. The re

microwave suscep

cylindrical refract

refractories were

Sodium silicate (Colmbus Chemical Industries INC, Coumbus, WI) was used as spin-on interlayer to join MgF_2. Sodium silicate is called 'water glass' and its system is a combination of almost equal proportions of silica and soda. Adding water can control viscosity. Sodium silicate is used as a deflocculent in ceramics and as a hardener in concrete [46].

2.2 Cold Pressing Ceramic Powder Compacts

Commercial powder ceramic materials, alumina, zirconia, alumina-zirconia composite, and HAP were pressed into powder compacts prior to microwave sintering. The mass of the powder to be pressed was first measured using an electronic balance (Mettler Instrument Corporation) with an accuracy of ± 0.001 gm. The green unfired powder compacts were about 2.2 cm in diameter and 0.2 cm thick after cold pressing at approximately 32 MPa (Figure 6 (a)). Up to seven powder compacts were sintered simultaneously using a 10.3 cm diameter refractory casket (Figure 6 (b)).

2.3 Preparation of Refractory Insulator Used in This Thesis

Refractory insulators were used during both microwave sintering and joining. Two types of cylindrical caskets were used, one 10.3 cm in diameter and the other 7.5 cm in diameter. The refractory caskets both (1) reduced heat loss and (2) provided microwave susceptors to allow heating at low temperatures. The wall thicknesses of the cylindrical refractories ZYC(Zirconia) were 1.3 cm for all caskets. The cylindrical refractories were composed of zirconia ZYC about 40 % densified.

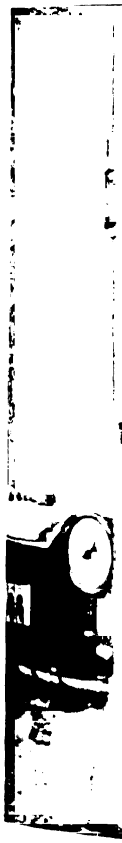

(a

Figure 6. (a) Ph
pressing powder

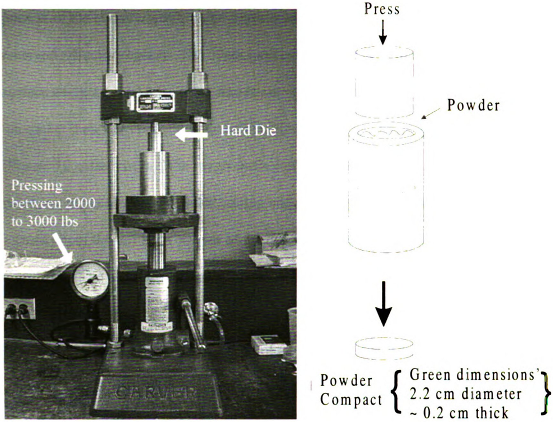

(a) (b)

Figure 6. (a) Photograph of the presser used in this thesis, (b) Schematic sketch of pressing powder compact in a steel die.

As-received c
portion of the casket
received refractory c
surface using a pencil.
the casket then was c
(Figure 7). After cutt
notebook paper (Figur
located about 0.5 cm fr
(Figure 7). The hole al
pyrometer.

Refractory end
diameter equal to the o
hacksaw blade. A spec
Figure 8).

2.4 Microwave Contr

In this thesis, a
Wavemat Inc., Plymou
ceramics (Figure 9). T
France) generates 0 w
microwave cavity was

An optical pyr
microwave heating. T

As-received cylindrical refractory was about 30 cm in long. The cylindrical portion of the casket used for microwave heating was 3 cm in height after cutting the as-received refractory casket. The 30cm long cylindrical casket was marked 3 cm on the surface using a pencil to suitable size to cut of refractory casket. The cylindrical part of the casket then was cut following the pencil mark on the surface using a hacksaw blade (Figure 7). After cutting, the rough surface of the casket was briefly polished using clean notebook paper (Figure 7). After cutting and polishing, a hole was made in the casket located about 0.5 cm from bottom of the cut cylindrical casket using a screw driver (Figure 7). The hole allows measurement of the specimen temperature using an optical pyrometer.

Refractory end plates composed of aluminosilicate 2 cm thick disks, with a disk diameter equal to the outer diameter of the cylindrical section of the casket using the hacksaw blade. A specimen setter was also cut using the hacksaw blade into 0.5 cm thick (Figure 8).

2.4 Microwave Control System

In this thesis, a 2.45 GHz single mode microwave cavity (Model CMPR-250, Wavemat Inc., Plymouth, MI) was the main heating source for sintering and joining ceramics (Figure 9). The microwave power supply (SAIREM, Model 24, Rue Louis, France) generates 0 watt to 2000 watts. For all sintering and joining work, the microwave cavity was operated using TM_{111} electro-magnetic mode.

An optical pyrometer (ACCUFIBER, Model 10) setting was performed prior to microwave heating. The optical pyrometer was set as following steps to measure

Figure 7. Schematic
of the refractory cas
refractory open cylin

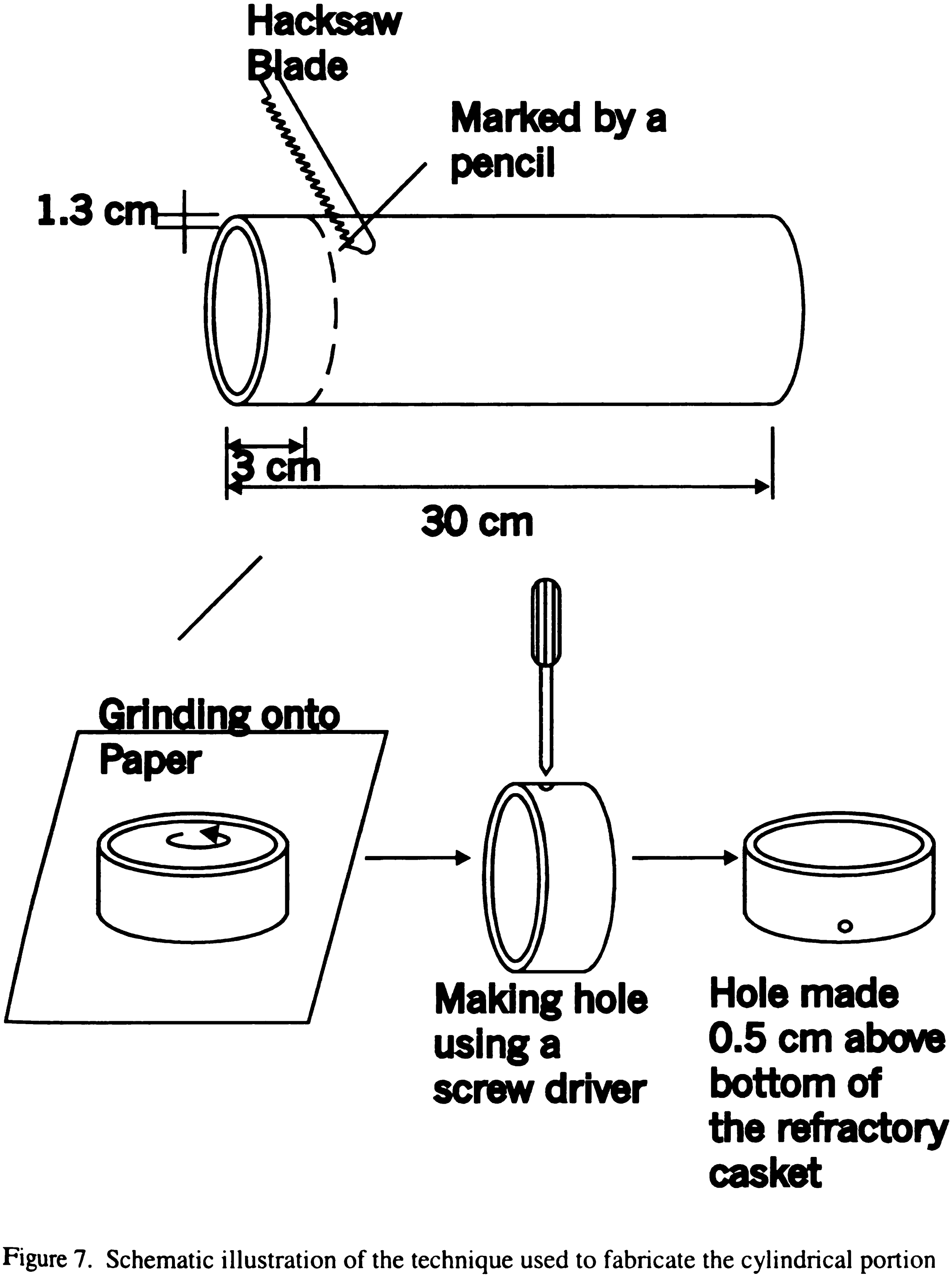

Figure 7. Schematic illustration of the technique used to fabricate the cylindrical portion of the refractory casket. The starting material was a 30 cm long section of a zirconia refractory open cylinder.

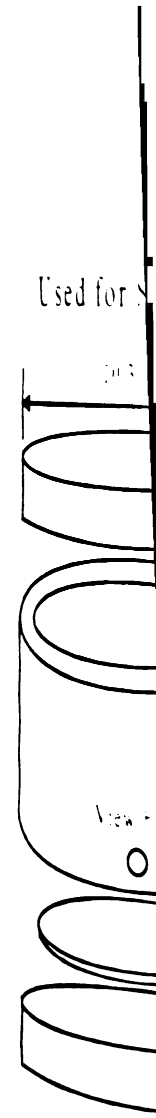

Figure 8. Illustration

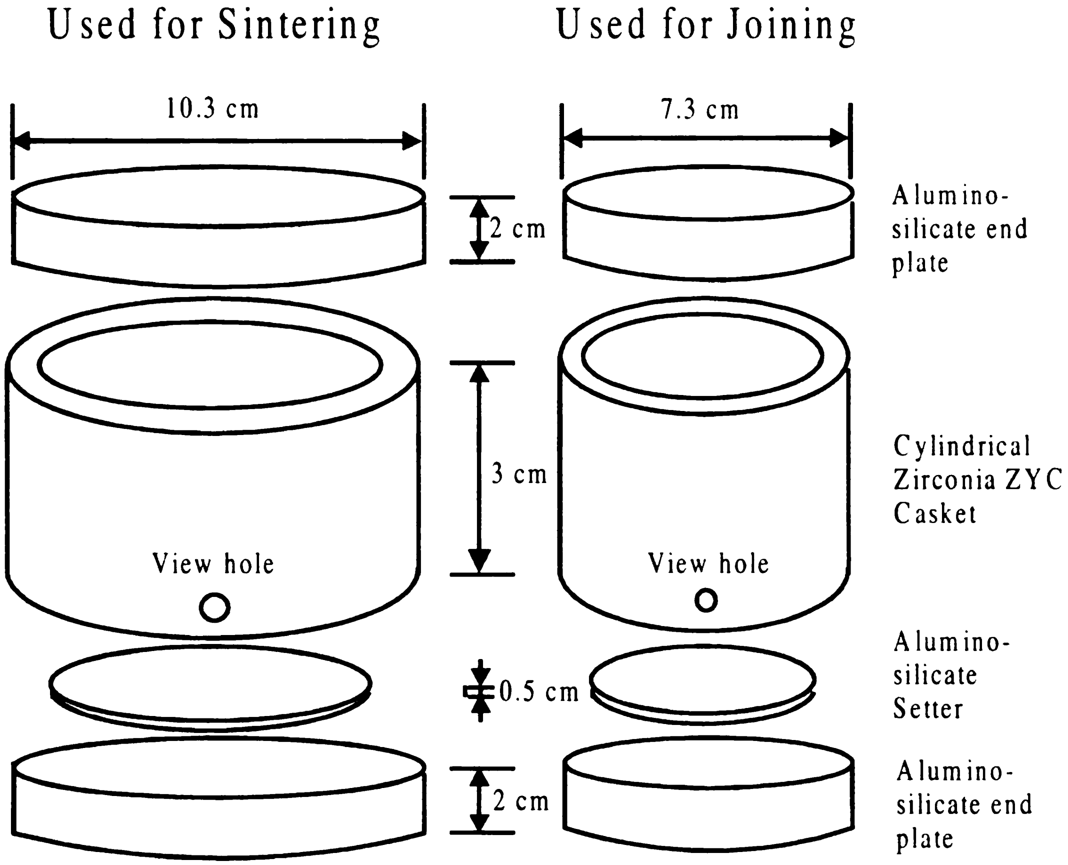

Figure 8. Illustration of refractory cavities used in this thesis.

inside microwave c
itself. First, the # 9
showed black body
one time and showed
pushing the enter key
showed sense type I
shown on the screen.
enter key was pushed
showing number 500 (

After placing s
on then the optical pyr
The computer controll
during heating. The r
position was set to app
initial position was fr

2.5 Sintering Proces

A maximum c
using a 10.3 cm in di
power was set to 10
was performed every
that material inside th
started heating after

inside microwave cavity. After power on the pyrometer, it was automatically calibrated itself. First, the # 9 key was pushed and then the number 1 key was pushed. The screen showed black body after pushing the down arrow key and the right arrow key was pushed one time and showed pyrometer on the screen. The enter key was then pushed. After pushing the enter key, the right arrow key was pushed one time and then the screen showed sense type. The down arrow key was pushed one time and sense factor was shown on the screen. Sense factor was pushed following the # keys 1572 and than the enter key was pushed. After setting sense factor, the upper arrow key was pushed until showing number 500.00.

After placing specimen inside the microwave cavity, the cooling water was turned on then the optical pyrometer, the microwave power, and the computer were turned on. The computer controlled the short and the probe position to minimize reflected power during heating. The reflected power meters were turned on. The initial value of the short position was set to approximately between from 10 cm to 10.05 cm while the probe's initial position was from about 0.2 cm to 0.3 cm.

2.5 Sintering Process Using Microwave Power

A maximum of seven compact powder specimens can be sintered simultaneously using a 10.3 cm in diameter refractory casket (Figure 11). First, the microwave input power was set to 100 watts and the input power was increased in 100 watt increments was performed every 3 minutes before coupling. The coupling was heat-starting point that material inside the microwave casket started to absorb the microwave energy then started heating after increment of power about 300 watts.

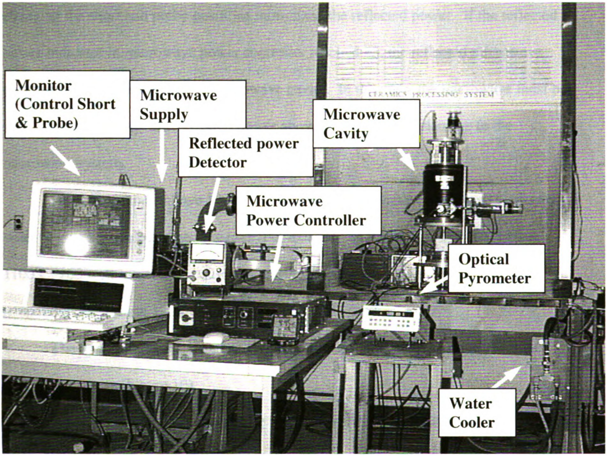

Figure 9. Photograph of the microwave cavity and the microwave power supply used in this thesis.

One proble

using the microwave

Coupling typically

microwave heating

tness. Thus, increas

problem of decreasi

changing the short an

power indicator in mi

power might cause ar

shut off immediately

microwave system.

For temperatu

order to give a prese

1100°C, 100 watt inc

temperature was abo

The temperat

microwave cavity (F

After reachin

be constant if the ten

determined hold tim

changing the short a

time, and heating ra

microwave-sintered

One problem encountered when heating the 7.5 cm diameter refractory casket using the microwave was that the temperature tended to decrease after coupling. Coupling typically occurred in the temperature range of 900°C to 1000°C. The microwave heating rate cannot be controlled at temperatures less than 1000°C in this thesis. Thus, increasing input power in 100 watt increments every 3 minutes solves the problem of decreasing temperature after coupling. Every time the input power increased, changing the short and probe positions minimized the reflected power. If the reflected power indicator in microwave power controller reached 45, the reflected microwave power might cause arcing in the microwave cavity. In this case, the microwave must be shut off immediately. The reflected power above 45 could cause damage to the microwave system.

For temperatures above 1000°C, increases in microwave power were controlled in order to give a preselected heating rate. For example, at 9 minutes temperature was 1100°C, 100 watt increments causes increasing temperature. After 19 minutes, if temperature was about 1200°C, heating rate was 10°C/min.

The temperature was measured by an optical pyrometer though a view port in microwave cavity (Figure 10).

After reaching a desired sintering temperature, the temperature was considered to be constant if the temperature changed by less than ± 2°C for 5 minutes. After a pre-determined hold time at the sintering temperature, decreasing the input power without changing the short and probe position did cooling. Table 7 shows sintering temperature, time, and heating rate for of the each powder material used in this thesis. The microwave-sintered specimens were fractured using a hammer. The sintered specimens

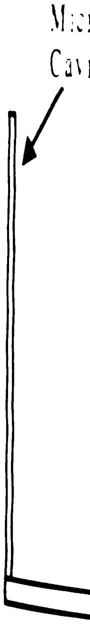

Figure 10. Sc
thesis.

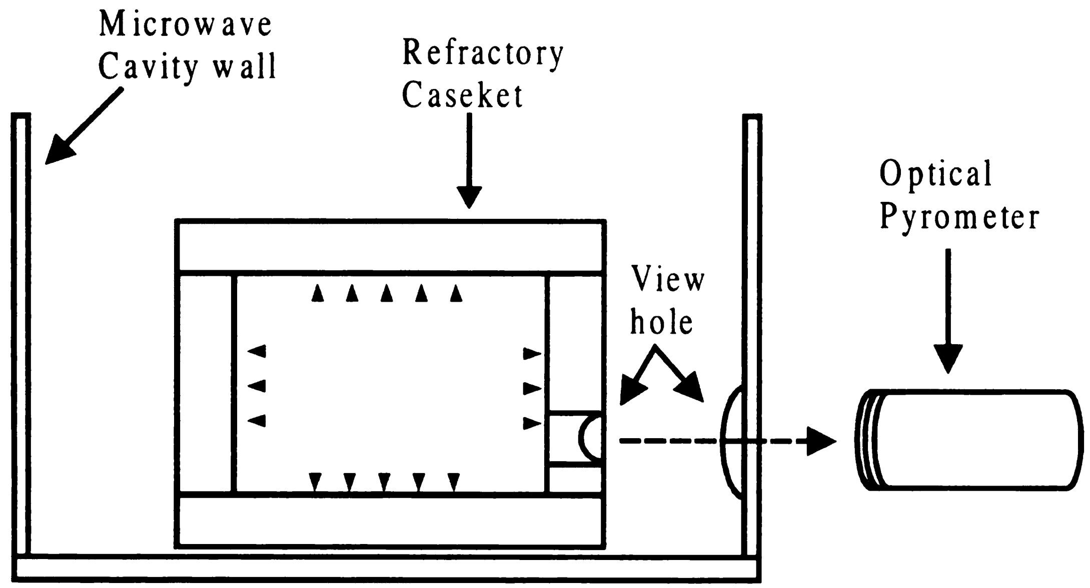

Figure 10. Schematic of specimen temperature measurement technique used in this thesis.

Table 7. Conditions
thesis.

Material
Alumina
3mol% Y_2O zirconia
8mol% Y_2O zirconia
Alumina –zirco composites

Table 8. Polishing t
in this thesis. The t
fewer specimens are

Material
Alumina
3mol% Y_2O_3 zirconia
8mol% Y_2O_3 zirconia
Alumina –zircon composites
Silicon Nitrid
Silicon Carbid
MaCor™
MgF_2

Table 7. Conditions of sintering for each of the commercial powder material used in this thesis.

Material	Mass	Sinter Temp	Hold time	Heating rate
Alumina	2 grams	1300°C	1 hour	10°C/min
3mol% Y_2O_3 zirconia	3 grams	1375 °C	1 hour	10°C/min
8mol% Y_2O_3 zirconia	3 grams	1350 °C	1 hour	10°C/min
Alumina –zirconia composites	3 grams	1350 °C	1 hour	10°C/min

Table 8. Polishing time and diamond grit size for each of the ceramic materials included in this thesis. The time corresponds to seven mounted specimens being polished. If fewer specimens are polished simultaneously the times are reduced.

Material	35 μm	17 μm	15 μm	10 μm	6 μm	1 μm
Alumina	20 min	30 min	30 min	30 min	30 min	30 min
3mol% Y_2O_3 zirconia	20 min	30 min	30 min	30 min	30 min	30 min
8mol% Y_2O_3 zirconia	20 min	30 min	30 min	30 min	30 min	30 min
Alumina –zirconia composites	20 min	30 min	30 min	30 min	30 min	30 min
Silicon Nitride	5 min	10 min	10 min	10 min	10 min	10 min
Silicon Carbide	5 min	10 min	10 min	10 min	10 min	10 min
MaCor™	2 min	10 min	10 min	10 min	10 min	10 min
MgF_2	N/A	10 min	10 min	10 min	10 min	10 min

A
s
e

Seve
comp

A
s
e

Figure 11
[illegible]

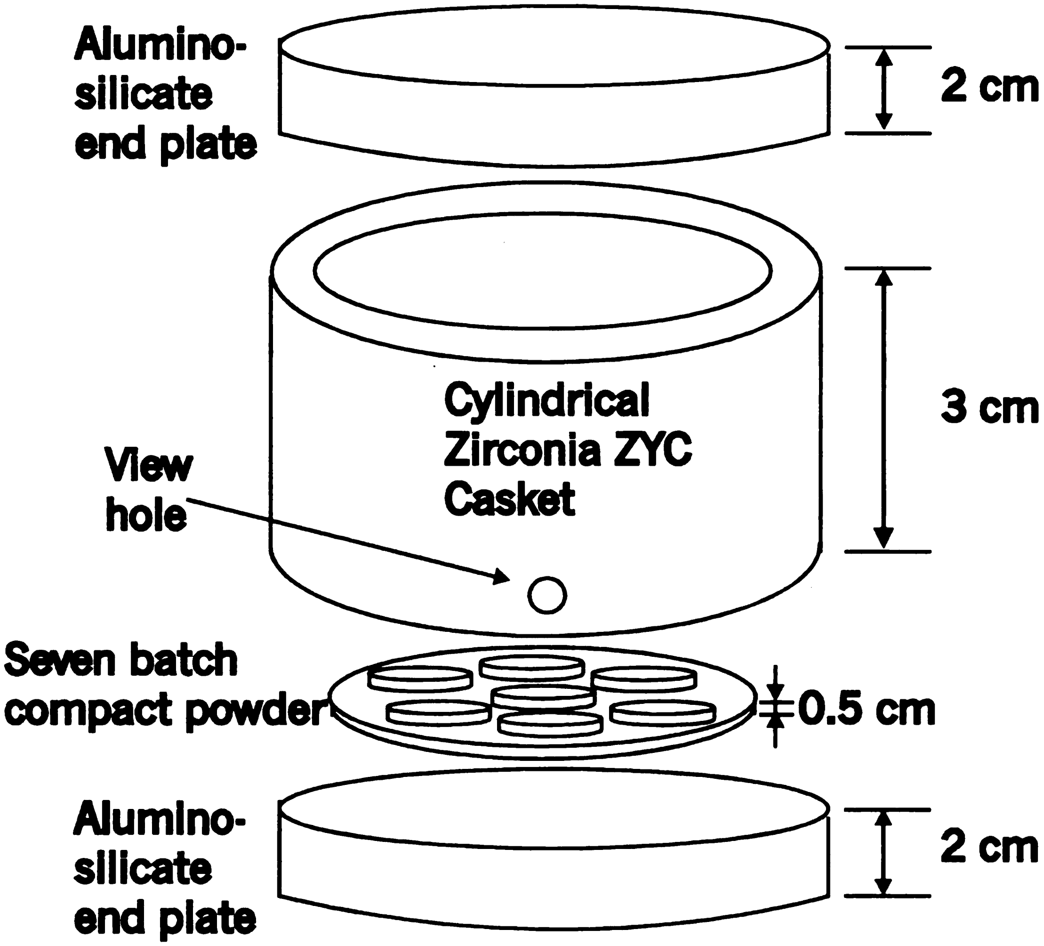

Figure 11. Schematic illustration of refractory casket arrangement used batch sintering of ceramic specimens in this thesis.

were hit by the har

pieces hit the sinte

The grain mea

fracture surfaces us

factor of 1.5.

2.6 Specimen Prep

The specime

using an automatic

Mn. The grit sizes

PA) used for polish

12). For polishing

2 cm thick, 20 cm

for about 10 minu

BUEHER, Lake B

the surface of the

were cooled for a

Polishing

pastes were appl

each time. The p

mounted polishi

cloth. The polis

specimens. Wh

were hit by the hammer to break into several pieces. The hammer to break into several pieces hit the sintered specimens.

The grain mean size of the specimens was calculated from SEM micrographs of the fracture surfaces using the liner line intercept method with a stero-graphic projection factor of 1.5.

2.6 Specimen Preparation

The specimens sintered and the as-received commercial specimens were polished using an automatic polisher (Model Vari/PoL^{TM} VP-50, LECO Corporation, St. Joeph, MI). The grit sizes of the diamond paste (Warren Diamond powder Co. Inc, Olyphant, PA) used for polishing included 35 μm, 17 μm, 15 μm, 10 μm, 6 μm, and 1 μm (Figure 12). For polishing, the specimens were first mounted onto an aluminum plate disk about 2 cm thick, 20 cm in diameter, with 0.5 cm diameter center hole. The plate was heated for about 10 minutes on a heater to allow a thermoplastic (Thermoplastic Cement, BUEHER, Lake Bluff, IL) to melt which was the adhesive between the specimens and the surface of the aluminum plate (Figure 13). After mounting, the plate and specimens were cooled for about 20 minutes to allow the thermoplastic to densify.

Polishing oil (Microid Diamond, LECO Corporation, St. Joeph, MI) and diamond pastes were applied to the polishing cloth after placing a polishing plate in the polisher each time. The polishing oil was applied each time diamond grit changed. For newly mounted polishing cloths about 1 gram of diamond paste was applied to the polishing cloth. The polishing oil gave a good contact between the polishing cloth and the polished specimens. When the polishing for each diamond grit size was complete, the specimens

were cleaned usin
water and 1 % liqu
diamond grit. The
lubricated during p
over heating of the
polishing plates wa
specimens' surfaces
µm was indicated b
surfaces were very
ensured good polis
appropriate polishi
in this thesis.

After polis
mounted from the
The specimens w
minutes to remov
Ultra-Met III Son
contamination by
was removed fro

As-recei
low speed saw ,
brittle than the
saw arm and th

were cleaned using liquid soap, which was strong resolve liquid mixed with water 99 % water and 1 % liquid soap (Liquid-Nox, Alconox, Inc, New York, NY), to remove oil and diamond grit. The polishing oil was applied when the cloth was not sufficiently lubricated during polishing since not enough oil caused tearing of the polishing cloth and over heating of the polisher. For all polishing done in this thesis, the spin rate of polishing plates was fixed at 120 rpm. After finishing with the 35 μm polishing, the specimens' surfaces were the same color. For example, insufficient polishing after 35 μm was indicated by an apparently dark color through the specimens. The specimens' surfaces were very shinny after finishing with the 17 μm. Thus, a shiny specimen surface ensured good polishing after polishing with the 17 μm grit. Table 8 shows the appropriate polishing time and diamond grits size for each of the ceramic materials used in this thesis.

After polishing with the 1 μm grit was complete. The specimens were dis-mounted from the aluminum disk by heating the disk for 5 minutes to melt thermoplastic. The specimens were then taken from the aluminum plate and put into acetone for 1 or 2 minutes to remove residual thermoplastic in a beaker. An ultra-sonic cleaner (Model Ultra-Met III Sonic Clearner, Burhler LTD, Evanston, IL) was used to remove contamination by ultras-sonification for 20 minutes using de-ionized water. Excess water was removed from the ultra-sonically cleaned specimens using a clean tissue.

As-received MgF_2 billets were cut into 1 cm X 1 cm X 0.2 cm specimens using a low speed saw (Buehler IsoMet^{TM}, low speed saw, Lake Bluff, IL). MgF_2 is much more brittle than the oxide ceramic materials, thus, a mass of about 1.5 kg was applied to the saw arm and the cutting speed was set at between 5 rpm to 6 rpm. During cutting, the

MgF_2 specimens w
due to contacting w
cut specimens was
aluminum plate wa
heater was usually
specimen could be a
allowed to cool free

MgF_2 was p
polishing. Thus, af
aluminum plate was
were removed from
was removed using
water was removed
single unpolished s
sizes. After both si
beaker containing d
sonic cleaner where
in the DI beaker (a
minutes to remove

2.7 Coating Proce

Prior to joining
spin-on materials (

MgF_2 specimens were wrapped with a small piece of paper towel to reduce scratching due to contacting with metal specimen holder during cutting. After cutting, each of the cut specimens was mounted onto the aluminum polishing plate using thermoplastic. The aluminum plate was first placed on a heater to melt the thermoplastic. The set point of heater was usually 8 and after 10 minutes heating, melted thermoplastic so that the cut specimen could be attached to onto the aluminum plate. The specimens were then allowed to cool freely for 20 minutes to avoid failure of the thermoplastic bond.

MgF_2 was polished on both sides to examine the infrared transmittance after polishing. Thus, after one side was polished, specimens were dis-mounted. The aluminum plate was heated to melt the thermoplastic. After 10 minutes, the specimens were removed from the aluminum plate and the residual thermoplastic on the specimens was removed using acetone. The specimens were cleaned using water and any excess water was removed using a clean tissue. The specimens were then remounted with the single unpolished side up. Polishing was done using the same series of diamond grit sizes. After both sides were polished, the specimens were dismounted and placed in beaker containing de-ionized water. The beaker was placed in the middle of an ultra-sonic cleaner where the height of the water in the beaker matched the height of the water in the DI beaker (about 5 cm). The specimens were cleaned ultrasonically for about 20 minutes to remove contamination during cutting and polishing.

2.7 Coating Procedure Prior to Joining.

Prior to joining, the ceramic materials used in this thesis were coated with various spin-on materials (Table 6). Silica film were used most often as the interlayer for the

Figure 12.
polishing

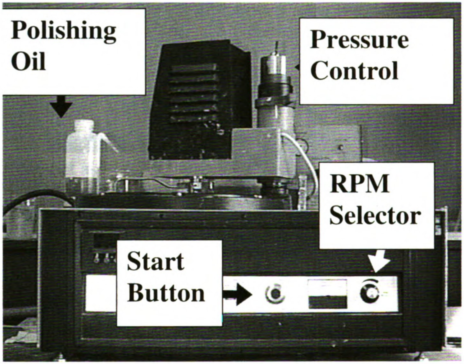

Figure 12. Photograph of the automatic polisher with the aluminum plate in place for polishing.

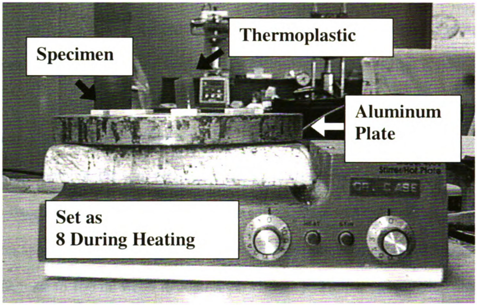

Figure 13. Photograph of heater and aluminum plate used in mounting the specimens for polishing. Note that several specimens have been fixed to the plate via thermoplastic.

ceramic/ceramic j
spinning at 500 rp
20 seconds.

First, double s
mounted on the pe
then the roughing v
The spin rate and th
Figure 14, the spin-
fully covered the spe

After spinnin
smooth. Except for
cured after spinning
sodium alginate to 1
sodium alginate and
furnace.

For MgF_2 wi
material, but film wa
sodium silicate on p

2.8 Microwave Joi

Ceramic/cera
cavity (Figure 15). T
mode. Microwave p

ceramic/ceramic joining done in this thesis. A high speed spinner was capable of spinning at 500 rpm to 6000 rpm. For this thesis, the spin rate was fixed at 3000 rpm for 20 seconds.

First, double sided adhesive tap was applied to the petri dish, and then specimen was mounted on the petri dish. The petridish was placed in high speed spinner holder and then the roughing vacuum pump (which held petri dish during spinning) was turned on. The spin rate and the spin time were set to the desired value (Figure 14). As shown in Figure 14, the spin-on material was liquid. Two or three pipette drops of spin-on material fully covered the specimen surface.

After spinning, the spin-on liquid material that had been applied was thin and smooth. Except for the silica film and sodium alginate, the spin-on materials were not cured after spinning. Water was added to the sodium alginate, at a ratio of 3 grams of sodium alginate to 100 ml water to control the viscosity. Following spinning, both the sodium alginate and silica film was cured at 200°C for 20 minutes in a conventional furnace.

For MgF_2 with MgF_2 joining, sodium silicate solution was used for the spin-on material, but film was not cured after spraying. MgF_2 specimens were coated with sodium silicate on polished side using a high speed spinner at 3000 rpm for 20 seconds.

2.8 Microwave Joining Procedure

Ceramic/ceramic joining was performed in a 2.45 GHz single mode microwave cavity (Figure 15). The particular resonant cavity mode used for this thesis was TM_{111} mode. Microwave power from 0 watts to 2000 watts was generated by a Sariem (Sairem

24 Rue Lo

input power

prepared an

deadweight

Figure 16

of approxim

power was

occurred at

microwaves

coupling oc

Coupling oc

level about

Afte

to control th

For

attached the

Holding 70

reached abo

step by step

seconds per

Tabl

temperature,

24, Rue Louis, France) power supply. The Microwave power controller controlled the input power. Cylindrical refractory caskets, 7.3 in diameter and 1.3 cm thick, were prepared and placed in the microwave cavity (Figure 16 (a)). Alumina (AKP 30) deadweight disks were placed of the specimens to provide low pressure during joining (Figure 16 (b)). The microwave power control is discussed in section 2.4. A heating rate of approximately 45°C per minute was used in this thesis. During joining, the reflected power was minimized by adjusting sliding the short and probe positions. Coupling occurred at input powers between 200 watts and 250 watts within 7 or 8 minutes for most microwaves heating. The probe position was changed from 0.3 cm to about 1.7 cm after coupling occurred, while short position was changed between 10.2 cm to 9.3 cm. Coupling occurred when the specimen absorbed microwave energy at critical energy level (about 250 or 300 watts).

After coupling the temperature quickly rose to 800°C. Thus, it was very difficult to control the heating rate for the temperatures less then 1000°C.

For MgF_2 joining, the maximum joining temperature was 700°C. The pyrometer attached the microwave system in this thesis can measure temperatures from 500°C. Holding 700°C was not easy operation since after coupling, specimen temperature was reached about at 900°C. However, it was possible to hold temperature at 700°C, after step by step power decrement (one time per 5 or 6 watts decrement) approximately 30 seconds per one power decrement.

Table 9 summarizes the interlayer materials, joining materials, joining temperature, joining time, and deadweight loading for the ceramic/ceramic materials

Figure 14. Schem

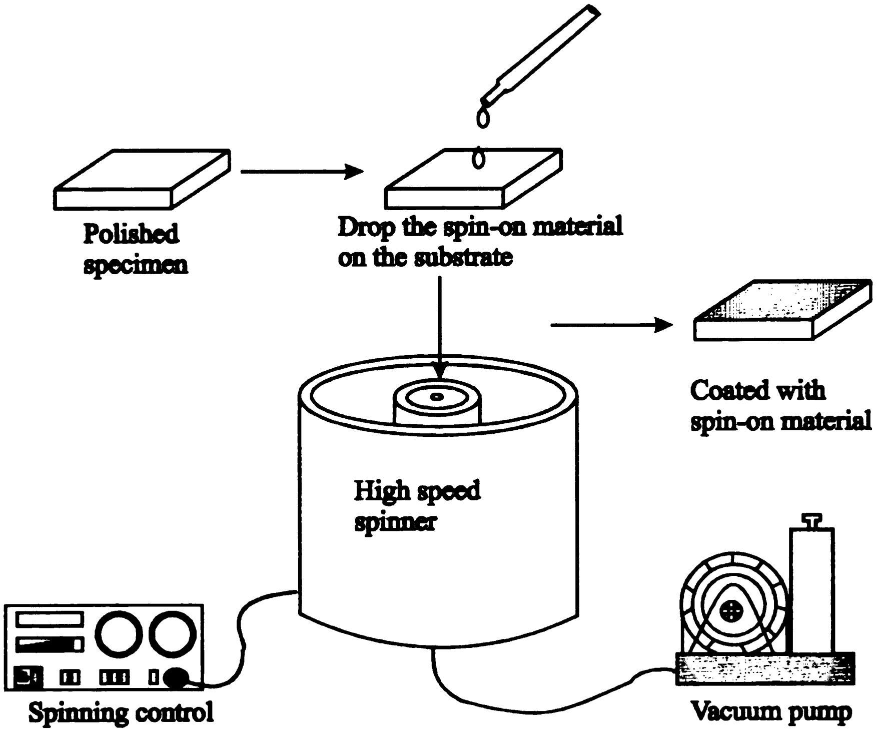

Figure 14. Schematic illustration of coating procedure using a high speed spinner.

joined in this th

partially stabili

partially stabil

ZrO_2-Al_2O_3, an

2.9 Joining tec

Nitride

furnace (Therm

flowing nitrog

silicon carbid

seconds but th

silicon carbid

holder to join

joining. The

flow rate was

limited to ten

grams was ap

2.10 Produc

As pa

specimens pr

Polis

specimen ho

joined in this thesis including (MgF_2/ MgF_2, AKP 30/AKP 30, partially stabilized ZrO_2/ partially stabilized ZrO_2, fully stabilized ZrO_2/ fully stabilized ZrO_2, HAP/MaCor^{TM}, partially stabilized ZrO_2/MaCor^{TM}, SiC/Al_2O_3/MaCor^{TM}, and partially stabilized ZrO_2/Al_2O_3, and alumina-zirconia composites alumina zirconia composites).

2.9 Joining technique for Non-Oxide Ceramics

Nitride and carbide ceramics joining attempts were made in a conventional furnace (ThermoCo Products Corporations, Model Mini Brute, Orange, CA) with a flowing nitrogen atmosphere and a flow rate of about 120 sccm. Only one polished silicon carbide or nitride specimen was coated with Blackglas^{TM} spun at 300 rpm for 20 seconds but the other polished silicon nitride specimen was not coated at all. Pair of silicon carbide or nitride specimen was first squeezed by hand then placed onto specimen holder to join using the conventional furnace without Blackglass^{TM} curing prior to joining. The heating rate for conventional joining was 20°C per minutes and the nitrogen flow rate was 120 sccm during heating. The conventional furnace used for joining was limited to temperatures of 1000°C or less. During joining, a deadweight of 20 to 60 grams was applied.

2.10 Producing Notch Mechanically Using A Low Speed Saw

As part of the ceramic/ceramic joining work, notches were cut into selected specimens prior to joining.

Polished and silica-coated specimens were mounted in a low speed diamond saw specimen holder, with the silica-coated side faced toward the saw blade (Figure 17). The

Figure 15. A
thesis.

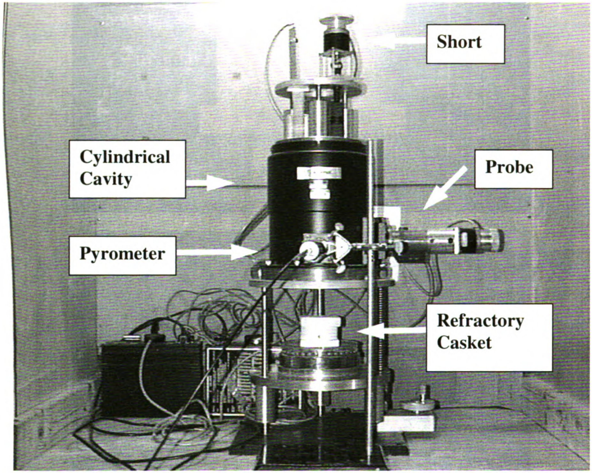

Figure 15. A photograph of the 2.45 GHz single mode microwave cavity used in this thesis.

Figure 16. (a) P
during ceramic
refractory caske

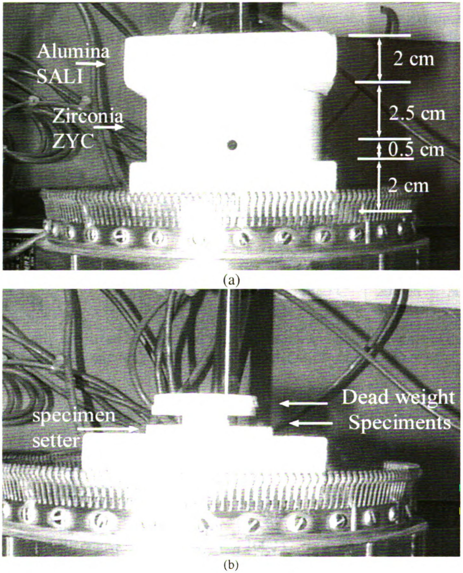

Figure 16. (a) Photograph of the type of zirconia/aluminosilicate refractory casket used during ceramic/ceramic joining, (b) Photograph of the bottom SALI plate of the refractory casket with the specimen, with the specimen setter and dead weights in place.

Table 9. A
hold time.
thesis.

Attemp ma
MgF$_2$
AKP 30
*ZrO$_2$
*ZrO$_2$
HAP w
*ZrO$_2$ w
SiC M
Al$_2$O Al
**ZrO

*ZrO$_2$ is
HAP is h

Table 10.
carbide.

Materi
SiC
Si$_3$N$_4$
Si$_3$N$_4$

Table 9. A summary of the interlayer materials, joining materials, joining temperature, hold time, and deadweight loading for all of the ceramic/ceramic joining included in this thesis.

Attempted joining materials	Spin-on interlayer	Joining Temp(°C)	Hold time	Dead Weight
MgF_2 with MgF_2	Sodium silicate solution	700°C	20 min	60 grams
AKP 30 with AKP 30	Sodium alginate	1400°C	20 min	60 grams
*ZrO_2 with *ZrO_2	Silica film	1500°C	20 min	60 grams
*ZrO_2 with Al_2O_3	Silica film	1500°C	20 min	50 grams
HAP with MaCor™	Silica film	1020°C	20 min	20 grams
*ZrO_2 with MaCor™	Silica film	1020°C	20 min	20 grams
SiC/Al_2O_3 with MaCor™	Silica film	1020°C	20 min	20 grams
Al_2O_3/ZrO_2 with Al_2O_3/ZrO_2	Silica film	1450°C	20 min	50 grams
**ZrO_2 with **ZrO_2	Silica film	1500°C	20 min	50 grams

*ZrO_2 is partially stabilized zirconia and **ZrO_2 is fully stabilized zirconia in this thesis. HAP is hydriteappitite and SiC/Al_2O_3 is a SiC platelet reinforced alumina

Table 10. Experimental condition of conventional joining of silicon nitride and silicon carbide.

Material	Spin-on material	Spin-rate	Max Temp (°C)	Hold time	Atmosphere
SiC	Blackglas™	5000 rpm	900°C	20 minutes	N_2
Si_3N_4	Blackglas™	3000 rpm	900°C	20 minutes	N_2
Si_3N_4	Blackglas™	5000 rpm	1000°C	20 minutes	N_2

weight applied t

the specimens.

than about 1 kg

18 shows a sche

notch were join

determine the

microwave he

211 Procedu

Notch

approximate

of the die pu

at 1.75 MPa

The p

which had n

MPa (Figure

Alu

heating rate

enclosed no

Alumina-z

1375°C for

for 20 min

weight applied to the saw during notching was much less than weight used during cutting the specimens. Often 1.5 kg of deadweight was used to produce notch, but a mass greater than about 1 kg was detrimental to the life of the low speed diamond saw blades. Figure 18 shows a schematic of the notch processing technique. After specimens containing a notch were joined with another specimens, the specimen was cut in half in order to determine the stability of the notch dimensions. The notched specimen was then microwave heated in an attempt to join the notched specimen.

2.11 Procedure of Producing Notch Prior to Sintering

Notched were "stamped" prior to sintering. Monofilament fishing line (approximately 250 mm in diameter) was cut into 1.5 cm lengths and then glued onto one of the die punch faces. Approximately 2.5 gm of alumina powder was uniaxially pressed at 1.75 MPa using a uniaxial press.

The powder was put into the hard die then smoothed using the second die punch which had no glued fishing line on it. Upper punch was replaced and then pressed at 17.5 MPa (Figure 19).

Alumina (TM-DAR) enclosed notches was sintered at 1300°C for 1 hour with heating rate 10°C/min using the microwave energy. Also, alumina-zirconia composites enclosed notches was sintered at 1300°C for 1 hour with a heating rate 10°C/min. Alumina-zirconia composites was then joined with zirconia (3 mol % Y_2O_3 sintered at 1375°C for 1 hour using the microwave energy), which was without notches at 1400°C for 20 minutes.

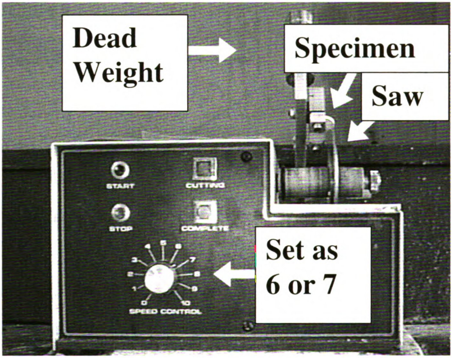

Figure 17. Photograph of a low speed diamond saw after the specimen had been in the saw.

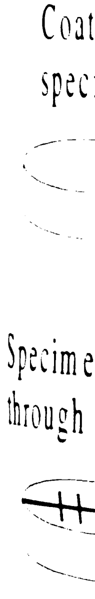

Figure 18.
specimens

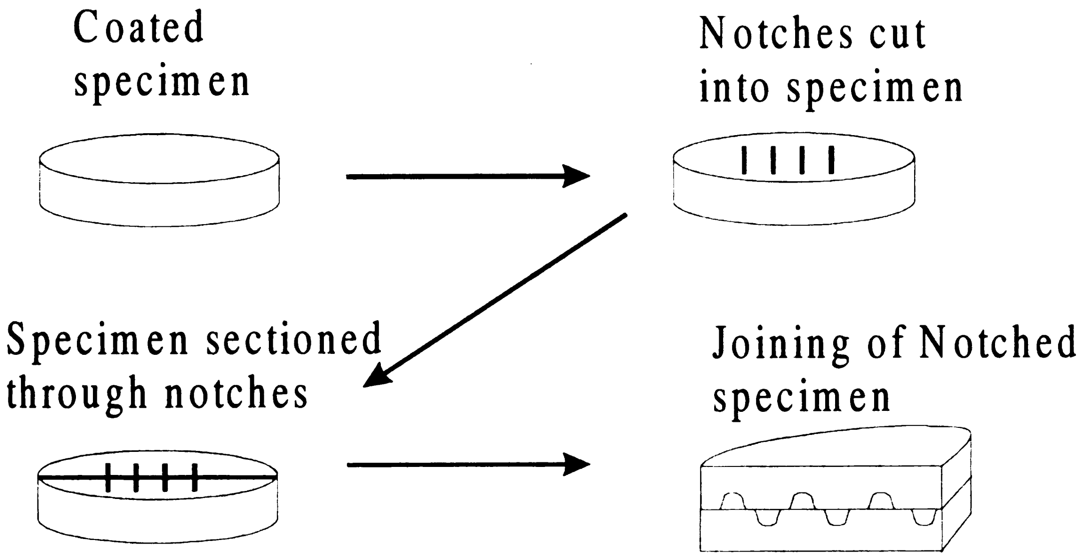

Figure 18. Schematic of the technique used to mechanically cut notches into the specimens.

Figure 19. S
prior to sinter

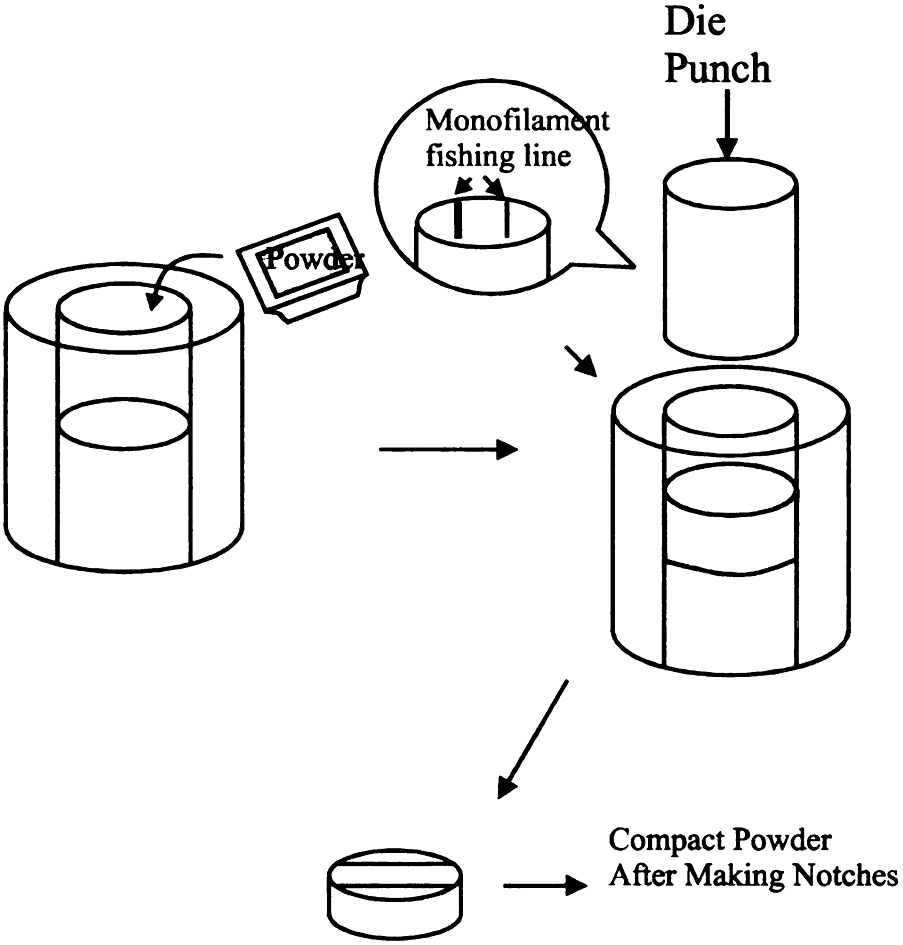

Figure 19. Schematic of "stamping" notches into the green (unfired) powder compacts, prior to sintering.

2.12 Mountin

Joined

saw. Joined

Compression

a 1 inch diam

At le

automatic p

inclining of

specimens w

polishing, cl

minutes.

2.13 Vicker

The

deflection

away from

more inden

were appli

compared

2.14 SEM

Jo

(Emscope

2.12 Mounting and Polishing of Joined Specimen

Joined specimens were cut into two or more pieces using a low speed diamond saw. Joined and cut specimens were then mounted in diayllyl-phthalate powder (Compression Mounting Powders, LECO Corporation, St. Joeph, MI) using a press with a 1 inch diameter rum (Figure 20).

At least 3 of the joined and mounted specimens were required to polish using the automatic polisher. During polishing, 3 mounted specimens were balanced without inclining of a polishing holder. As mentioned in section 2.6, joined and mounted specimens were polished as using diamond grit size from 35 μm to 1 μm. After polishing, cleaning was performed in DI water using the ultra-sonic cleaner for 20 minutes.

2.13 Vickers indentation Testing of Joined Specimen

The fracture toughness of joined specimens was estimated from the crack deflection at an interface using Vikers indentation (Figure 21). Indentation was applied away from the interface to near the indentation using Vikers indentation then applied more indentations to near interface as shown in Figure 21. Same load and load speed were applied onto joined specimen to observe the deflection of bond layer after joining compared with mother material.

2.14 SEM Observation of Bond-layer

Joined and mounted specimens were coated with gold using a sputter coater, (Emscope SC 500) coating for 1 minute produced 7 nm gold coating. Carbon paint,

Figure 20. S

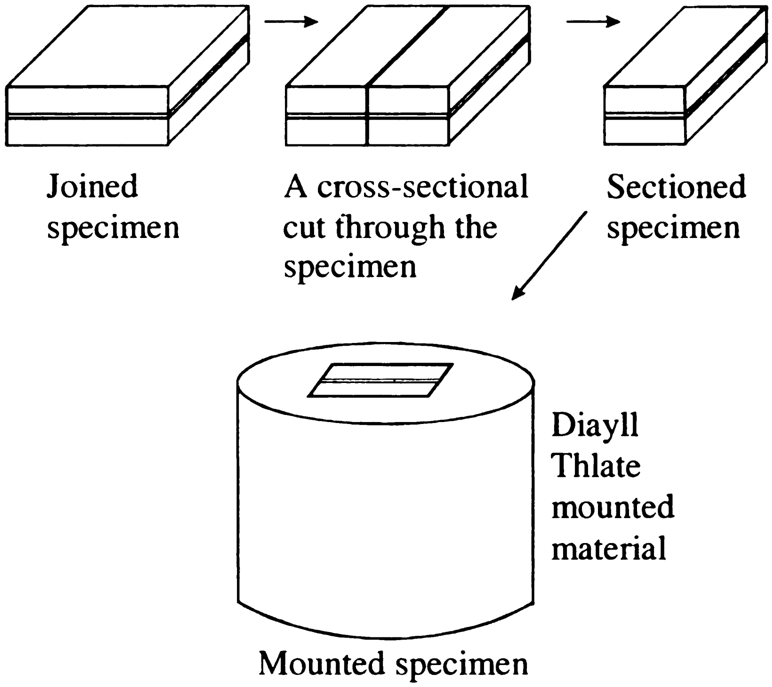

Figure 20. Schematic illustration of mounting the specimen after joining and cutting.

Vicker
Indent

Figure 21. S

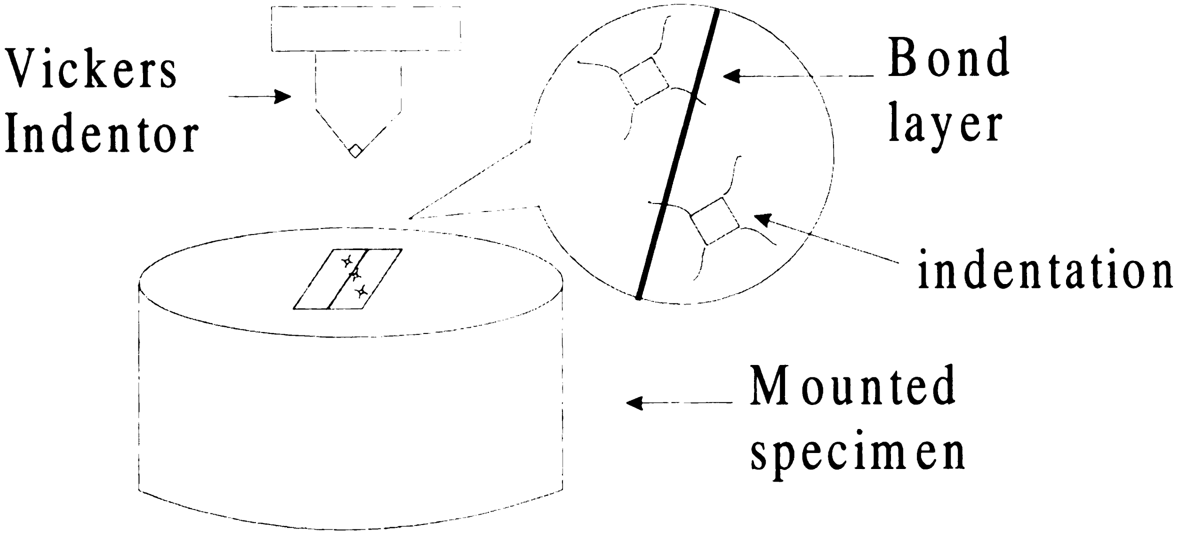

Figure 21. Schematic of Vikers indentation near the bond layer.

Table 11.
specimens

Figure
specim

Table 11. Type of filters and detectors used to measure the IR transmittance of the MgF_2 specimens.

Wavelength range	Types of filters	Types of detectors
400-650nm	Transparent filter	813-SL
650-840nm	Red filter	813-SL
850-1650nm	Black filter	800-IR

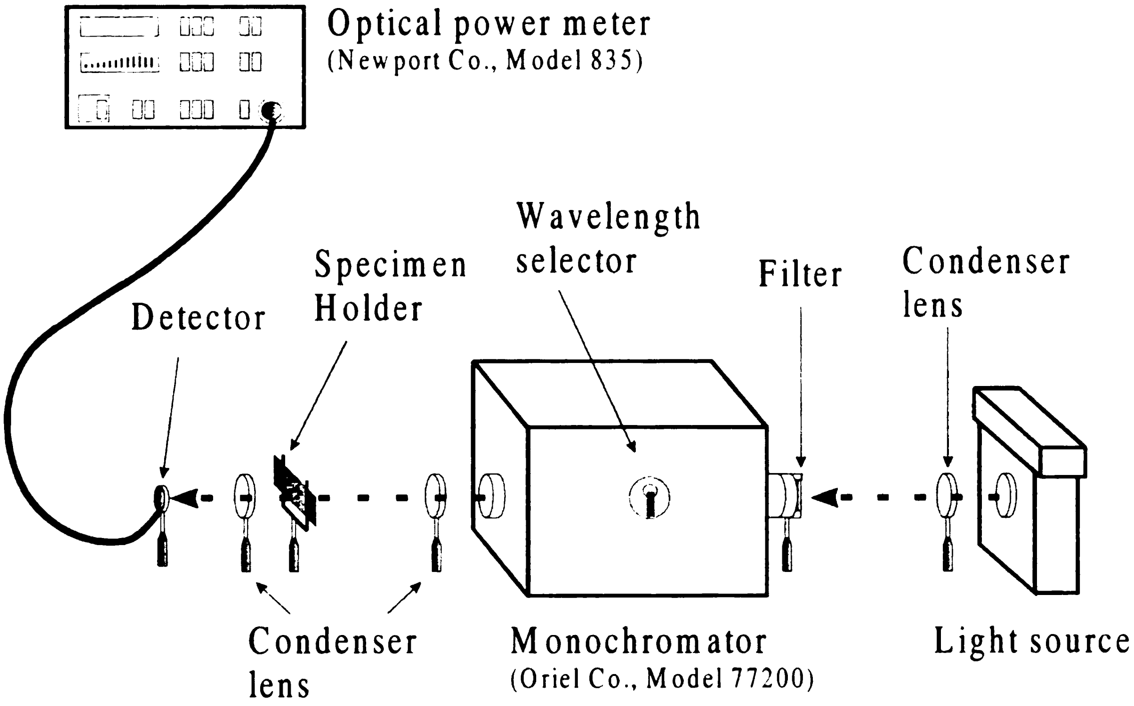

Figure 22. Schematic of the apparatus used for measuring the IR transmittance of MgF_2 specimens.

whic

gold

speci

exam

of 20

carbo

The s

2.15

for w

7720

and th

calcul

calcul

with s

red fil

transm

detect

which was carbon based black liquid (Ted Pella, Inc. Redding, CA), was applied before gold coating from edge of the joined specimen to end of the mounted side to the specimen to prevent charging during SEM observation. A JEOL 6400 SEM was used to examine bond layer. The best image resolution was obtained using accelerating voltage of 20 kV, a working distance 15 cm, and condenser lens intensity setting of 9.

A set of notched and joined specimens was mounted to an aluminum stub using carbon tape in order to observe changes in notch dimensions before and after joining. The specimens mounted onto aluminum stub also were coated with gold for 1 minute.

2.15 Infrared Transmittance Measurement of MgF_2

The transmittance of polished, coated, and heated MgF_2specimens was measured for wavelength from 400 nm to 1650 nm using a spectrophotometer (Oriel Co, Model 77200) (Figure 22).

Transmittance was first measured without the specimen in the spectraphotometer and then measured with the specimen in the spectrophotometer. Transmittance was calculated after measuring both without specimen and with specimen. Transmittance was calculated from dividing the measurement of without specimen data into measurement of with specimen data. Which was

$$\frac{\text{Transmittance measurement from with specimen}}{\text{Transmittance measurement from without specimen}}.$$

Transparent filter transmitted UV light only in range of wavelength 400-650nm, red filter transmitted infrared only in range of wavelength 650-840nm, and black filter transmitted only infrared in range of 850-1650nm shown in Table 11. Two types of detectors were used to get correct data at each range.

2.1

the s

micr

Ribb

and t

are g

micro

to pre

the sh

micro

finger

the mi

probe

the mi

plate is

cleaned

sweeps a

often u

2.16 Microwave cavity cleaning

The microwave cavity was cleaned every each month. Volatile components of the spin-on coatings deposit on the water-cooled microwave cavity walls. The microwave cavity is cleaned using metal polish (No. 22 Metal and Chrome Polish, Blue Ribbon Products Division, Indianapolis, IN) and commercially pure alcohol.

The microwave cavity is composed of the main cavity, the sliding short assembly, and the probe (Figure 23). Inside the microwave cavity, the short assembly and the probe are gold coated.

Before removing either the short assembly or the probe assembly from microwave cavity, the short was positioned at 17 cm and the probe positioned at 0.0 cm to prevent possible damage while removing the short and probe parts. After setting both the short and the probe to the proper position, they were removed from the main microwave cavity using proper screwdriver. The short and the probe assembly each have finger stock (Figure 23, 24, and 25). Finger stock distributes microwave energy inside the microwave cavity during heating are very brittle. Thus, separating the short and the probe parts must be done carefully to avoid breaking the finger stock.

The inside of the main microwave cavity is coated with gold and the bottom of the microwave cavity (which does not move) has finger stock (Figure 23). The cavity top plate is the sliding short, which has also finger stock, and is goal coated (Figure 24).

Each of the separated parts (short, probe, and main microwave cavity) were cleaned by first applying metal polish to metal part and then cleaned by alcohol. Cotton swaps and cotton balls were used to clean the microwave cavity. Cotton swaps were often used inside the microwave cavity, the short assembly, and the probe part that can be reach

finge

assem

17 cm

positi

cavity

reached with one's hands. The cotton balls were used to clean the finger stock since the finger stock is very fragile.

After cleaning the main microwave cavity, the short assembly, and the probe assembly, careful reassembly is required. In this case, the short was positioned at about 17 cm and the probe was positioned at 0.0 cm. After replacement, the short was positioned to about 10.2 cm and the probe was positioned at about 0.6 cm to prepare the cavity for its next use.

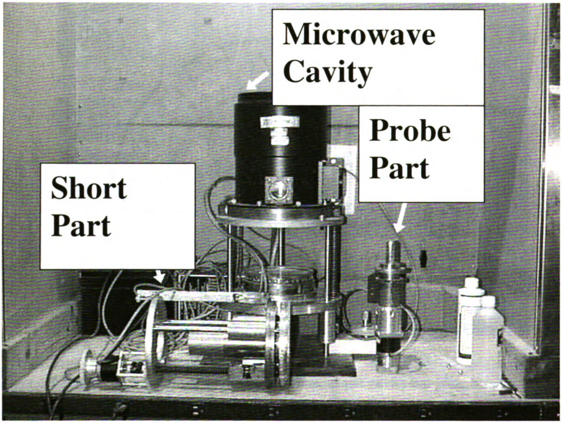

Figure 23. A view of the microwave cavity disassembled for cleaning. Shown are the main microwave cavity, the lanch probe, and the sliding short.

Figure 24.
physical co
effective ca

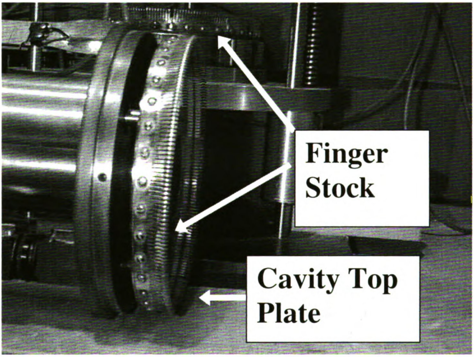

Figure 24. Cavity top plate showing finger stock. The finger stock makes electrical and physical contact with the inner cavity wall. Thus, as the cavity top plate moves, the effective cavity length changes.

Figure 25.

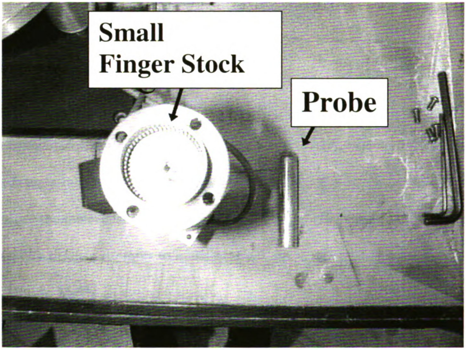

Figure 25. For the launch probe part of the probe assembly includes small fingers stack.

3. Results

3.1 Joining o

JOININ(

ABSTRAC

Many

spectrum (s

protect such

difficult, sin

deposition.

diamond film

1. INTROD

Ceram

ceramic mate

joined alumin

J. G. Lee, K. Y. L
Ceramic Transact

3. Results

3.1 Joining of Diamond Thin Film to Optical and IR Materials

JOINING OF DIAMOND THIN FILM TO OPTICAL AND IR MATERIALS

J. G. Lee, K. Y. Lee and E. D. Case
Materials Science and Mechanics Department,

Michigan State University
East Lansing, MI 48824

ABSTRACT

Many materials that are transparent in both the visible and infrared regions of the spectrum (such as ZnS and MgF_2) are easily scratched. Hard coatings may help to protect such materials, but direct deposition of diamond films onto such substrates is difficult, since the materials tend to degrade at the temperatures required for diamond deposition. We discuss attempts to make MgF_2/MgF_2 joins, as well as efforts to bond diamond films to MgF_2.

1. INTRODUCTION

Ceramic/ceramic joining has been done successfully for a variety of structural ceramic materials, including alumina, SiC, and zirconia. For example, Case et al. has joined alumina, Macor^R, and zirconia using spin-on layers [1-2]. In addition to structural

---

J. G. Lee, K. Y. Lee and E. D. Case, "Joining of Diamond Thin Films to Optical and IR Materials," Ceramic Transactions, Volume 94, American Ceramic Society, Inc., Westerville, OH. pp. 509-520 (1998)

ceramics, optical

pressures. Yen e

technique at tem

Yen et al. attrib

in the polycryst

This pa

diamond thin f

measured as a

to compare th

2. EXPERIM

2.1. Materi

As re

pressed poly

26). Specim

speed diamo

Afte

Corporatio

specimens

and after jo

(Columbu

spinning a

smooth.

ceramics, optically-transmitting ceramics have been joined, usually at high joining pressures. Yen et al. [3] joined MgF_2 specimens using a direct diffusion bonding technique at temperatures of 800°C and greater, using pressures of 17 MPa to 25 MPa. Yen et al. attributed a drop in the joined MgF_2 specimens' transmittance to grain growth in the polycrystalline MgF_2 specimens.

This paper discusses attempts to bond (1) MgF_2 to MgF_2 and (2) polycrystalline diamond thin films to MgF_2. For successfully joined specimens, the transmittance is measured as a function of wavelength and the optical absorption coefficient, α, in order to compare the optical qualities of joined and unjoined specimens.

2. EXPERIMENTAL PROCEDURE

2. 1. Materials

As received commercial MgF_2 (Itran I, Eastman Kodak Company) is a hot-pressed polycrystalline material with a mean grain size of approximately 2.8μm (Figure 26). Specimens were sectioned into roughly 1cm X 1cm and 2mm thickness using a low speed diamond saw.

After cutting, the specimens were polished by an automatic polisher (LECO Corporation) using the following series of diamond grit sizes 17, 10, 6, and 1μm. The specimens were polished on both sides to facilitate IR transmittance measurements before and after joining. The polished specimens were coated with a sodium silicate solution (Columbus Chemical Industries Inc.) using a high-speed spinner (Figure 27). After spinning at a rate of 2000 rpm to 5000 rpm, coating was uniform in thickness and smooth.

Figure

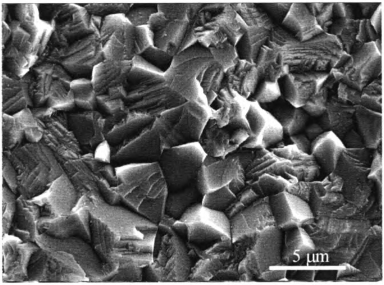

Figure 26. SEM image of the fracture surface of MgF_2.

Figure 27.
MgF_2 subs

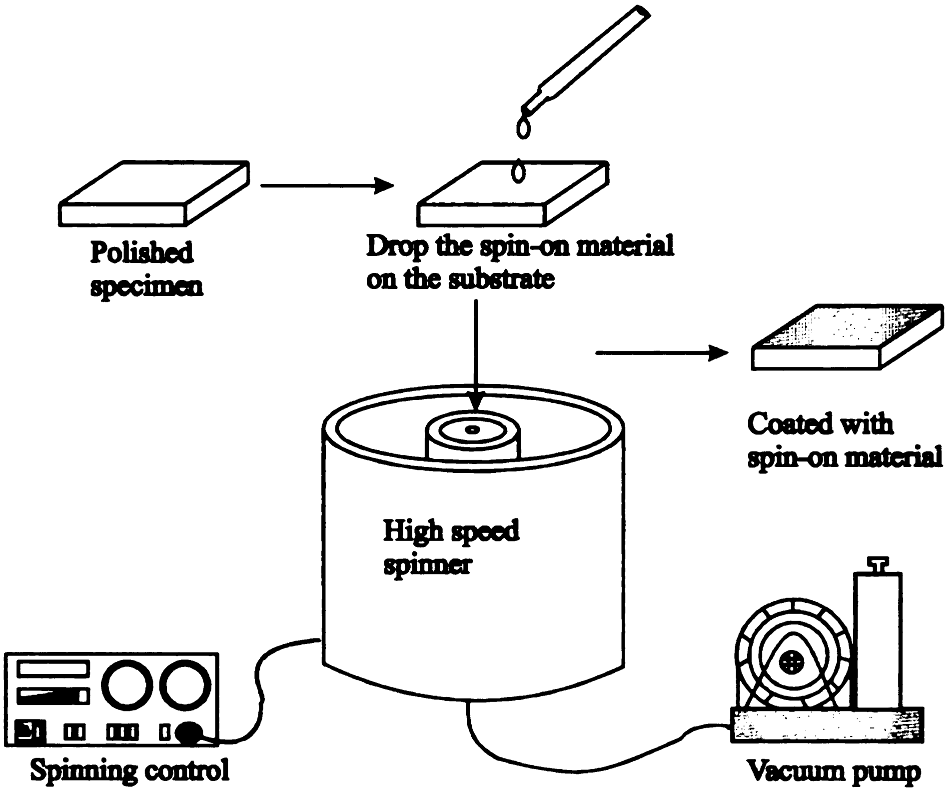

Figure 27. Schematic showing the high-speed substrate spinner used in coating to the MgF_2 substrates.

sodi
med
subs
was
conn
bond

mean
at 40
that w
specin
ultraso
onto M
were p
the sod

pipette.
MgF_2 su
high-spe

2.2 Joi

C
Model M

In this study, two silicate solutions were used as bonding agents. A commercial sodium silicate solution (Columbus Chemical Industries, Inc.) was used as one of the joining media. Although the sodium silicate was very viscous, after spinning on the high-speed substrate spinner, the coatings were quite smooth. A second bonding agent that was used was an organically-based silica solution, which pyrolyses to an amorphous silica film upon curing at 200°C. However, the silica film was not successful in either the MgF_2/MgF_2 bonding or the diamond film/MgF_2 bonding.

The diamond films used in this study were between 3 to 4 microns thick, with a mean grain size of approximately one micron. The films were microwave plasma-deposited at 400°C to 500°C under 28 torr pressure onto (100) oriented single crystal silicon wafers that were 0.048 to 0.053 cm thick and 5.08 cm in diameter. The diamond-coated silicon specimens were fractured into 1 cm X 1 cm sections using a razor blade. Following ultrasonic cleaning in deionized water, the diamond-coated silicon specimens were placed onto MgF_2 substrates that had been coated with sodium silicate solution. The specimens were placed such that the diamond film coating on the diamond-silicon specimens contacted the sodium silicate coating on the MgF_2 substrates.

Prior to joining, the bonding agents were spun onto the MgF_2 substrates. Using a pipette, a few drops of either sodium silicate or the silica film was placed onto a polished MgF_2 substrate and the film was spun between 2000 and 5000 rpm using a high-speed substrate spinner (Figure 27).

2.2. Joining Procedure

Coated specimens were heated in either a single mode microwave cavity (Sairem, Model MWPS 2000) or in a conventional electrical resistance furnace. For joining the

MgF_2 to M

1200°C wi

using the s

weights of

2.3. IR Tr

All IR

Co. Model

Prior to

experiment

at or near th

(but not joi

done on the

(1) As-poli

(2) Polished

(3) Polished

air.

In additio

listed above, p

specimens we

specimens (en

MgF_2 to MgF_2 using the silica film, the annealing temperatures ranged from 500°C to 1200°C with applied dead weight loads of 20 gm to 85 gm. The MgF_2/MgF_2 joining using the sodium silicate solution utilized temperatures of 500°C to 800°C and dead weights of 20 gm to 85 gm.

2.3. IR Transmittance Measurements

All IR transmittance measurements were performed using a monochromator (Oriel Co, Model 77200) over wavelength range of 800 nm to 1600 nm (Table 12).

Prior to the transmittance measurements on the joined specimens, a series of experiments was done to determine the effect of (1) heating the polished but uncoated MgF_2 at or near the temperature used for joining and (2) coating and heating the MgF_2 substrates (but not joining them). In order to examine these effects, transmittance measurements were done on the MgF_2 substrates having the following surface treatments:

(1) As-polished specimens,

(2) Polished specimens which were subsequently heated at 700°C in air,

(2) Polished specimens that were coated (without joining) and then heated at 700°C in air.

In addition to the three "comparison" surface treatment/heat treatment conditions listed above, polished specimens were coated, and then the coated surfaces of the two specimens were placed in contact. The specimens were then heated in an effort to join the specimens (either MgF_2/MgF_2 joining or diamond/MgF_2 joining).

Figure 28
weight loa

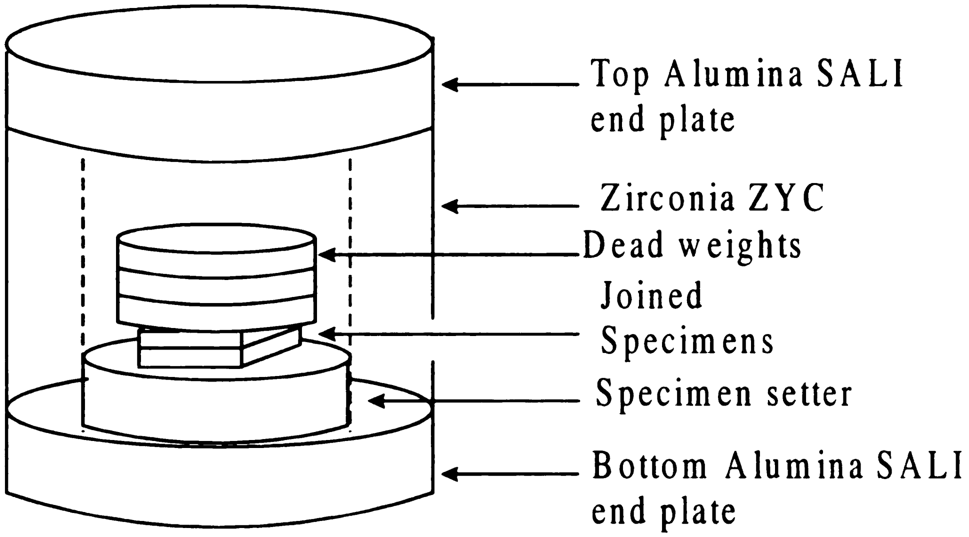

Figure 28. Schematic of the refractory casket used for microwave joining. The dead weight loading also is illustrated [2].

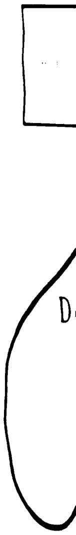

Figure 29

measurem

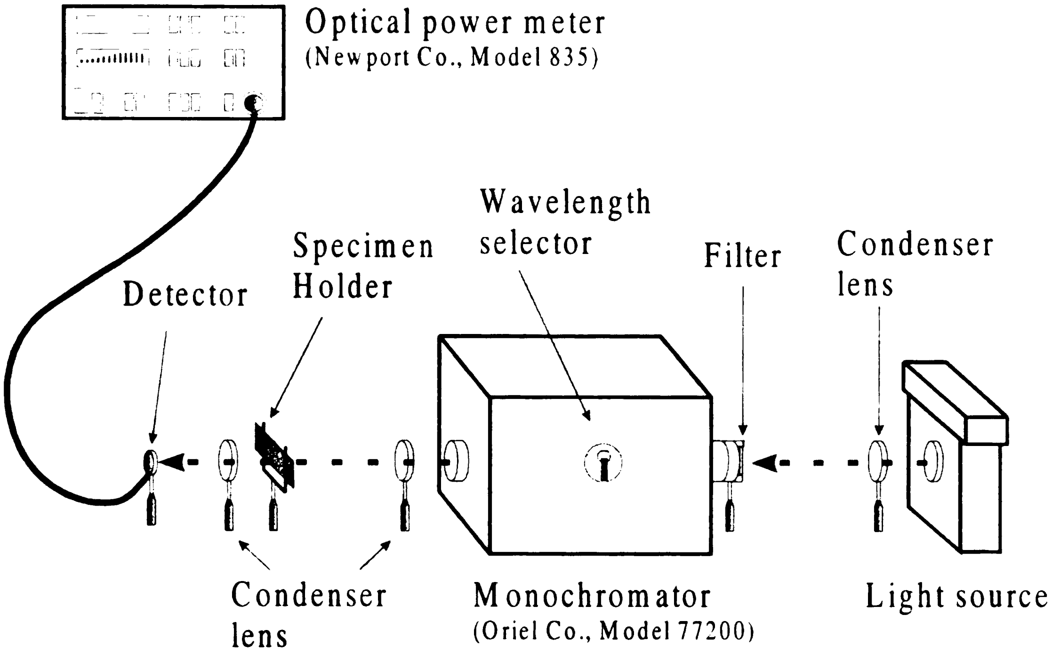

Figure 29. Schematic of the spectrophotometer used for the IR transmittance measurements.

Joine

of the sectio

polisher, the

17, 10, 6, an

SEM

specimens.

sectioned an

SEM exami

3. RESULT

3.1. Joining

For t

700°C using

conventiona

The mean b

microwave-j

conventiona

MgF_2/MgF_2s

30). Microst

joined $MgF_2/$

The coupling

the temperatu

can be generat

Joined specimens were cross-sectioned using a low speed diamond saw. A portion of the sectioned specimen was mounted in thermosetting powder. Using an automatic polisher, the mounted specimens were polished using a series of diamond grit, including 17, 10, 6, and 1μm.

SEM examination determined the bond-layer thickness in the sectioned specimens. Since ceramic materials are not electrically conductive materials, the sectioned and mounted specimens were coated with a 0.7 nm thick layer of gold prior to SEM examination.

3. RESULTS AND DISCUSSION

3.1. Joining MgF_2 using sodium silicate solution

For the sodium silicate bonding agent, the MgF_2/MgF_2 joining was successful at 700°C using both microwave and conventional heating. For both the microwave and conventional heating, dead weight loading was used during joining (Table 13).
The mean bond layer thickness for the MgF_2/MgF_2 specimens was 10 microns for the microwave-joined specimens and 15 microns for the specimens joined in the conventional furnace. The microwave and the conventionally-joined MgF_2/MgF_2specimens showed very different microstructures near the bond layer (Figure 30). Microstructural differences between the microwave-joined and the conventionally-joined MgF_2/MgF_2 specimens may be related to the nature of microwave heating itself. The coupling of a material with microwave energy is a function of both the material and the temperature of the material, but if the material does absorb microwave power, heat can be generated within the specimen [4,5]. In this case, the microstructural differences

Table 1

Table 1

Hea

Co

M

Table 12. Type of filters and detector for various wavelengths.

Wavelength range	Types of filters	Types of detectors
400-650nm	Transparent filter	813-SL
650-840nm	Red filter	813-SL
850-1650nm	Black filter	800-IR

Table 13. The conditions of joining both microwave and conventional furnace.

Heating method	T_{max}(°C)	Hold time(min)	Dead weight(gm)	Heating rate (°C/min)
Conventional	700°C	20min	85gm	10°C/min
Microwave	700°C	20min	60gm	45°C/min

(Figure 30

conventio

reaction la

difference

Future stu

A

Vickers in

specimen

stopped a

material.

bond laye

The I

IR transm

to the IR

coating.

similar t

to signif

The

than the

transmi

be discu

3.2. Ca

MgF_2 us

(Figure 30) may be a function of differing chemical reaction kinetics between the conventional and microwave heating (hence forming differing sodium silicate/MgF_2 reaction layers). Alternatively, the microstructural differences may be linked to differences in microwave and conventional heating at and near the interfacial region. Future studies should address these points.

A rough estimate of the bond-layer toughness was obtained by placing a 98N Vickers indentation crack near the bond-layer of a sodium silicate bonded MgF_2/ MgF_2 specimen (Figure 31). For the microwave joined MgF_2, the Vickers indentation crack stopped at bond-layer, indicating the bond-layer material is not as strong as the matrix material. Similar results were obtained for Vickers indentation cracks placed near the bond layer for conventionally-joined specimens.

The IR transmittance of the polished and heated (but not coated) specimens and the IR transmittance of the polished coated, and heated (but not joined) were nearly identical to the IR transmittance of the polished specimens (Figure 32). Thus, (1) heating without coating, (2) coating, heating and not joining gave an IR transmittance that was very similar to the as-polished specimens, and therefore heating and coating alone do not seem to significantly affect the IR transmittance of the MgF_2 specimens.

The microwave joined MgF_2/MgF_2 shows a considerably higher IR transmittance than the conventionally joined MgF_2/MgF_2 specimens (Figure 33). The differences in transmittance lead to differences in the calculated optical absorption coefficients, as will be discussed in Section 3.2 of this paper.

3.2. Calculation of Absorption Factor for microwave and conventionally joined MgF_2 using sodium silicate solution

Figure 3
MgF_2 sho
with 60g
with 55gr

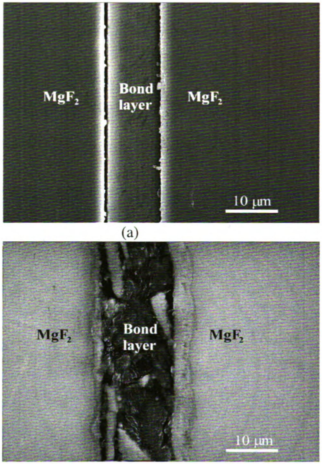

(a)

(b)

Figure 30. SEM micrographs of both the microwave and the conventionally joined MgF$_2$ showing the bond-layer. (a) Microwave joined MgF$_2$ (joining at 700°C for 20min with 60gm weight loading), (b) Conventional joined MgF$_2$ (joining at 700°C for 20min with 85gm weight loading).

Figure
solutio
60gm

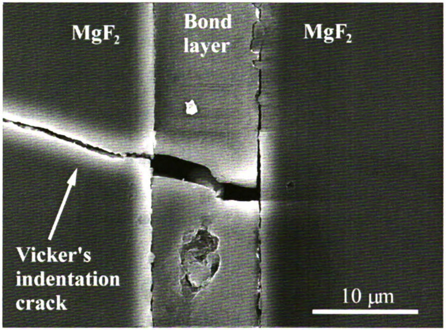

Figure 31. SEM image of a MgF$_2$/ MgF$_2$ specimen joined using the sodium silicate solution. The specimen was joined by microwave heating at 700°C for 20min with a 60gm dead weight loading.

To d

microwave

was used, w

radiation. (

If th

where R is

optical ind

The ratio

At normal

Solving fo

The o

zero thick

specimen

An op

index of r

absorption

microwav

To determine the optical absorption factor, α, for both the conventionally and the microwave joined MgF_2/ MgF_2 specimens, the Lambert-Bouger law [6]

$$I_T = I_I e^{-\alpha x} \tag{1}$$

was used, where I_T is intensity of transmitted radiation, I_I is the intensity of the incident radiation, α is absorption factor, and x is the specimen thickness.

If the optical reflection at each interface is taken into account, I_T/I_I is given by

$$I_T/I_I = (1-R)^m e^{-\alpha x} = T \tag{2}$$

where R is the reflectivity for normal incidence angles. R is a function of the optical index of reflection, *n*, and *m* is the number of interfaces for the specimen. The ratio I_T/I_I is the transmittance, *T*. For a planar slab, $m = 2$.

At normal incidence, *R*, is given by

$$R = \frac{(n-1)^2}{(n+1)^2} \tag{3}$$

Solving for optical absorption factor, α, gives

$$\alpha = -\frac{1}{x}\ln\frac{T}{(1-R)^m} \tag{4}$$

The optical properties of bond-layer are unknown, but we estimated α by assuming a zero thickness bond-layer in equation (2) for the joined MgF_2. For MgF_2/ MgF_2 specimens, *m* is set equal to 3 (Figure 34).

An optical absorption factor, α, was calculated from equation (4) using an optical index of refraction, *n*, of 1.3749 at a wavelength 1500nm [7]. The calculated optical absorption coefficients, α, were similar for the polished (unjoined) and for the microwave-joined

Figure 3
Conventi
and MgF

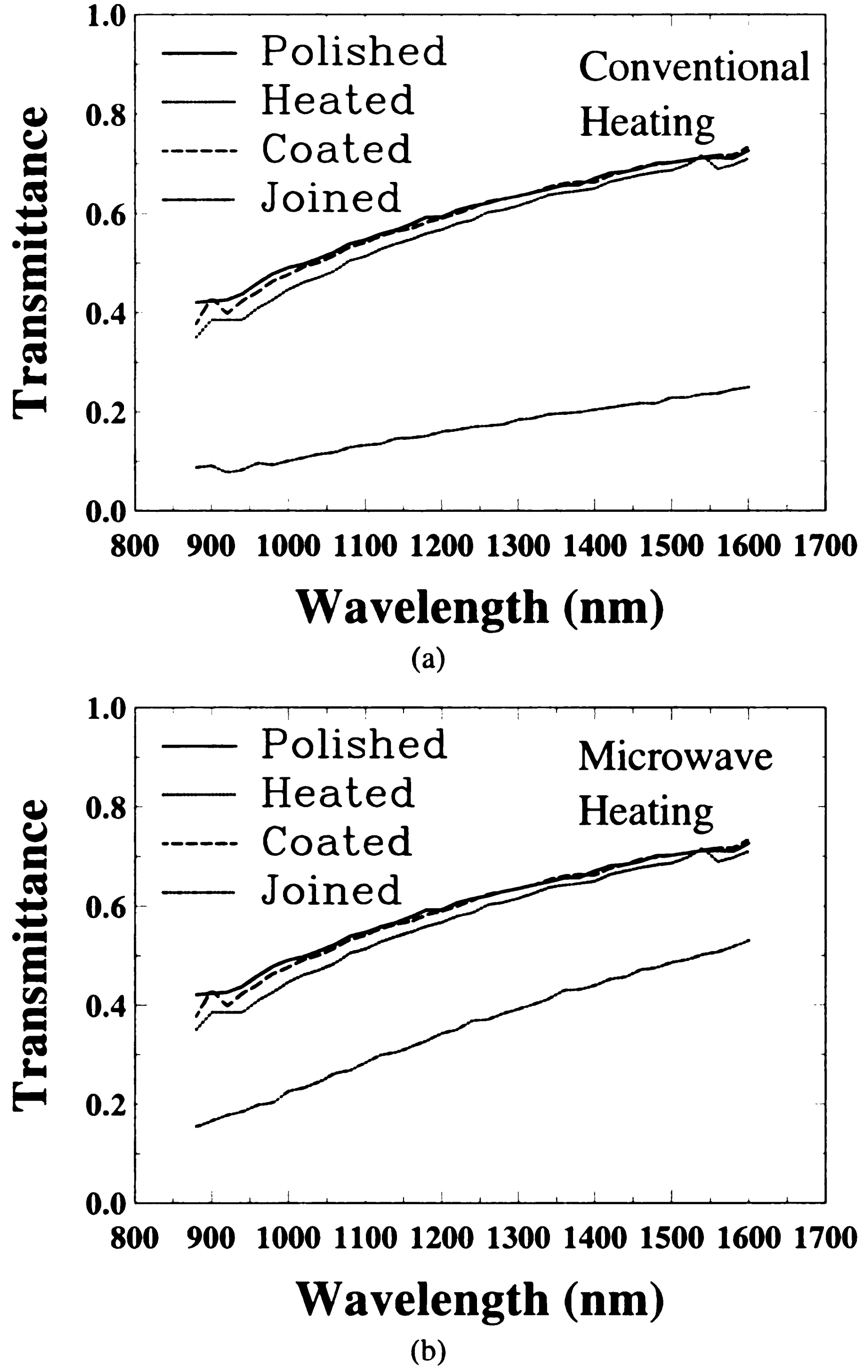

Figure 32. Transmittance for both microwave and conventionally heated MgF_2. (a) Conventionally-heated MgF_2 and MgF_2/ MgF_2 joined and (b) Microwave-heated MgF_2 and MgF_2/ MgF_2 joins.

Transmittance

33. Co
Figure 3

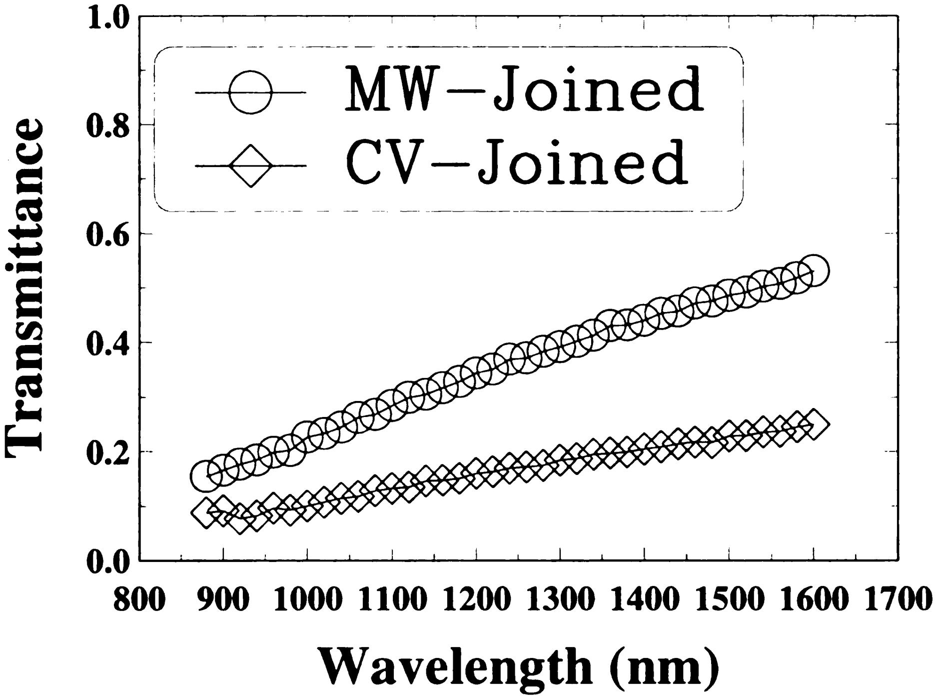

Figure 33. Comparison of transmittance for microwave and conventionally joined MgF_2(From Figure 32).

Figure .
specime

Table 1-

Process
Polish
MW-joi
CV-joir

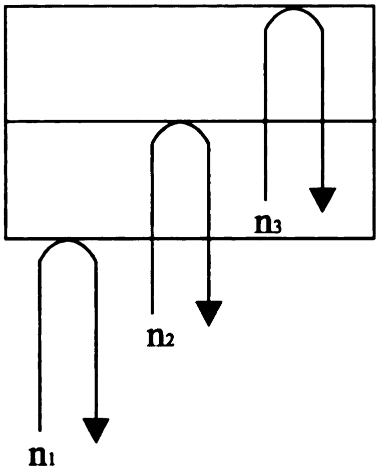

Figure 34. As schematic showing the reflections at the various interfaces of a two-layer specimen (which gives $m = 3$).

Table 14. Calculation of the optical absorption factor, α.

Processing	Measured T	R	x(mm)	$\alpha(mm^{-1})$
Polished	0.703	0.025	2.029±0.002	0.149
MW-joined	0.486	0.025	4.134±0.009	0.156
CV-joined	0.229	0.025	4.209±0.012	0.342

specim
polishe
and th
conver
induce

includ
the ma
wavele
center a
$\lambda/a < 1$
scatteri
visible
micron
microns
theoreti
micron
one-perc
centers (
several m
waveleng
since λ/a
scattering

specimens ($0.149mm^{-1}$ and $0.156mm^{-1}$, respectively Table 14). The α values for the polished (unjoined) and the microwave-joined specimens implied that the polished MgF_2 and the microwave-joined MgF_2 had a similar optical quality. The higher α for conventionally-joined MgF_2 indicated optical losses resulting from IR scattering [8,9] induced by crystallographic phases formed in and near the bond region (Figure 30).

The scattering of electromagnetic radiation depends on a number of factors, including (1) the mismatch in optical indices of refraction between the scattering center and the matrix material, and the (2) the relative size of the scattering center, compared to the wavelength of the incident radiation [9, 10]. If we let a = characteristic size of the scattering center and λ = the wavelength of the incident light, then for scattering is significant for $0.1 < \lambda/a < 10$, with a maximum in scattering at about $\lambda/a = 1$. As an example of how effectively scattering can reduce the transmitted light intensity in a ceramic, consider the scattering of visible light by pores in a ceramic [10]. At the wavelength of red light (700 nm or 0.7 micron), a 3 percent volume-fraction porosity consisting of pores with a diameter of 2 microns reduces the transmittance to about 0.01 % compared to the transmittance for a theoretically-dense material [10]. When the pores have a diameter of 0.7 micron, then 0.7 micron radiation will be reduced by a similar amount for a volume fraction porosity of only one-percent [10]. From Figure 30, we see that the characteristic dimension of the scattering centers (second phase particles) is roughly a few microns. Thus, second phases that are several micron diameter should scatter the incident radiation used in this study (a wavelength range from 880 nm to 1600 nm, or equivalently 0.88 micron to 1.6 micron), since λ/a should be very roughly in the range from about 0.1 to 0.5. However, a detailed scattering study for non-spherical particles that are not uniform in size is extremely complex

[8-10].

(Figures

3.3. Di

the silic
rpm an
a dead
of flow
minute
experim
in flow
presum
magnes
higher

MgF_2/M
a conve
atmosph
MgF_2/M
that tem
specimen
MgF_2 spe

[8-10]. Therefore, attempts to extract further information from the transmittance curves (Figures 32 and 33) will be a topic of future study.

3.3. Diamond joining on MgF_2 using sodium silicate solution

Diamond/MgF2 joining was attempted for both the sodium silicate solution and for the silica film. For the sodium silicate bonding agent, the films were spun between 3000 rpm and 5000 rpm from for 20 seconds. Then, using a heating rate of 10^{O} C per minute and a dead weight loading of 85 gm, the diamond/MgF2 specimens were heated in a atmosphere of flowing nitrogen at maximum temperatures of 500^{O}C to 800^{O}C for hold times of 20 minutes. However, the joining was not successful at any of these conditions. In separate experiments involving single-slab specimens of magnesium fluoride, it was found that even in flowing nitrogen, the specimens were discolored at temperatures above 800°C, presumably due to point defects that evolve during heating. Due to the degradation of the magnesium fluoride's optical properties, no joining attempts were made at temperatures higher than 800°C.

In addition to the sodium silicate solution, the silica film was used to attempt both MgF_2/MgF_2 bonding and the diamond film/MgF_2 bonding. The specimens were heated by a conventional furnace at maximum temperatures between 500^{O}C and 1200^{O}C in an atmosphere of flowing nitrogen. Dead weight loads ranged from 20 gm to 85 gm. The MgF_2/MgF_2 bonding occurred only at for a maximum anneal temperature of 1200^{O}C, but at that temperature (despite the flowing nitrogen atmosphere) the surface of the MgF_2 specimen was milky-colored (likely due to oxidation). The resulting transmittance of the MgF_2 specimen was severely degraded by the high-temperature reaction.

has bee

a KOH

could r

4. CO

silicate

applied

microv

the IR

absorp

specim

a consi

betwee

related

REFER

1. K.Y
Cera
Ann.
Cera

2. K.N.
Cera
Tech.

3. T.F.
Optic

Had the joining been successful, the silicon substrate (on which the diamond film has been microwave-plasma deposited) would have been etched away using a nitric acid or a KOH etching solution. The transmittance of the specimen, without the silicon substrate, could then have been measured.

4. CONCLUSIONS

The MgF_2/MgF_2 specimens were successfully joined using: (1) spun-on sodium silicate interlayers, (2) both conventional and microwave heating and (3) low externally applied pressures. The microstructure of the bonded region was quite different for the microwave and the conventionally bonded MgF_2/MgF_2 materials (Figure 30). In addition, the IR transmittance of the microwave-bonded specimens, as determined from the optical absorption factor, α, was similar in optical quality to the polished but unjoined MgF_2 specimens (Table 14). In contrast, the α for the conventionally-joined MgF_2/MgF_2 indicates a considerably degraded optical transmittance (Table 14). The difference in optical quality between the microwave-joined specimens and the conventionally-joined specimens may be related to IR scattering induced by second phases [8,9] in the bond region (Figure 30).

REFERENCES

1. K.Y. Lee and E.D. Case, "Microwave Joining and Repair of Ceramics And Ceramic Composites," *Ceramic Engineering and Science Proceedings, 21st Annual Cocoa Beach Conference and Exposition on Composites, Advanced Ceramics, Materials and Structure*, Cocoa Beach, Florida, **V18** 543-550, 1997.

2. K.N. Seiber, K.Y. Lee, and E.D. Case, "Microwave and Conventional Joining of Ceramic Composites Using Spin-On Materials," *Proceeding of the 12th Annual Technical Conference Dearborn, MI*, 941-949, 1997.

3. T.F. Yen, Y.H. Chang, D.L. Yu and F.S. Yen, "Diffusion Bonding of MgF_2 Optical Ceramics," *Material Science and Engineering*, **A147** 309-321, 1991.

4. M.L.
the A

5. I. A
Mate

6. I.W.
Jour

7. Mos
Hugh

8. P. D

9. C.F.
Part

10. W. D
2nd

4. M.L. Santella, "A review of Techniques for Joining Advanced Ceramics," *Journal of the American Ceramic Society Bulletin*, **71**[6] 947-953 (1992).

5. I. Ahmad and R. Silberglitt, "Joining Ceramics Using Microwave Energy," *Materials Research Society Proceedings*, **314**, 119-130, 1993.

6. I.W. Donald and P.W. Mcmillan, "Review Infrared Transmitting Materials," *Journal of Materials Science*, **13**, 1151-1176 (1978).

7. Moses "Refractive Index of Optical Materials in the Infrared Region"; pp7-16, Hughes Aircraft Company, Culver City, CA 1970.

8. P. Debye, H.R. Anderson, and H. Brumberger, *Journal of Apply Physics.*, **28**: 679, 1957.

9. C.F. Boren and D.R. Huffman, Chaper 3 in Absorption and Scattering Light by Small Particles, John Wiley and Sons, New York, 1983.

10. W. D. Kingery, H. K. Bowen, and D. R. Uhlmann, *Introduction to Ceramics*, 2nd Edition, pp 674-677, John Wiley & Sons, New York, NY (1976)

3.2

MI(

J. C
Ma
Mi
Ea

ABS

cera

com

give

was

by th

ceram

INTR

5]. bon

-12]. A

such as

interlaye

J. G. Lee
Comp site
571-581 (

3.2 Microwave Joining of Particulate Composites

MICROWAVE JOINING OF PARTICULATE COMPOSITES

J. G. Lee and E. D. Case
Materials Science and Mechanics
Michigan State University
East Lansing, MI 48824

ABSTRACT

Using various spin-on materials with submicron initial coating thickness, oxide ceramics have been joined using microwave heating. Four different ceramic material combinations were joined in this study, where either one or both of the materials in a given pair was a particulate ceramic composite. The microstructure of the bond region was examined using Scanning Electron Microscopy. This study builds upon earlier work by the authors and co-workers, in which a variety of non-composite polycrystalline ceramics were joined.

INTRODUCTION

Recently, there has been considerable activity in bonding ceramics with metals [1-5], bonding ceramics with other ceramics [6 - 10] and bonding ceramics with polymers [11 -12]. A number of researchers have used brazing techniques to join metals with ceramics such as silicon nitride [1], sialon [2], molybdenum disilicide [3], and aluminum nitride [4].

In addition, ceramics have been joined to ceramics using brazing, where a metallic interlayer is used to join the ceramic components. However, if ceramics are joined via

---

J. G. Lee and E. D. Case, "Microwave Joining of Particulate Composites", Advances in Ceramic Matrix Composites V, Ceramic Transactions Volume 103, American Ceramic Society, Inc., Westerville, OH, pp. 571-581 (2000)

brazing

minimu

include

(2) SiC

zirconi

comme

BACK

heating

numbe

alumin

hydrox

cerami

the int

Vicker

the int

transm

joining

cerami

previou

brazing the final bond thickness can be 40 to 50 microns thick or more [5].

In contrast, work done by the current authors and co-workers [6 - 10] has focused on minimizing the bond area thickness using spin-on interlayers. The joining work has included joining of the following particulate ceramics; (1) alumina/zirconia- 3 mol% yttria, (2) SiC platelet reinforced alumina/glass ceramic, (3) hydroxyapatite/glass ceramic, and (4) zirconia - 3 mol% yttria/glass ceramic, where the glass ceramic used was MaCor^{TM}, a commercial glass ceramic reinforced by mica platelets.

BACKGROUND

Microwave heating of ceramic materials gives efficient, volumetric, and rapid heating [13-15]. The authors and co-workers have used microwave heating to join a number of polycrystalline ceramic materials, including the following pairs: alumina with alumina, zirconia with zirconia, MaCorTM with MaCorTM, hydroxyapatite with hydroxyapatite, and magnesium fluorite with magnesium fluorite [6 - 10]. In ceramic-ceramic joining in these previous studies [6 - 10] produced high-quality joins. For example, the interfaces of the alumina-alumina joins were relatively tough, as indicated by the fact by Vickers indentation cracks placed near the joined interface did not deflect as they transited the interface [6]. For the joined IR transmitting material magnesium fluoride, the infrared transmittance was especially unchanged by the presence of the interface for microwave joining [8]. However, the joining in the earlier studies [6 - 10] was limited to like ceramics, and none of the joined ceramics were composites. This study extends the previous work to include the joining of particulate-reinforced ceramic materials.

EXPI

(a) Z

cerar

reinf

mate

parti

using

micr

cerar

were

hard

green

3YS,

in a 2

sinter

Archi

-3 mo

particu

powder

EXPERIMENTAL PROCEDURE

The ceramics joined in this study included two polycrystalline materials, namely (a) ZrO_2 -3 mol % Y_2O_3 and (b) hydroxyapatite (HAP) and three particulate-reinforced ceramic composites, including (a) Al_2O_3/ZrO_2 particulate composites, (b) a mica platelet reinforced glass ceramic (MaCor^{TM}) and (c) SiC platelet reinforced alumina. Of these materials, the ZrO_2 -3 mol % Y_2O_3, the hydroxyapatite (HAP), and the Al_2O_3/ZrO_2 particulate composites were sintered as part of this study, with all sintering being done using commercial powders. The sintering, as described below, was done either using a microwave cavity or a conventional tube furnace. The mica platelet reinforced glass ceramic (MaCor^{TM}) and SiC platelet reinforced alumina were commercial materials which were received in billet form.

Prior to the sintering that was performed as part of this study, all specimens were hard die pressed at 32 MPa in a uniaxial die, resulting in disc-shaped specimens with green dimensions of approximately 2.0 cm in diameter and 2.0 mm thick.

Seven powder compact specimens of the zirconia - 3 mol % yttria powders (TZ-3YS, Tosoh Ceramic Division, Bound Brook, New Jersey) were sintered simultaneously in a 2.45 GHz single mode microwave cavity at 1375°C for 1 hour. The densities of sintered zirconia were about 97 % of the theoretical density, as measured using Archimedes method.

For the 85 wt % alumina (TMDAR, Taimi Chemicals Co. LTD)/ 15 wt % zirconia - 3 mol % yttria powders (TZ-3YS, Tosoh Ceramic Division, Bound Brook, New Jersey) particulate composites, the powders were prepared by milling the alumina and zirconia powders together for 24 hours using alumina grinding media in a plastic ball mill to produce uniform alumina/zirconia powder mixture. The alumina/zirconia compact powders were microwave sintered at 1350°C for 1 hour using a heating rate of approximately 10°C/min.

Unlike the alumina/zirconia composites and the zirconia specimens included in this study, the calcium hydroxyapatite ($Ca_{10}(OH)_2(PO_4)_6$) powder (Cerac™ Incorporated Specialty Inorganics) was sintered in a conventional furnace at 1300°C for 11 hours. The heating and cooling rate was approximately 10°C/minute.

The as-received billets of MaCor™ (Corning Code 9658, a flurophlogopite mica platelet reinforced glass ceramic) and billets of the as-received 80 vol% Al_2O_3 / 20 vol % SiC platelet composites (Max Tech, Inc, Lansing MI) were cut using a low speed diamond saw. The final specimen dimensions were approximately 1 cm × 1 cm × 0.1 cm for the MaCor™ and about 1 cm × 1 cm × 0.5 cm for the 80 vol% Al_2O_3 / 20 vol % SiC platelet composites.

All specimens used in this study were polished using an automatic polisher at 1200 rpm with a series of diamond paste grit of size ranging from 35 µm to 1 µm. After polishing, each of the specimens were cleaned first with acetone and then cleaned again in deionized water using an ultrasonic cleaner.

After polishing and cleaning the specimens, the silica coating was applied to the specimens. An organic liquid (SilicaFilm, Emulsitone Company, Whippany, New Jersey) was utilized for the spin-on interlayer. Several drops of silica film on the specimens were deposited on the specimen surface using a pipette. The coatings were spun at 3000 rpm for 20 seconds, then coated specimens were cured in a conventional furnace at 200°C for 20 minutes. When heated, the SilicaFilm is pyrolyzed to an amorphous silica coating.

The cur
with the

For
nm thic
MaCor

For
heating
electron
used du
plate of
stabiliz
(1) to
and (2
alumin
gram t

(Accu
cm dia
allowe
was co
watts
run.

The cured silica coating is thin and uniform (Figure 35a), where the film thickness varies with the spin rate (Figure 35b).

For the coated materials in this study, the cured silica coating was about 100 to 200 nm thick. Figure 35 a is a SEM micrograph of a 130 nm thick silica coating on one of the MaCorTM specimens used in this study.

For all of the joining work included in this paper, the specimens were joined by heating in a 2.45 GHz single-mode microwave resonant cavity using the TM_{111} electromagnetic mode. A cylindrical zirconia refractory specimens enclosure (casket) was used during joining (Figure 36a). The refractory casket consisted of a top and bottom plate of an aluminosilicate fiber board (SALI, Zircoa) and a hollow yttria-partially stabilized zirconia cylinder (ZYC, Zircoa). The refractory casket serves two purposes: (1) to serve as a microwave susceptor to aid in heating the specimens at low temperatures and (2) to provide thermal insulation. Within the casket, the specimens were placed on a aluminosilicate setter (Figure 36b) and alumina dead weights of mass ranging between 20 gram to 50 gram were used to apply a normal load during joining (Figure 36b).

The specimen temperature was measured via an optical pyrometer system (Accufiber Optical Fiber Thermometer, Model 10, Luxtron Co., Beaverton, OR). A 0.5 cm diameter circular hole in the zirconia-cylinder section of the casket (Figure 36b) allowed the optical pyrometer to be sighted on the specimen. The joining temperature was controlled by input power where the maximum input power ranged from about 400 watts to 900 watts. The heating rate was approximately 40°C/min for each experimental run.

After joining, the joined specimens were sectioned using a low speed diamond

Figure 3
function

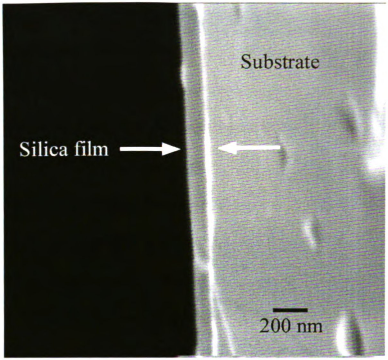

(a)

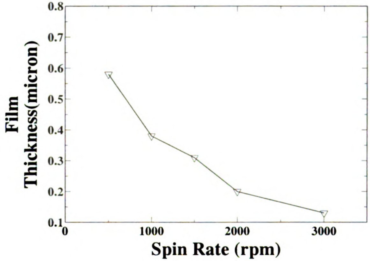

(b)

Figure 35. (a) SEM micrograph of a cured silica film on a MaCor™ substrate, (b) as a function of spin rate for cured silica coatings on MaCor™ [after 6]

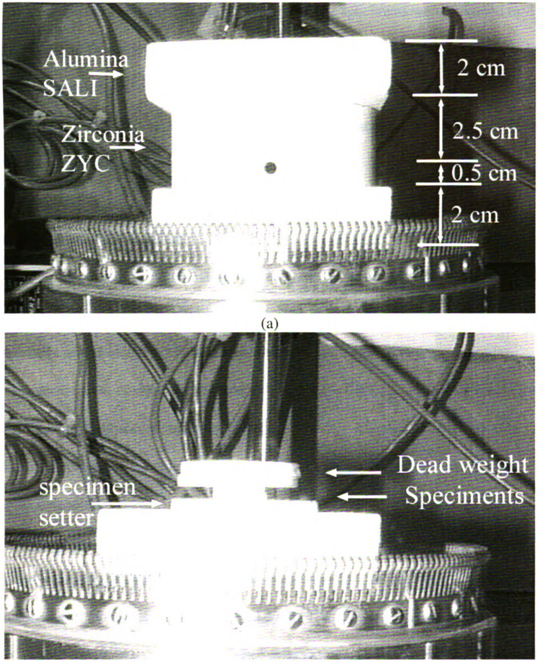

(a)

(b)

Figure 36. (a) Photograph of the zirconia/aluminosilicate refractory casket during specimen joining, (b) Photograph of the bottom SALI plate of the refractory casket with the specimen, specimen setter and dead weights in place.

s

c

s

o

el

R

wa

suc

zirc

(4)

com

rem

micr

dead

top o

if a b

pores

20 mir

alumin

saw to allow SEM observation of the bond region. The specimens were mounted in dially pthlate and then polished with a series of diamond grit. The surfaces were made sufficiently conductive for SEM examination by sputtering a 7 nm thick coating of gold onto the specimen surfaces. In conjunction with the SEM analysis, x-ray line scans and elemental mapping was performed.

RESULTS AND DISCUSSION

For the pairs of ceramic materials joined, either one or both of the materials joined was a particulate reinforced ceramic material. The ceramic materials that were successfully joined include: (1) alumina-zirconia composites joined with alumina-zirconia composites, (2) MaCor™ joined with ZrO_2, (3) HAP joined with MaCor™, and (4) SiC platelet reinforced alumina with MaCor™. Of these materials, the particulate composites include the alumina-zirconia composites, MaCor™, and the SiC platelet reinforced alumina.

The alumina/zirconia particulate composite specimens were joined using microwave heating at 1400°C, 1450°C, and 1500°C for 20 minutes. During joining, a deadweight of approximately 50 grams was applied via sintered alumina disks placed on top of the specimen. As viewed in the SEM micrographs, no bond phase is apparent, and if a bond phase exists, it must be less and one μm thick (Figure 37). Quasi-elliptical pores are occasionally observed at the interface (Figure 37).

MaCor™ was joined with zirconia - 3 mol % yttria upon heating at 1020°C for 20 minutes using a 20 gram deadweight loading. In contrast to the specimens of alumina/zirconia composite joined with alumina/zirconia composite (Figure 37), a bond layer

of 0.

inter

H

using

com

phas

plate

max

1050

those

Lans

dead

attem

since t

observ

the orig

bond la

alumina

combina

process.

layer is visible at the MaCor^{TM} /zirconia interface, where the bond region is on the order of 0.5 - 1 micron thick (Figure 38). Numerous micron-scale pores were visible along the interface region between the MaCor^{TM} /zirconia interface.

Hydroxyapatite was successfully joined with MaCor^{TM} at 1020°C for 10 minutes using a 20 gram deadweight (Figure 39). As was the case with the alumina/zirconia composites specimens joined with alumina/zirconia composites (Figure 37), a bond phase at the interface was not apparent in the SEM (Figure 39). In Figure 39, the mica platelet reinforcement in the MaCor^{TM} is evident to the right of the indicated interface.

MaCorTM has a relatively low use temperature material, with a vendor-specified maximum use temperature of 1000°C. The attempted joining of HAP with MaCor^{TM} at 1050°C and 1070°C using a 50 gram deadweight failed since the MaCor^{TM} melted under those conditions, when in contact with the HAP.

Polycrystalline alumina reinforced with 20 vol% SiC platelets (Max Tech Inc., Lansing, MI) was joined with MaCor^{TM} by heating at 1020°C for 20 minutes using a deadweight loading of about 20 grams. As was the case with joining HAP with MaCor^{TM}, attempts at joining the alumina/SiC platelet composite with MaCor^{TM} at 1050°C failed since the MaCor^{TM} partially melted. After joining, a 10 micron-thick bond layer was observed at MaCor^{TM}-alumina/SiC platelet interfaces (Figure 40). Since the thickness of the original silica coating layer (before joining) was roughly 130 nm, the 10 micron thick bond layer thickness likely represents a reaction zone between the SiC platelet reinforced alumina and the MaCor^{TM}. Thus, only one of the four ceramic/ceramic material combinations included in this study formed a significant reaction zone during the joining process.

Figur

minu

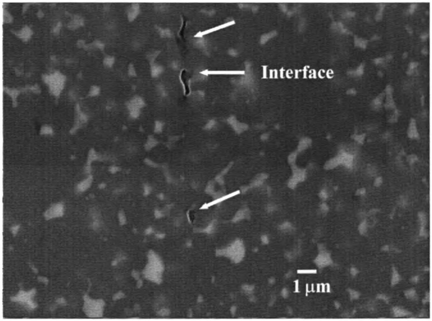

Figure 37. SEM micrographs of alumina/zirconia composites joined at 1450°C for 20 minutes showing interface.

Figu
192

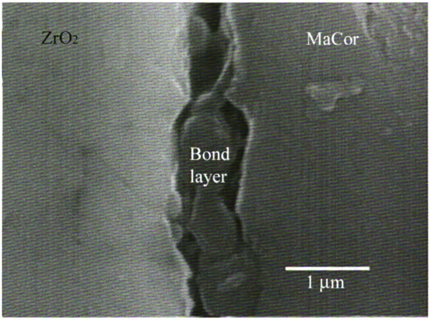

Figure 38. SEM micrographs of zirconia (3 mol % Y_2O_3) with MaCor™ joined at 1020°C for 20 minutes showing interface.

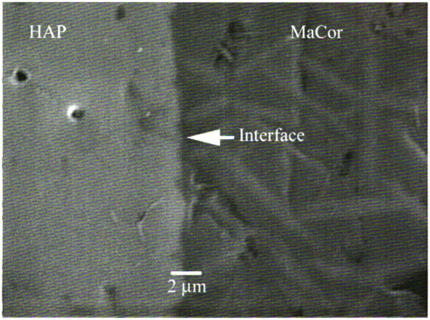

Figure 39. SEM micrograph of HAP with MaCor™ joined at 1020°C for 10 minutes. The mica platelet rainforcement in the MaCor™ is evident in the micrograph.

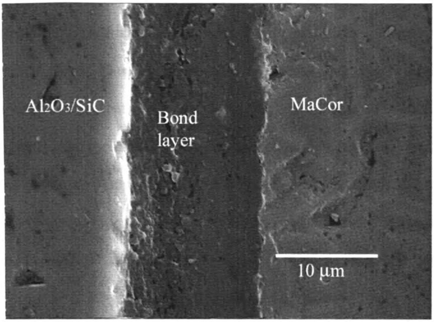

Figure 40. SEM micrograph of SiC platelet reinforced alumina with MaCor^{TM} joined at 1020°C for 10 minutes.

re

H

in

th

in

se

m

pro

the

sho

enh

the p

CON

Partic

glass

hydro

interfa

specim

joined s

hydroxy

X-ray line profiling of the composition of the bond region and the near-bond region was performed for each of the four ceramic material pairs joined in this study. However, for each of the joins (except the MaCor™-alumina/SiC platelet joined interface, Figure 40) no "bond layer" could be identified, which was to be expected since the radius of the interaction volume [16] is typically large enough that the compositional information from the x-ray line profile is averaged over subsurface volumes that are several microns in radius. Thus the composition differences on the size scale of the sub-micron bond region (if present) would be impossible to detect with the x-ray line profiling. However, the preliminary x-ray line scan measurements of the bond region in the specimens consisting of alumina/SiC platelet composite joined with MaCor™ did show evidence of the reaction zone (for example, the concentration of aluminum ions was enhanced near the MaCorTM/reaction zone interface). Also, an elemental map indicated the possible presence of Mg and K rich precipitates in the reaction zone.

CONCLUSIONS

In this study, we joined the following particulate ceramics: (1) alumina/zirconia particulate composites with alumina/zirconia composites (2) a mica platelet reinforced glass ceramic (MaCor™) with zirconia -3mol % yttria, (3) MaCor™ with polycrystalline hydroxyapatite and (4) SiC platelet reinforced alumina with MaCor™. Except for the interface was relatively free of porosity. For the alumina/zirconia particulate composites specimens in which the alumina/SiC platelet was bonded to MaCor™, the region near the joined with alumina/zirconia composites and the MaCor™ joined with polycrystalline hydroxyapatite, no bond layer was apparent on the SEM micrographs.

re

be

th

pr

th

AC

St

En

ele

RE

1.

2.

3.

4.

5. I

C

(

6. K

C

A

In future work, Vickers indentation will be used to aid in estimating the nature of the residual stresses near the join. In addition, Transmission Electron Microscopy (TEM) will be performed in order to further analyze the interface region of the joined specimens. For the reaction layer alumina/SiC platelet composite - MaCor^{TM} specimens, additional x-ray profiling of the bond layer compositions will be performed in order to better characterize the nature of the interface regions.

ACKNOWLEDGMENTS

The authors acknowledge the financial support of the Composite Materials and Structures Center and the Electronic Surface and Properties of Materials Center, College of Engineering, Michigan State University. The authors also acknowledge the use of the electron microscopy facilities at Michigan State University's Center for Electron Optics.

REFERENCES

1. G. Chaumat, B. Drevet, and L. Vernier, "Reactive brazing study of silicon nitride to a metal joining", J. European Ceram. Society, 17[15-16]: 1925 - 1927 (1997).

2. A. P. Xian, "Joining of sialon ceramics by Sn-5 at% Ti based ternary active soders", J. Materials Science, 32[23]: 6387 - 6393 (1997).

3. S. D. Conzonne, D. P. Butt, A. H. Bartlett, "Joining of $MoSi_2$ to 316L stainless steel", J. Mater. Sci, 32[13]: 3369-3374 (1997).

4. D. Huh and D. H. Kim, "Joining AlN to Cu using In-base active brazing fillers", J. Materials Res., 12[4]: 1048 - 1055 (1997).

5. L. Esposito, A. Bellosi, S. Guicciardi, G. de Portu, "Solid state bonding of Al_2O_3 with Cu, Ni, and Fe: characteristics and properties", J. Mater. Sci., 33[7]: 1827 - 1836 (1998).
6. K. N. Seiber, K. Y. Lee, and E. D. Case, "Microwave and Conventional Joining of Ceramics using Spin-on Materials," pp. 941-949 in Proceedings of the 12th Annual Advanced Composites Conference, Technomic Publishing Co., Lancaster, PA (1997).

7. E. D. Case, K. Y. Lee, and J. G. Lee, "Joining of Polycrystalline Ceramics and Ceramic Composites Using Microwave Heating," pp. 17 - 20 in Proceedings of the 33rd International Microwave Power Symposium, International Power Institute, Manassas, VA (1998).

8. E. D. Case, J. G. Lee, and K. Y. Lee, "Joining of Optical and Infrared Materials Using Spin-On Layers", pp. 17 - 26 in Joining of Advanced and Specialty Materials, M. Singh, J. E. Indacochea, and D. Hauser, eds., ASM International, Materials Park, OH (1998).

9. E. D. Case, K. Y. Lee, J. G. Lee, and T. Hoepfner, "Geometrical Stability of Holes and Channels During Joining of Ceramics and Ceramic Composites," pp. 27 - 34 in Joining of Advanced and Specialty Materials, M. Singh, J. E. Indacochea, and D. Hauser, eds., ASM International, Materials Park, OH (1998).

10. J. G. Lee, K. Y. Lee and E. D. Case, "Joining of Diamond Thin Films to Optical and IR Materials," pp. 509 - 520 in Ceramic Transactions, Volume 94, American Ceramic Society, Inc., Westerville, OH (1998).

11. C. Mukherjee, E. D. Case and A. Y. Lee, "Thin, Protective Silica Layers on Polymeric Materials", Accepted for publication, Ceramic Eng. and Sci. Proc., Volume 20 (1999).

12. C. Mukherjee, E. D. Case, K. Y. Lee, and A. Lee, "Silica Coatings on BMI Polymeric Substrates," submitted, Journal of Materials Science.

13. K. Y. Lee and E. D. Case, "Steady-State Temperature of Microwave-Heated Refractories as a Function of Microwave Power and Refractory Geometry," Accepted for publication, Materials Science and Engineering.

14. K. Y. Lee and E. D. Case, "Microwave Sintering of Alumina Matrix Zirconia Composites Using a Single-Mode Microwave Cavity," J. Mater. Sci. Lett., 201-203 (1999).

15. K. Y. Lee, P. H. Dearhouse, and E. D. Case, "Microwave Sintering of Alumina Using Four Different Single-Cavity Modes," Journal of Materials Synthesis and Processing, 7[3] Page numbers not yet determined (1999).

16. P. J. Grundy and G. A. Jones, pp. 26 - 36 in Electron Microscopy in the Study of Materials, Crane Russak, Publishers, New York, NY (1976).

3.3 Geometrical Stability of Holes and Channels During Joining of Ceramics and Ceramic Composites

Geometrical Stability of Holes and Channels During Joining of Ceramics and Ceramic Composites

E. D. Case, K. Y. Lee, J. G. Lee, and T. Hoepfner

Materials Science and Mechanics Department,

Michigan State University

East Lansing, MI 48824

Abstract

An ultrasonic mill has been used to machine precise channels and holes in ceramic components that are subsequently joined via microwave heating. Microscopic inspection of the channels then indicates the stability of the channels during the microwave joining process. The information gained from joining such specimens can be crucial in the development of techniques for joining ceramics with complex geometries, including channels for fluid flow in intricate components that are joined from simpler ceramic subcomponents.

E. D. Case, K. Y. Lee, J. G. Lee, and T. Hoepfner, "Geometrical Stability of Holes and Channels During Joining of Ceramics and Ceramic Composites," Joining of Advanced and Specialty Materials, M. Singh, J. E. Indacochea, and D. Hauser, eds., ASM International, Materials Park, OH. pp. 27 – 34 (1998)

Introduction

This paper deals with joining densified ceramic bodies that include channels or holes cut into one or more of the subcomponents. The need for such a technique is related to the nature of ceramic processing, which often involves (1) a difficulty in processing components of complex geometry and (2) the considerable shrinkage that is typical during densification.

This paper discusses and compares work done by Case and co-workers on joining polycrystalline alumina and MaCor^{TM} [1, 2] with more recent work in joining polycrystalline zirconia and hydroxyapatite.

Background

Ceramic Processing: Difficulty in Forming Complex Shapes

Ceramic components are typically processed using a powder processing technique, that is, ceramic powders are formed into a shape, then the powders are densified at temperatures corresponding to homologous temperatures, T_H, of 0.6 or greater. T_H may be defined as the ratio $T_{AMBIENT}/T_{MP}$, where the ambient temperature, $T_{AMBIENT}$, and the melting point temperature, $T_{MP.}$ are both expressed in units of degrees Kelvin. In some processing methods, the shape forming and densification steps are combined (such as in hot-pressing or hot-isostatic pressing), but typically the shape-forming and densification steps are performed in sequential fashion [3].

The shape-forming techniques often used in industry often involve either a pressing operation or slip casting. Pressing powders in a die usually required that the processed shaped be relatively simple disk or plates [3]. Rods of constant cross-section may be extruded from a die [3]. Slip casting allows a greater range of geometry, but still the shapes produced are limited and the introduction of precise channels or holes within the part is problematic.

Components With Complex Geometry: Fabricated From Ceramic "tapes"

A technique that does offer more flexibility in terms of component geometry is that of building-up a complex shape for tape-casting ribbons. The unfired tape-cast materials are typically quite thin (on the order of one millimeter or less in thickness), and when cast with a high fraction of a plastic binder phase, the unfired tape-cast elements can be cut and compacted into a shape of relatively complex outer geometry.

Organic binders are widely used in the ceramics industry. Organic binders, typically at the level of several volume percent, are added to increase the green (unfired strength) of a variety of components pressed from ceramic powders [3]. In the electronics industry, large volumes of organic binders and solvents are added to ceramic powders resulting in "tapes" that are flexible in the green state. Cutting and hole punching operations then are relatively straightforward in the flexible tapes, enabling the fabrication of multilayer ceramic capacitors and piezoelectrics. In addition, 50 volume percent or more of binder and lubricants are added to ceramic powders for injection molding of ceramic components.

Difficulties with binder burnout in ceramic tapes.

The benefits of adding organic binders to ceramic powders are at least partially offset by several disadvantages. The problems inherent to having a large volume fraction of binder in a ceramic compact focus on binder burnout, where the burnout process (1) can be very time consuming, (2) binder burnout can leave chemical residues that lead to flaws and defects in the final sintered ceramic, and (3) the high shrinkage associated with binder burnout can lead to mechanical stresses that cause cracking.

When the volume fraction of the binder phase is high and/or the ceramic components are thick (such as is the case for electronic components from multilayers of binder-laden ceramics) then the time required for binder burnout can be very long. For example, in multilayer ceramic piezoelectrics which may consist of 150 layers or more of ceramic "tape" [4] or mutilayer ceramic capacitors [5], delaminations (cracks) between the layers can occur at extremely low heating rates. Heating rates on the order of 0.015°C per minute, corresponding to a total binder burnout time of 250 hours (approximately 1.5 weeks) may still be rapid enough to induce delamination between layers of a multilayer ceramic piezoelectric component [4]. Binder burnout treatments can require up to several days for injection-molded ceramic components [6].

In addition to the long times required for burnout of multi-layered, binder-laden ceramic powders, binders also can leave a carbon or sulfur residue [7, 8], which has been shown to persist even after elevated (1500°C) heat treatments. Many researchers have linked binder residues with defects in the final, sintered ceramic bodies [9-11].

The high shrinkage inherent to the binder burnout process induces mechanical stresses which in turn can lead to flaws and cracking in the processed ceramics [12, 13]. It is worth noting that densification for a ceramic compact containing binders is essentially a two step process in which (1) the binder is first removed from the compact and (2) the densification of the ceramic powders themselves takes place. That is, after binder burnout is complete, the sintered powders must still densify. At the point that the binder is removed (typically at temperatures of a few hundred degrees Celsius), the remaining ceramic powders have a volume fraction porosity of roughly 50 percent. During densification of the ceramic powders, the component thus must undergo considerable addition shrinkage upon sintering.

When the fraction of binder is high enough to allow the green (unfired) tape cast material to plastically deform and therefore form a complex part by building it up layer by layer, then binder burnout can be a problem. As discussed above, the binder burnout problems can include: (1) the binder burnout step can be very lengthy for parts composed of many layers, (2) chemical residues from binder burnout can lead to defects in the final sintered part, and (3) cracks can form in the part as a result of the very high shrinkages that are inherent to the binder burnout process. Thus, the plasticity afforded to green (unfired) ceramics by virtue of their high binder concentrations can come at with a high cost in terms of processing difficulties. In addition, the act of compacting layer upon layer to build up the component from tape cast materials might deform precise channels or holes within the ceramic body, if such channels or holes were desired.

One alternative way to fabricate ceramics of complex geometric shape is to joined simpler subcomponents of densified ceramics, in order to more the final component. This can have benefits in terms of quality control (the detection of flaws) and in terms of allowing one to include precisely machined channels and holes into the ceramic component.

Ceramic/Ceramic Joining

The joining of ceramic materials can help circumvent some of the difficulties associated with processing components of complex geometry. The fabrication of complex parts can be accomplished by the joining of simpler subcomponents. In addition to avoiding the difficulties associated with the burnout of large volume fractions of a binder phase, a potential benefit of joining simple ceramic subcomponents is that the detection of flaws in simple subcomponents is easier than the detection of flawed components of complex shape. Thus, if a flaw is discovered in a subcomponent, it may be discarded before it is included in the final part.

Often, joining is performed with the assistance of a flux that is placed between the ceramic pieces that are to be joined. Different joining techniques are distinguished in part by the (1) magnitude of the externally applied pressure and (2) the joining temperatures used. Diffusion bonding, for example, uses very high stresses and temperatures to join ceramics, such that the joining is accomplished under conditions conducive to creep in that material [14, 15]. In this paper, we use relatively low externally applied loads to join a variety of specimens, but in each instance we use a spin-on interlayer to assist in joining.

Experimental Procedure

Materials Used

The materials joined in this study include polycrystalline alumina, hydroxyapatite, zirconia, and a mica-platelet reinforced glass ceramic. The alumina, hydroxyapatite, and the zirconia were sintered from commercial powders, while the glass ceramic was a commercial material, MaCor^{TM} (Corning Code 9658).

The alumina specimens were microwave-sintered from Sumotomo AKP 50 powders using a single-mode microwave cavity, described in the next section. The

AKP50 powders have a vendor-specified initial particle size of 0.23 microns and a purity of 99.95 percent. Alumina is used in a wide variety of electronic and structural applications of ceramics, due to its high hardness, good resistance to chemical attack, and low electrical resistivity.

The calcium hydroxyapatite powder (HAP) used in this study (Cerac Inc., Specialty Inorganics, Milwaukee, WI, Item #C-2071-1, Lot#X16907) had a nominal purity (as reported by Cerac) of "typically 99% pure". Calcium hydroxyapatite is an "bioactive" ceramic material, such that when exposed to blood or to a simulated biological fluid (SBF), HAP promotes the formation of bone on its surfaces [16]. HAP coatings have been used to coat biological implant materials. The HAP coatings can act to reduce corrosion of the metallic substrate materials, since the corrosion can lead to the release of toxic ions into the body [16, 17].

The MaCor™ specimens were cut from as-received billets of the material. Macor is a machineable glass ceramic material of the composition SiO_2-$Al2O_3$-MgO-K_2O-F. The machinability of the material stems from the flurophogopite mica platelets that are randomly dispersed in the material. Macor is used in a variety of electronic substrate applications, due to its good dielectric properties and its ability to be precisely machined by metal-working tools.

The zirconia specimens were formed from 3-mol percent yttria partially-stabilized zirconia powders (TZ-3Y Grade zirconia powders, Tosoh Ceramics Division, Bound Brook, New Jersey) with a vendor-specified specific surface area of approximately 16 m^2/gram. The standard vendor chemical assay shows that the major impurities in the zirconia powders are alumina, silica, iron oxide, and soda, with weight percentages of less than 0.1, 0.02, 0.01, and 0.04, respectively. The initial particle size is roughly in the 0.1 micron range. Zirconia is used in a wide variety of ceramic applications, including as grinding media, high-temperature insulation, and in electronic components.

Two materials were used as bonding agents in this study. "Silicafilm" (Emulsitone Company, Whippany, New Jersey) is an organically-based silicate, which upon heating at relatively low temperatures (say, 200^{O}C) yields an amorphous silica film. The second bonding agent used was a sodium silicate solution

Specimen Preparation

Microwave and Conventional Sintering of the Specimens

The alumina, hydroxyapatite, and zirconia powders were each dry pressed in a uniaxial, double-acting die at approximately 32 MPa. For the alumina, the nominal mass of each specimen was about 2 grams, with an as-pressed diameter of about 2 cm and an as-pressed thickness of about 2 mm. The alumina and zirconia specimens were then sintered in a single-mode microwave cavity (described below) while the HAP specimens were sintered in a conventional, radiant energy furnace (also described below).

The HAP specimens were fired at maximum 1300^{0}C for 30-60 minutes in a conventional tube furnace (MRL Thermtec, with an Eurotherm Controller and SiC heating elements), at a ramp rate of 10C/ minute. For the alumina and zirconia, the maximum temperatures ranged from about 1500 to 1600^{O}C for the alumina, while the zirconia and the HAP powders were sintered at about 1450 and 1300^{O}C, respectively. For both the microwave sintering and the microwave joining, the temperature was measured by an optical pyrometer (Accufiber Optical Fiber Thermometer, Model 10, Luxtron Co., Beaverton, OR).

Cutting and coating the specimens

The as-received Macor^{TM} billets were approximately 7.8 cm X 7.8 cm X 0.18 cm. These billets were cut into 1 cm X 1 cm X 0.18 cm specimens using a low-speed diamond saw. Following sintering, the sintered HAP specimens were sectioned by a low-speed diamond saw into 12-15 mm square billets which were about 3-5 mm thick. The alumina and zirconia specimens were disk-shaped in the as-sintered form, and were not sectioned prior to coating, notching, and joining.

The microstructures of the as-sintered specimens of alumina, zirconia, and the hydroxyapatite were characterized by Scanning Electron Microscope (SEM) micrographs of fracture surfaces (Figure 41). The fracture surfaces of the alumina and zirconia show relatively equiaxed grains with low porosity (Figure 41). However, the HAP material has a volume fraction porosity of about 0.10 and exhibits considerable transgranular failure on the fracture surface.(Figure 41) In addition, the fracture section of the MaCorTM material clearly shows the randomly oriented mica phase (Figure 41).

All specimens were polished prior to joining using an automated polishing machine (Leco Corporation, St. Joseph, MI). Prior to beginning the polishing procedure, the edges of the specimens were slightly beveled to reduce wear on the polishing cloth. After beveling, three or more specimens were simultaneously mounted onto an aluminum disk, using a thermal plastic to hold the specimens in place. Polishing was done using a series of diamond grit ranging from 25 microns to 1 micron.

After polishing the specimens were coated with one of the bonding agents described above. A few drops of the coating was applied to the specimen using a pipette, and then the specimen was spun on a substrate spinnner to distribute the coating material over the surface of the material to be joined. The spinning rates varied from about 500 to 5000 rpm. After spinning, the Silicafilm coatings were cured in air, in a conventional furnace, using curing temperatures of $200^{O}C$ and curing times of 20 minutes. For the PCS and the sodium silicate bonding agents, the film was not cured prior to bonding.

Notching the Specimens

Following the polishing, coating, (and in some cases, curing) steps, the specimens were then notched using a ultrasonic vibratory mill (Sonic Mill. Albuquerque, NM). The principal of operation of the vibratory mill is that a tool is mechanically vibrated at ultrasonic frequencies (say between about 1 - 10 kHz), and the vibrating tool in turn causes vibration in a boron nitride slurry which is placed at the tip of the tool. The cutting is then accomplished by the boron nitride itself, rather than the tool. The cutting tool used for many of the notches was a single-edge razor blade that had been mounted via silver soder on a "stub" supplied by the vendor (Sonic Mill) that allows one to fabricate cutting tools of a variety of shapes. In addition to the "razor-blade tool", some wider notches were placed in polycrystalline alumina specimens using a tool made from a cold-rolled steel piece which also had been attached by silver soder to a stub. (The razor blade tool was capable of cutting notches of widths ranging from roughly 200 to 330 microns, while notches cut using the cold-rolled steel tool were on the order of 900 microns across).

Following the notching procedure using the sonic mill, a 3 to 5 mm section of each specimen was cut from the notched end of the specimen using a low-speed diamond saw (Figure 42). The section of the notched specimen was used as the reference for the dimensions of the notch prior to the joining procedure. Both the notched specimen and the reference piece were examined in the SEM to determine the geometrical stability of the notch during joining.

Microwave and Conventional Processing

A 2000 Watt, 2.45 GHz power supply (Sairem, Model MWPS 2000, Wavemat Inc., Plymouth, MI) was used to heat a 17.78 cm diameter cylindrical single-mode cavity (CMPR-250, Wavemat Inc., Plymouth, MI, Figure 43) [18, 19]. As the specimen's temperature increased, the dielectric constants (both the real and the imaginary parts) of the heated ceramics changed, and thus the microwave system was tuned continuously to re-establish the resonant condition in the cavity. Cavity tuning entailed separate but coordinated movements of the cavity short position and the launch probe position via stepper motors that were interfaced with a computer [18, 19]. The specimens were joined using a TM111 cavity mode, with an initial input power of 100 Watts. The power was incremented by 50 Watts approximately every three minutes until the processing temperature was reached.

During joining, the specimens were placed in an refractory enclosure (called a "casket"). The casket (Figure 44) consisted of a hollow zirconia cylinder (ZYC, Zircar, Inc.) and two disc-shaped end caps made of an aluminosilicate refractory board (SALI, Zircar, Inc.) Before the specimens were loaded into the zirconia casket, from zero to 60 grams of dead weight were placed on the specimens. (The dead weights consisted of disc of microwave-sintered Sumitomo alumina, which each weighed about 20 grams and were about 4.1 cm in diameter and 4 mm thick.). The specimens were loaded into the casket near its cylinder axis, and the casket was in turn centered along the cylinder axis of the microwave cavity.

The conventionally joined specimens were joined in one of two radiant-heat furnaces. The MaCor™ specimens were joined in an electrical box-type furnace (CM, Inc.) which employed MoSi2 heating elements. The specimens were placed on an alumina setter, and an alumina crucible was inverted and placed over the specimen.

Results

The alumina and the MaCor™ were joined well using the silica spin-on layer, and notches cut into the specimens were quite stable during the joining process. Micrographs of the specimens obtained via the Scanning Electron Microscope (SEM) indicated that the width and depth of the channels machined into the alumina and MaCoR™ The alumina and the MaCor™ were joined well using the silica spin-on layer, and notches cut into the specimens were quite stable during the joining process. For notches widths in the range of about 200 to 330 microns, and for large notches about 900 microns in width, the "after joining dimensions" were within about 2 to 5 percent of the "before joining" dimensions.

For the zirconia specimens, the geometrical stability of the notches has not yet been quantified, since the zirconia specimens (microwave sintered from 3 mol% Tosoh TZ-3Y Grade zirconia powders), however the authors believe that using 8 mol% zirconia powders and/or a different bond phase might assist in the joining of the zirconia. While the polycrystalline HAP ceramics did not join using the silica spin-on interlayers, the HAP did join when the sodium silicate was used.

The zirconia specimens did not join well at 1450^{O}C using microwave heating of the spin-on silica film, thus the stability of the notches can not be assessed that this time. Although the zirconia specimens were joined , the specimens broke apart upon cutting.

Using the silica spin-on interlayers, the polycrystalline HAP ceramics did not join using either microwave or conventional heating at 1200^{O}C. After the joining attempt using the silica solution and both heating modes (conventional and microwave) the HAP specimens showed no indication of bonding whatsoever. However, when the sodium silicate solution was used as the bonding agent in place of the silica film, the HAP did bond at 1250^{O}C in air in the microwave cavity (Figure 45). The silica spin-on interlayers, the HAP did join when the sodium silicate was used. For the notch shown in Figure 45, for example, the notch width and depth before joining was about 166 microns and 322 microns, receptively. After joining, the width and depth was 169 and 319 microns, respectively. Thus, the joining process induced only a about a two-percent change in width and a one-percent change in depth, compared to the "before-joining state. Additional notches in the joined HAP showed similar results, with changes in individual notch dimensions uniformly within about 4-percent or less.

Summary and Conclusions

The alumina and the MaCor^{TM} were joined well using the silica spin-on layer, and notches cut into the specimens were quite stable during the joining process. For the zirconia specimens, the geometrical stability of the notches has not yet been quantified, since the zirconia specimens (microwave sintered from 3 mol% Tosoh TZ-3Y Grade zirconia powders), however the authors believe that using 8 mol% zirconia powders and/or a different bond phase might assist in the joining of the zirconia. While the polycrystalline HAP ceramics did not join using the silica spin-on interlayers, the HAP did join when the sodium silicate was used. In addition, the stability of the notches during the HAP was excellent, as was seen for alumina and MaCor^{TM} specimens also. These results mean that precise channels can be cut into polycrystalline ceramics, and the dimensions of the channels can be maintained very well during joining.

Acknowledgments

The authors acknowledge the financial support of the Michigan Research Excellence Fund provided through the Electronic and Surface Properties of Materials Center, Michigan State University and by the Composite Structures and Materials Center. The authors also acknowledge the use of the Scanning Electron Microscope facilities at the Center for Electron Optics, Michigan State University.

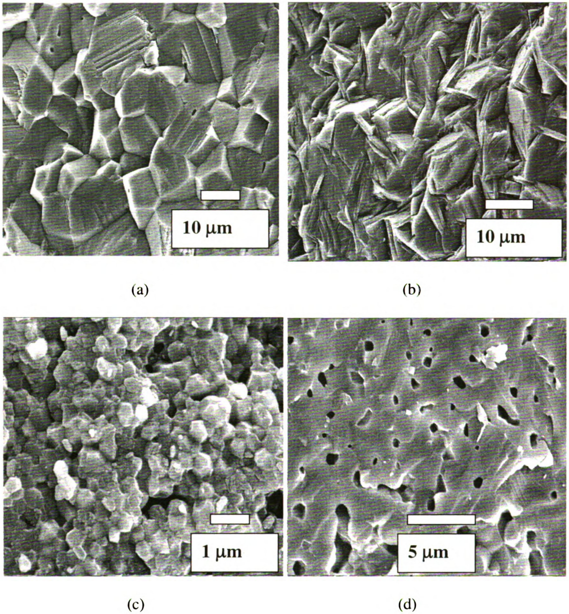

(a) (b)

(c) (d)

Figure 41. SEM micrographs of the fracture surfaces for the four materials included in this study, namely (a) alumina, (b) MaCor™, (c) zirconia, and (d) hydroxyapatite.

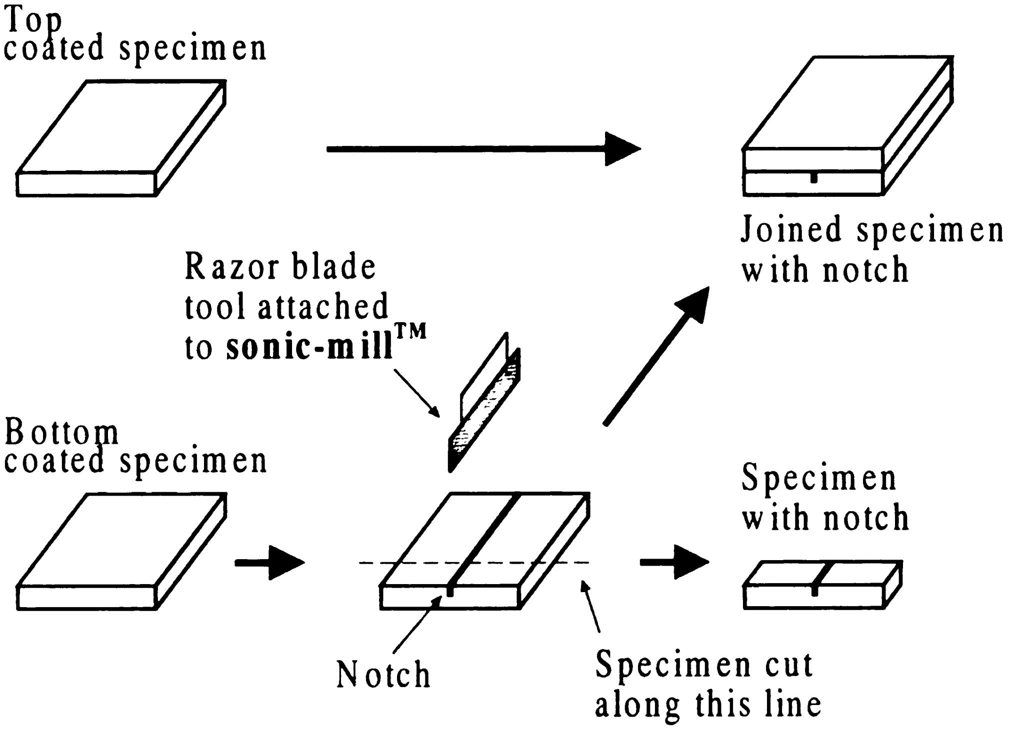

Figure 42. Procedure for sectioning the reference specimen for notch geometry in the "pre-joined" state (after [1]).

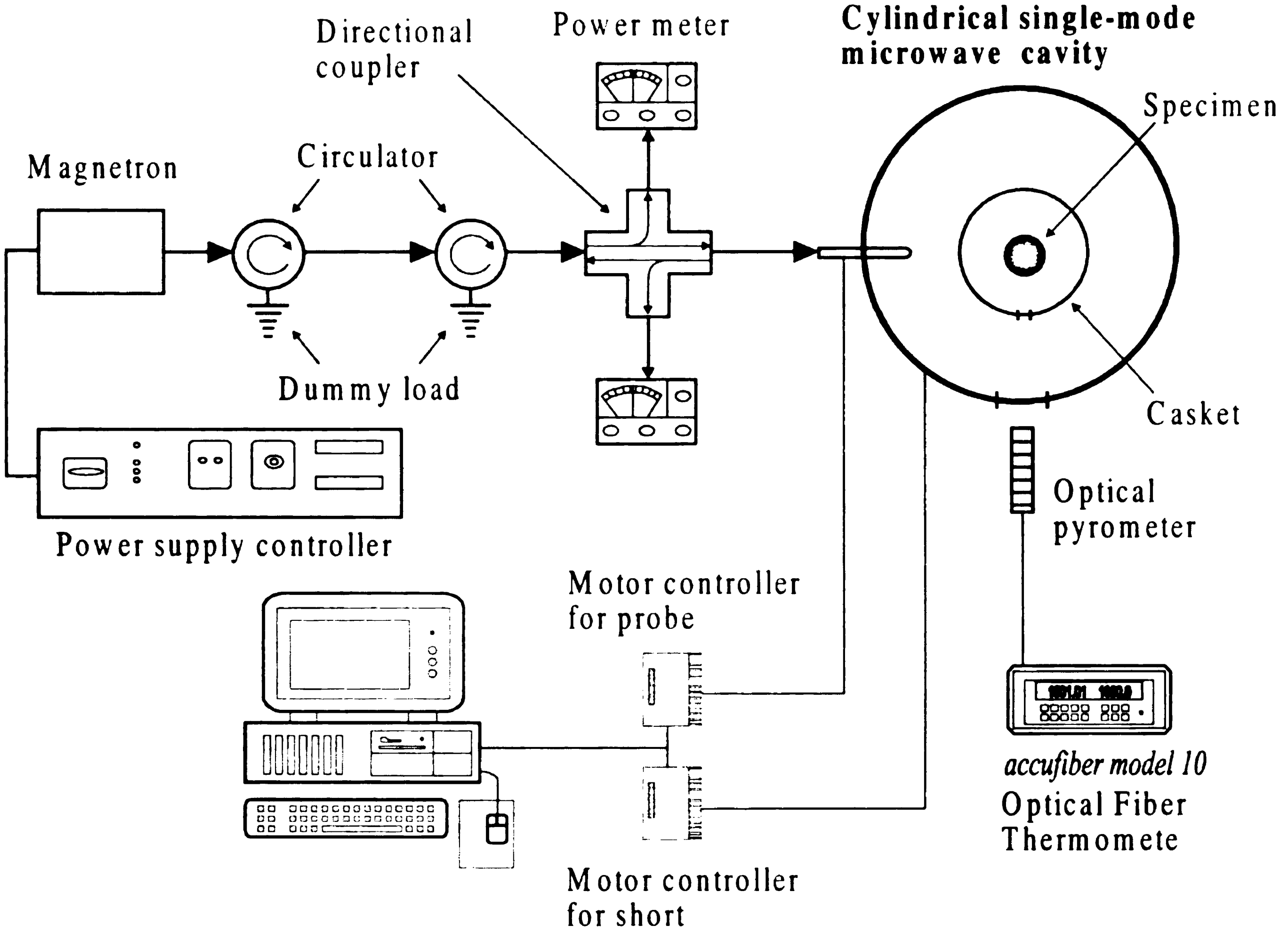

Figure 43. Schematic of the microwave processing system, showing the microwave cavity and the power supply (after [20]).

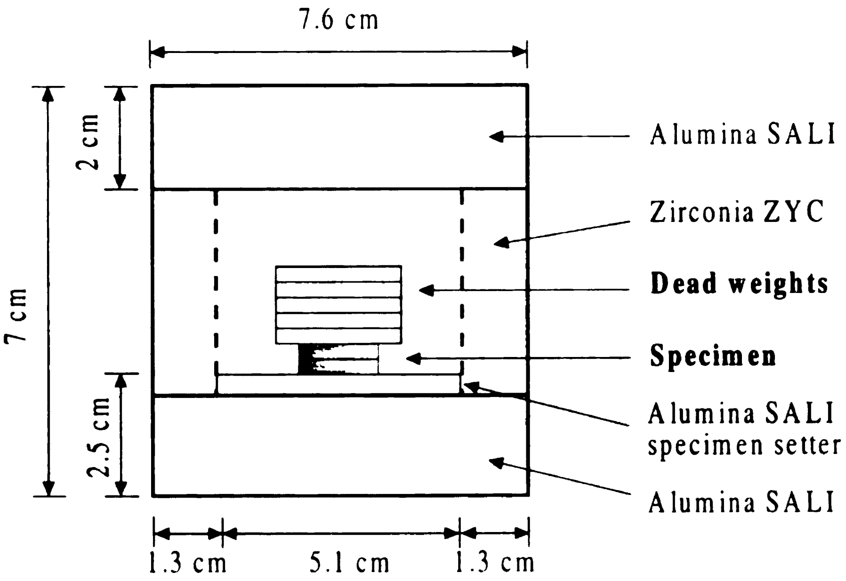

Figure 44. Schematic of the refractory casket used during joining (after [1]).

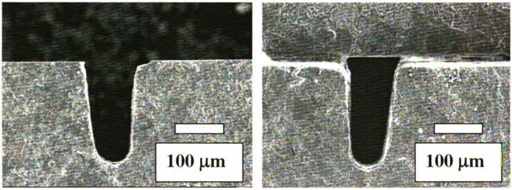

(a) (b)

Figure 45. Microstructures of the joint regions of the joined HAP specimens.

References

1. K. N. Seiber, K. Y. Lee, E. D. Case, pp. 941-949 in Proceedings of the 12th Annual Advanced Composites Conference, Technomic Publishing Co., Lancaster, PA (1997)

2. K. Y. Lee, E. D. Case, and D. Reinhard, Ceramic Eng. and Sci. Proc., 18: 543-550 (1997)

3. D. W. Richerson, *Modern Ceramic Engineering*, 2nd edition, p. 496-497, Marcel Dekker, Inc., New York (1992)

4. M. Kahn and M. Chase, J. Am. Ceram. Soc., 75[3]: 649-656 (1992)

5. S. Masia, P. D. Calvert, W. E. Rhine, and H. K. Bowen, J. Mater. Sci, 24: 1907-1912 (1989)

6. M. J. Edirisinghe and J. R. C. Evans, Int. J. High Technol. Ceram., 2: 249-258 (1986)

7. H. Yan, W. R. Cannon, and D. J. Shanefield, J. Am. Ceram. Soc., 76[1]: 167-172 (1993)

8. F. J. Klug, W. D. Pasco, and M. P. Borom, J. Am. Ceram. Soc, 65: 619- 626 (1982)

9. S. J. Bennison and M. P. Harmer, J. Am. Ceram. Soc., 68, 591-597 (1985)

10. F. F. Lange, B. I. Davis, and E. Wright, J. Am Ceram. Soc., 69: 66-69 (1986)

11. C. H. Hseuh, A. G. Evans, and R. C Coble, Acta. Metall., 30, 1269-1279 (1982)

12. G. Bandyopadhyay and K. W. French, J. Europ. Ceram. Soc., 11[1]: 23-24 (1993)

13. R. M. German, K. F. Hens, S.T.P. Lin, Am. Ceram. Soc. Bull., 70[8]: 1294-1302 (1991)

14. T. F. Yen, Y. H. Chang, D. S. Tsai, S. L. Duh, and S. J. Yang, Mat. Sci. and Engineering, A154, 215-221 (1992)

15. G. Elssner, W. Diem, and J. S. Wallace, pp. 629-639 in *Surfaces and Interfaces in Ceramic and Ceramic-Metal Systems*, Edited by J. Pask and A. G. Evans, Plenum Press, New York (1981)

16. Ravaglioli and A. Krajewshi, *Bioceramics*, pp. 5 – 7, 413-415, Chapman and Hall, New York (1992)

17. A.Krajewshi, A. Ravaglioli and V. Biasin, "Plasma spray coating of prevalently titanium supports with various ceramics", paper presented at the International Conference of 'Bioceramics and the Human Body', Faenza, Italy (1992)

18. K. Y. Lee, E. D. Case, and J. Asmussen, Jr. , Ceramic Transactions, 59, 473-480, American Ceramic Society, Inc., Columbus, OH. (1995)

19. K. Y. Lee, E. D. Case, J. Asmussen Jr., and M. Siegel, Scripta Materialia, 35[1]:107-111 (1996)

20. K. Y. Lee, E. D. Case, J. Asmussen Jr., and M. Siegel, *Binder Burnout in a Controlled Single-Mode Microwave Cavity*, Scripta Materialia, 35[1]:107-111 (1996)

3.4 Joining Ceramics to Produce Components with Precise Internal Channels

JOINING CERAMICS TO PRODUCE COMPONENTS WITH PRECISE INTERNAL CHANNELS

J. G. Lee* and E. D. Case
Materials Science and Mechanics Department,
Michigan State University, East Lansing, MI 48823

ABSTRACT

Geometrically complex ceramic parts are difficult to achieve, especially when one deals with an "internal" geometric complexity such as a component with internal channels, holes, or notches. Such components are potentially important for the flow of cooling fluids, fuel, or biological fluids through a ceramic component. This paper discusses microwave joining of ceramics (including alumina/zirconia composites, zirconia, MaCor^{TM}, and hydroxyapatite) to form components with precise internal notches. The microstructure near the joined/notched regions also will be characterized.

J. G. Lee and E. D. Case, "Joining Ceramics to Produce Components with Precise Internal Channels", in Innovative Processing and Synthesis of Glass, Composite, and Ceramic Materials III, Volume 108, Ceramic Transactions, American Ceramic Society. pp. 433 – 442 (2000)

INTRODUCTION

The difficulty of fabricating near net-shape components, due to the brittle characteristic of ceramic materials, has been a limitation for machining ceramic [1-4]. However, joining allows one to make complex shape from simpler subcomponents [1-4]. Features such as of interest channels, holes, or notches, are interesting in high temperature heat exchanger and engine application as well as biological fluids.

Direct ceramic-ceramic joining utilizing microwave energy has been successfully done in recent year. The ability of rapid and volumetric heating is attractive advantages of microwave heating [3]. Desirable temperature can be reached at lower power compared to conventional heating. Case and Lee have been joined alumina, zirconia, MaCor™ and MgF_2 also including notch stability before and after joining using spin-on materials [6-10].

In this study, notches were induced in alumina/zirconia composites, zirconia, MaCor™, and hydroxyapatite. In order to observe the dimension difference before and after joining, notched and notched/joined specimens were compared by SEM micrograph. The joining was attempted in 2.45 GHz single mode microwave cavity with a low external pressure, provided by dead weight loading in air. The joined regions were characterized by Vikers indentation near the interface to perceive the toughness.

EXPERIMENTAL PROCEDURE

Materials used in this study

Zriconia

In this study, a 3 mol % yttria-ziconia and an 8 mol % yttria-zirconia powder (Tosoh

Ceramics Division, Bound Brook, New Jersey) were sintered in a 2.45 GHz single mode microwave. Microwave heating could achieve higher density after sintering when compared to that of conventionally annealed specimen [5]. Table 15 showed the sintering conditions for both powers including alumina/zirconia composites.

Alumina/zirconia composites

Alumina/zirconia composies composed of 85 wt % alumina powder (99.9 % pure alumina, TMDAR, TAIMI chemicals Co. LTD) and 15 wt % zirconia powder (3 mol % yttria-zirconia powder, Tosoh Ceramics Division, Bound Brook, New Jersey) were mechanically mixed for 24 hours using alumina grinding media in a plastic ball mill. After ball milling, the powder was sintered at 1350°C for 1 hour in the microwave cavity.

MaCor™

MaCor™ (Corning Code 9658) is commercial machinable glass ceramic with a good tolerance for thermal shock that is used as an electrical or thermal insulator. The composition of MaCor™ is SiO_2-Al_2O_3-MgO-K_2O-F. As received MaCor™ billets were cut into 1 cm × 1 cm using a low speed saw.

Hydroxyapatite

Nomially 99 % pure hydroxyapatite powder (Cerac Inc., Specialty Inorganics, Milwaukee, WI, Item#C-2071-1, Lot#X 16907) is an "bioactive" ceramic material which used for human bone and had a nominal purity. Unlike other power materials used in this study, hydroxyapatite(HAP) was sintered in an electrical resistance conventional furnace at 1300°C for 11 hours to a density about 2.974 g/cm^3.

Silica film

Silica film (Emulsitone Company, Whippany, New Jersey) was used for the bond phase. The film was cured at 200°C in a conventional furnace.

Specimen Preparation

The specimens of MaCor™ and sintered ZrO_2, Al_2O_3/ZrO_2 composites, and HAP specimens were polished followed a series of diamond grits size 35 μm, 17 μm, 15 μm, 10 μm, 6 μm, and 1 μm using an automatic polisher (LECO Corporation, St. Joseph, MI). After polishing, the specimens were cleaned in DI water using an ultrasonic cleaner for 20 minutes.

The silica film was dropped onto a substrate spun at 3000 rpm for 20 seconds using a high speed substrate spinner. Curing at 200°C for 20 minutes in a conventional furnace produce uniform and smooth films approximately, 0.13 μm thick.

After the applied silica films were cured, the specimens were notched on coated side using a low speed diamond saw (Figure 47). The coated and notched specimens were sectioned though the notches in order to observed the notch prior to joining.

A pair of half sectioned specimens were attempted joining in a single mode microwave cavity 17.78 cm in diameter (Model CMPR-250, Wavemat Inc) using microwave power supply (Sariem, Model MWPS 2000) generates from zero to 2000 watts of microwave power at frequency of 2.45 GHz (Figure 48). During microwave heating, the specimens were placed in a cylindrical refractory insulator to reduce heat loss during joining. During joining, alumina deadweights in range of 20 grams to 50 grams were placed on top of the specimen being joined to provide low external loads.

After joining, the specimens were sectioned using a low speed diamond saw, which produced one specimen for SEM examination and one specimen for Vickers indentations.

Sectioned specimen enclosed notches was mount on stub with just notched specimen not heated for observing the notch dimension difference before and after joining using scanning electron microscope (SEM). The other piece was mounted using hot pressing presser and then polished finished 1 μm. To examine the bond layer or interface toughness, Vickers indentation was introduced near the bond layer or interface (Figure 49).

Results and Discussion

HAP with MaCor^{TM}

Notches were cut into both HAP and MaCor^{TM} specimens (Figure 50). One set of MaCor^{TM} and HAP were joined at 1020°C with 20 grams applied dead weights. Joining was failed at temperature range 1150°C to 1050°C with 50 grams dead weights. Table 16 was showed conditions of attempted joining of MaCor^{TM} and HAP.

For MaCor^{TM} joined at 1020°C for 20 minutes, using a 20 grams deadweights, the difference between before and after joining was less than 6 %, which shows the geometrical stability of notches was quite stable after joining (Table 17 and Figure 51). For HAP, also three were introduced and measure (Figure 52) before and after joining (Table 17). The geometrical stability of HAP was in the range of 1 % to 4 %.

ZrO_2 (3mol% Y_2O_3) with MaCor^{TM}

ZrO_2 was joined with MaCor^{TM} at 1020°C for 20 minutes with applied 20 grams dead weights. Four notches were made in ZrO_2 but the MaCor^{TM} was not notched. Notch stability was determined from SEM mesurements of the notch dimensions, before and after joining. (Table 18 and Figure 53). The differences between before and after joining values of depth range from 1 % to 5 % while the width changes ranged from 1 % to 2 %. Thus, the notch dimension was quiet stable after joining.

ZrO_2 (8 mol % Y_2O_3) with ZrO_2 (8 mol % Y_2O_3)

Zirconia (8 mol % Y_2O_3) was joined to zirconia (8 mol % Y_2O_3) via microwave heating at 1500°C for 20 minutes with 50 grams dead weights. Notches were at into both the 8 mol % yttria-zirconia specimens. The differences in notch width and depth before and after joining was less than 3 % (Table 19). After heating at 1500°C using microwave energy, notches made in ZrO_2 (8 mol % Y_2O_3) were not effected in terms of difference dimension changing.

Al_2O_3 85 wt %/ ZrO_2 (3 mol % Y_2O_3) 15 wt % composites joining.

Al_2O_3/ZrO_2 composites were successfully joined using microwave heating at 1500°C, 1450°C, and 1400°C for 20 minutes. In each case, a silica film spin-on interlayer was used as the bonding phase and a 50 gram dead weight was placed on the top of the specimens during joining. Three notches were observed the joined specimen at 1450°C. The notches were changed the dimension in depth of range 1 % to 2 % and width of range 1 % to 4 % (Table 20).

CONCLUSIONS

A number of different ceramic materials were notched and then successfully joined. The ceramic-creamic material pairs that were joined include MaCor^{TM} with HAP, MaCor^{TM} with ZrO_2 (3 mol % Y_2O_3), ZrO_2 (8 mol % Y_2O_3), and Al_2O_3/ZrO_2 composites. In each case, a spin-on silica coating was used as the bond phase. The dimensions of the notches induced in joined specimens were quite stable (less than 6 % for every attempted joining specimen) during microwave joining process. These results indicate that channels and notches cut into in polycrystalline ceramics can maintain their dimensions during the joining process.

REFERNCES

1. D.Palaith and R.Silberglitt, " Microwave Joining of Ceramics," *Journal of American Ceramic Society Bulletin*, 68[9] 1601-1606 (1989).

2. R.E. Loehman and A.P. Tomsia, "Joining of Cermics," *Journal of American Ceramic Society Bulletin*, 67[2] 375-380 (1988).

3. M.L. Santella, "A Review of Techniques for Joining Advanced Ceramics," *Journal of American Ceramic Society Bulletin*, 71[6] 947-953 (1989).

4. R.Silberglitt, I. Ahmad, W.M. Black, and J.D. Katz, "Recent Developments in Microwave Joining," *MRS Bulletin*, 18[7] 47-50 (1993).

5. S.A. Nightingale, D.P. Dunne, and H.K. Nomer, "Sintering and Grain growth of 3 mol % Yttria Zirconia in A Microwave Filed," *Journal of Materials Science*, **31** 5039-5043 (1996).

6. E.D. Case, K.Y, Lee, J,G, Lee, and T. Hoepfner, "Geometrical Stability of Holes and Channels During Joining of Ceramics and Composites," *Proceedings from Materials Conference '98 on Joining of Advanced and Specialty Materials*, 12-15 October 1998, 27-34.

7. K.Y. Lee and E.D. Case, Microwave Joining and Repair of Ceramics And Ceramic Composites," *Ceramic Engineering and Science Proceedings, 21st Annual Cocoa Beach Conference and Exposition on Composites, Advanced Ceramics, Materials and Structure*, Cocoa Beach, Florida, 18 543-550, 1997.

8. K.N. Seiber, K.Y. Lee, and E.D. Case, " Microwave and Conventional Joining of Ceramic Composites Using Spin-On Materials," *Proceeding of the 12thAnnual Technical Conference Dearborn, MI*, 941-949, 1997.

9. J.G. Lee, K.Y. Lee and E.D. Case, "Joining of Diamond Thin Film to Optical And IR Materials," *Innovative Processing/Synthesis: Ceramics, Glasses, Composites II*, 509-520, 1999.

10. E.D. Case, J.G. Lee, and K.Y. Lee, "Joining of Optical and Infrared Materials Using Spin-On Layers," *Proceedings from Materials Conference '98 on Joining of Advanced and Specialty Materials*, 12-15 October 1998, 17-26.

Table 15. Sintering conditions for powder materials used in this study.

Materials	Mass	Pre-Pressing	Heating Rate	Sintering Temp (°C)	Hold Time(min)	Cooling Rate
ZrO_2 (3 mol % Y_2O_3)	3 gm	32 Mpa	10°C/min	1375°C	60 min	10°C/min
ZrO_2 (8 mol % Y_2O_3)	3 gm	32 Mpa	10°C/min	1350°C	60 min	10°C/min
Al_2O_3/ZrO_2 composites	2 gm	32 Mpa	10°C/min	1350°C	60 min	10°C/min

Table 16. Attempted joining conditions for joining MaCor™ and HAP.

T_{max} (°C)	Dead weights	Hold time	Heating rate	Result	Comments
1150°C	50 grams	20 min	~ 40°C/min	Not joined	MaCor melted
1100°C	50 grams	20 min	~ 40°C/min	Not joined	MaCor melted
1050°C	50 grams	20 min	~ 40°C/min	Not joined	MaCor melted
1020°C	20 grams	10 min	~ 40°C/min	Joined	
1000°C	No	20 min	~ 40°C/min	Not joined	

Table 17. Notch stability of joined HAP with MaCor™ before and after joining.

Material Notched	# of notches	Notch Width, before joining	Notch Width, after joining	Difference (%)	Notch depth, before joining	Notch depth, after joining	Difference (%)
HAP	1	364 μm	361 μm	1 %	632 μm	636 μm	1 %
HAP	2	343 μm	355 μm	-4 %	643 μm	614 μm	4 %
HAP	3	314 μm	321 μm	-2 %	518 μm	496 μm	4 %
MaCor™	1	343 μm	335 μm	2 %	371 μm	385 μm	-4 %
MaCor™	2	321 μm	335 μm	-4 %	514 μm	528 μm	-3 %
MaCor™	3	341 μm	321 μm	6 %	407 μm	421 μm	-4 %

Table 18. The notch change before and after joining for joined ZrO_2 with MaCor™

Material Notched	# of notches	Notch Width, before joining	Notch Width, after joining	Difference (%)	Notch depth, before joining	Notch depth, after joining	Difference (%)
ZrO_2	1	374 μm	367 μm	2 %	246 μm	240 μm	3 %
ZrO_2	2	375 μm	379 μm	-1 %	238 μm	225 μm	5 %
ZrO_2	3	379 μm	375 μm	1 %	267 μm	265 μm	1 %
ZrO_2	4	385 μm	379 μm	2 %	304 μm	296 μm	3 %

Table 19. The notch dimension change before and after joining for joined ZrO_2 (8 mol % Y_2O_3)

Material Notched	# of notches	Notch Width, before joining	Notch Width, after joining	Difference (%)	Notch depth, before joining	Notch depth, after joining	Difference (%)
ZrO_2	1	314 µm	319 µm	2 %	421 µm	407 µm	3 %
ZrO_2	2	319 µm	310 µm	3 %	381 µm	386 µm	-1 %
ZrO_2	3	319 µm	312 µm	2 %	402 µm	410 µm	-2 %
ZrO_2	4	329 µm	319 µm	2 %	460 µm	452 µm	2 %
ZrO_2	5	310 µm	314 µm	-1 %	433 µm	419 µm	3 %

Table 20. . The notch dimension change before and after joining for joined Al_2O_3/ZrO_2 composites.

Material Notched	# of notches	Notch Width, before joining	Notch Width, after joining	Difference (%)	Notch depth, before joining	Notch depth, after joining	Difference (%)
Al_2O_3/ZrO_2	1	321 µm	307 µm	4 %	321 µm	325 µm	-1 %
Al_2O_3/ZrO_2	2	309 µm	307 µm	1 %	313 µm	315 µm	-1 %
Al_2O_3/ZrO_2	3	321 µm	318 µm	1 %	352 µm	346 µm	2 %

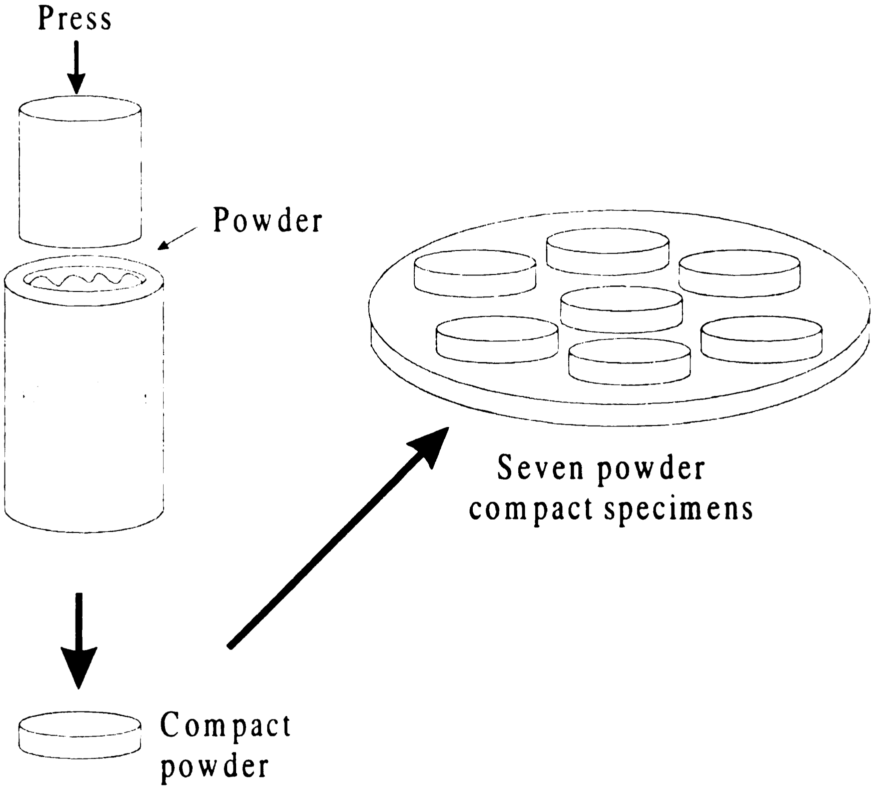

Figure 46. A schematic for compact powder materials and sintering.

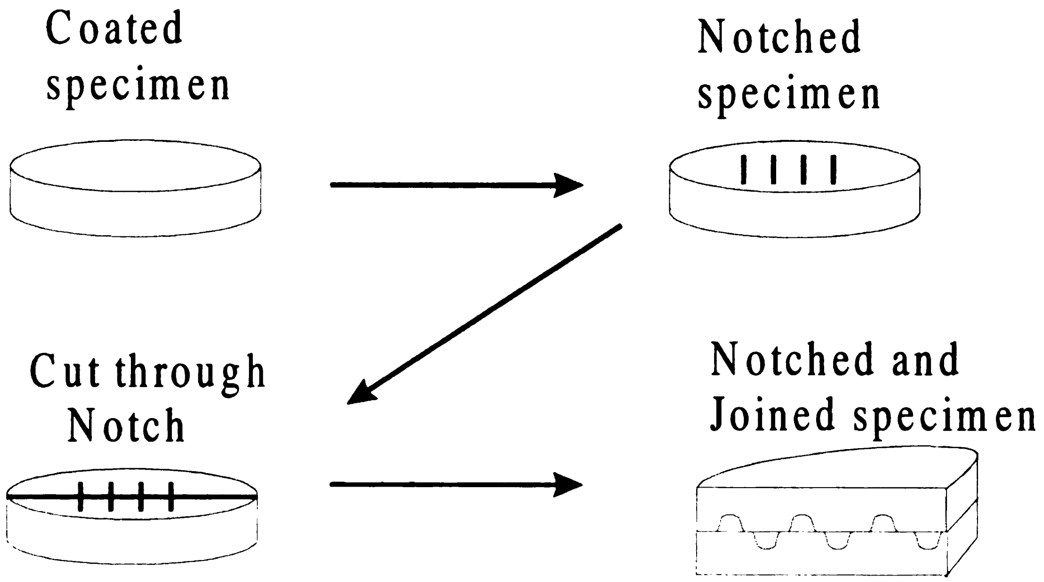

Figure 47. Schematic of producing notches.

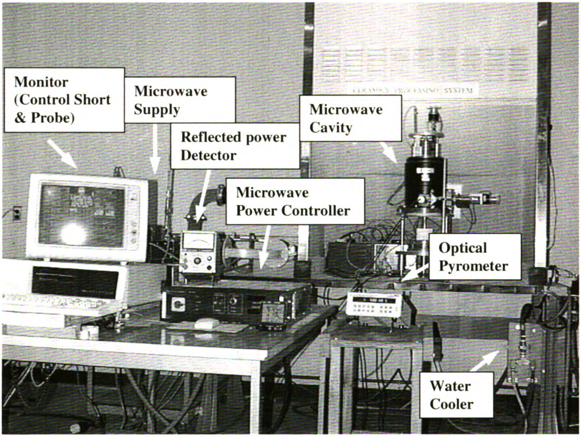

Figure 48. Schematic of microwave processing system, showing microwave cavity and microwave power supply.

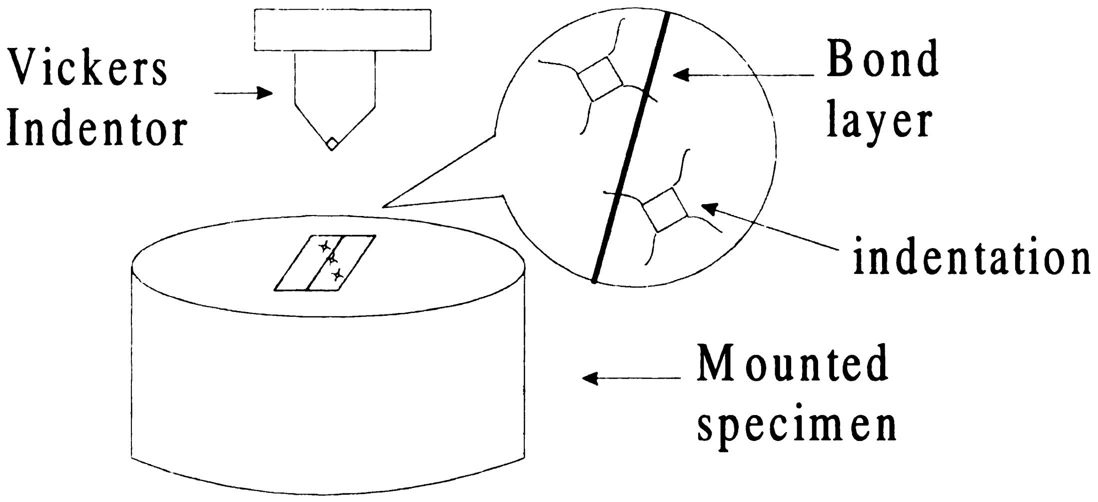

Figure 49. A schematic of showing Vickers indentations placed near the bond layer.

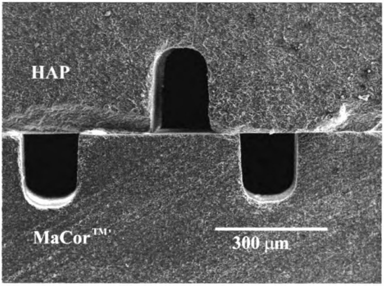

Figure 50. Notch configuration in both HAP and MaCor^{TM} specimens.

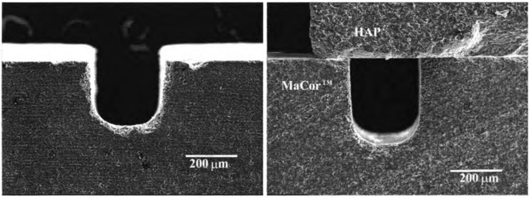

(a) MaCor^{TM} before joining (b) MaCor^{TM} after joining

Figure 51. MaCor^{TM} notched specimen before and after joining.

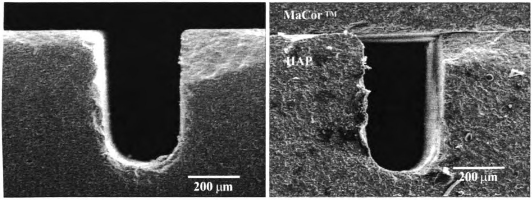

(a) HAP before joining (b) HAP after joining

Figure 52. HAP notched specimen before and after joining.

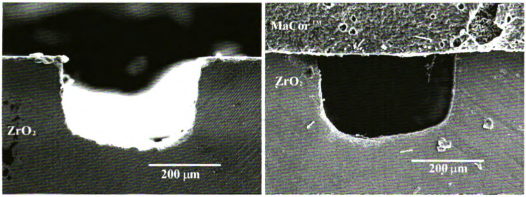

(a) ZrO_2 before joining (b) ZrO_2 after joining

Figure 53. ZrO_2 notched specimen before and after joining.

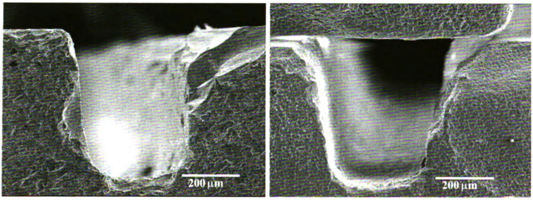

(a) ZrO_2 before joining (b) ZrO_2 after joining

Figure 54. ZrO_2 notched specimen before and after joining.

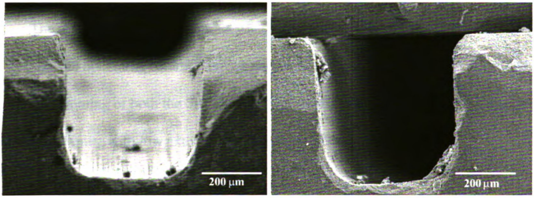

(a) Al_2O_3/ ZrO_2 before joining (b) Al_2O_3/ZrO_2 after joining

Figure 55. Al_2O_3/ ZrO_2 notched specimen before and after joining.

3.5 Joining of Non-Oxide Ceramics Using Conventional And Microwave Heating

JOINING OF NON-OXIDE CERAMICS USING CONVENTIONAL AND MICROWAVE HEATING

Jong-Gi Lee and E. D. Case
Materials Science and Mechanics Department
Michigan State University
East Lansing, MI 48824

ABSTRACT

The nonoxide ceramic materials silicon carbide (a structural ceramic) and magnesium fluoride (an optical/IR ceramic) have been joined using conventional and microwave heating. Joining of both the SiC and MgF_2 utilized a spin-on interfacial layer, which allowed joining with low external applied pressures.

INTRODUCTION

Non-oxide ceramics include many useful materials, including structural ceramics such as silicon carbide and silicon nitride, with their combination of relatively high toughness and low mass density. However, a second important category of non-oxide ceramics is infrared transmitting materials. Particular nonoxide ceramics are much better infrared transmitting materials than oxide ceramics due to basic physical nature of the metal-oxygen bond. The cutoff in infrared transmission as a function of wavelength is due to coupling of

---

J. G. Lee and E. D. Case, "Joining of Non-Oxide Ceramics Using Conventional and Microwave Heating", Ceramic Engineering and Science Proceedings 21[4], American Ceramic Society. pp. 589-597 (2000) the infrared photons with the lattice normal modes of vibration for the material [1]. High atomic mass and weak bonds tend to increase the effective cutoff wavelength such that in oxide ceramics, the metal-oxygen bond strongly absorbs infrared wavelengths longer than about 5 to 8 microns [2,3], but for nonoxides such as magnesium fluoride and zinc sulfide, the relatively low mass and weak bonds enhance the infrared transmission by pushing the IR cutoff to higher wavelengths. This paper addresses the joining of both optical/infrared nonoxide ceramics as well as structural ceramics.

As is the case for oxide ceramics, non-oxide ceramics also are difficult to process in complex shapes and one method of fabricating ceramic components with complex morphologies is to "build them up" by joining sub-components of relatively simple geometry. Thus, there have been a number of efforts to join nonoxides via either conventional or microwave heating [4 - 14].

Nonoxide ceramics have been joined by conventional heating using a variety of metallic interlayers or braze filler materials. Young et al. fabricated AlN-Ni-Cu-Ni-AlN "sandwiches" by vacuum hot pressing at 600^0C to 700^0C at a pressure of 6.5 MPa for 30 minutes [4]. The AlN plates were coated with nickel, then a copper foil was inserted between the Ni-coated AlN plates prior to joining, resulting in a low-temperature bond about 100 microns thick [4]. Wang et al. used a CuNiTiB paste brazing filler to join Si_3N_4/Si_3N_4. Before joining, an interfacial layer consisting of a slurry of the metal powders was applied to the specimens [5]. Joining was done at temperatures between about 1000^0C and 1120^0C in a conventional vacuum furnace, with final bond layer thicknesses ranging between about 48 microns and 58 microns thick [5].

A number of researchers used ceramic interlayers to join nonxoxide ceramics via either conventional or microwave heating. Xie et al. joined sintered Si_3N_4 using a slurry of α-Si_3N_4, Y_2O_3, SiO_2, and Al_2O_3 powders in a conventional furnace with a nitriding atmosphere [6]. The optimum joining conditions were 1650^0C with a 5 MPa applied load and a 30 minute hold time, giving bond layers approximately 15 microns thick [6]. Lee et al. joined sintered silicon carbide using a 1 mm thick MgO-Al_2O_3-SiO_2 (MAS) layer inserted between the two SiC plates [7]. Using zero applied external load, the SiC specimens were heated in a conventional graphite-element furnace from room temperature to 1000^0C in vacuum, then from 1000^0C to either 1500^0C or 1600^0C in an Ar atmosphere, yielding final bond thicknesses of 5 microns and 10 microns, respectively [7].

Silberglitt et al. used Si interlayers in the microwave joining of SiC at 1450^0C for 5 - 10 minutes under an external load of 2 - 5 MPa [8]. The final bond widths were a function of the interlayer processing technique, with Si powders, a Si slurry, and a plasma-sprayed Si coating yielding final (as-joined) bond layer thicknesses of 50 microns, 5 microns, and approximately 3 microns, respectively.

In addition to the joining of nonoxides using interlayers, Binner used a 2.45 GHz microwave cavity to directly join RBSN to RBSN [9]. However, although Binner et al. did not deposit an interlayer on the RBSN materials, the joining process itself generated a free-silicon interlayer between the joined RBSN specimens [9], where the free silicon was thought to “bleed” out the RBSN microstructure into the bond region due to the application of high temperature and pressure [9]. For the RBSN, a gap between the joined specimens diminished with increasing temperature and pressure, until at a joining temperature of 1350^{0}C, a joining time of about 15 minutes, and a joining pressure of 1.5 MPa, the silicon-filled bond layer had decreased to about 3 - 5 microns (whereas at 1190^{0}C and 0.5 MPa, the "gap" was about 10 - 20 microns wide and only partially filled with Si). [9]

Previously, the authors and coworkers successfully joined several ceramic oxide materials [10-14], including joining alumina, partially stabilized zirconia (PSZ), MaCor™, and hydroxyapatite. Also, a number of dissimilar ceramic oxide pairs have been joined [12, 14]. This paper focuses on the joining of two nonoxides, SiC (a structural material) and MgF_2 (an IR transmitting material).

EXPERIMENTAL PROCEDURE

The as-received billets of silicon carbide and magnesium fluoride were cut using a low speed diamond saw, with specimen dimensions of 1.6 cm X 0.4 cm X 0.3 cm for the SiC (Hexoloy) specimens and 1.0 cm X 1.0 cm X 0.2 cm for the magnesium fluoride specimens. After cutting, the specimens were polished using a series of diamond grit sizes, with a minimum 1 micron grit size.

The spin-on layers used were applied to the polished specimen surfaces in a liquid form. Four to five drops of the spin-on liquid (Blackglas™ for the SiC and sodium silicate for the MgF_2) were applied near the center of the polished specimen using a pipette. The specimen was spun for 20 seconds at speeds ranging from 3000 RPM to 5000 RPM using a substrate spinner. Following spinning, the coated surface of the specimen was placed in contact with another polished, uncoated specimen of the same material and was immediately loaded into the furnace (Figure 56).

The joining was done using both a conventional furnace and a microwave cavity. Conventional heating was done with a nitrogen flow rate of approximately 120 sccm and a heating/cooling rate of approximately $10^{O}C$ per minute. The microwave heating was done in air using a 2.45 GHz single-mode microwave resonant cavity. The specimen temperature was monitored via an optical pyrometer system. A cylindrical zirconia refractory specimen enclosure (casket) was used during joining [10-14].

The SiC specimens were heated first in the conventional furnace at $900^{0}C$ for 20 minutes, followed by microwave heating of selected specimens at $1200^{0}C$ for 20 minutes. The MgF_2 specimens were heated for 20 minutes either in the conventional furnace (with flowing nitrogen) at $700^{0}C$ or in air in the microwave at $700^{0}C$. After joining, the specimens were sectioned on a low speed diamond saw and examined in a Scanning Electron Microscope (JEOL Model JSM-6400V). Vickers indentation testing was also performed on the joined and sectioned specimens.

RESULTS AND DISCUSSION

The microstructure of the SiC (Hexoloy) materials is shown in Figure 57 (a micrograph of the fracture surface), while for MgF_2 a comparable fracture surface micrograph is given in reference 11.

Joining the SiC at $900^{0}C$ in flowing N_2 in a conventional furnace results in a dense bond layer that was roughly 2 to 3 microns thick (Figure 58a). For the MgF_2 specimens that were joined at $700^{0}C$ both in flowing nitrogen in a conventional furnace and in a microwave cavity in air at $700^{0}C$, the resulting bond thickness was about 10 microns (Figure 58b shows the MgF_2 bond due to microwave heating). For the SiC specimens that were heated conventionally at 900^{0}C, reheating the specimens at 1200^{0}C in the microwave cavity did not appreciably change either the appearance or mean thickness of the bond layer (Figure 59). Previously, the authors found that the IR transmittance of the joined MgF_2 was essentially the same as the unjoined MgF_2, if microwave heating was used. However, the IR transmittance was degraded if the specimens were joined by conventional heating, in part due to IR scattering from the second phases formed in MgF_2 bond layer in conventionally heated specimens [11, 14].

In order to investigate the relative interfacial toughness of the bonds in the joined specimens, a series of 49 N Vickers indentation cracks were placed near the interface of the conventionally and the microwave joined MgF_2 and SiC specimens, such that the radial cracks were oriented approximately normal to the joined interface. In general, cracks approaching an interface can deflect at the interface (forming "T-shaped" cracks along the interface) if the interfacial fracture energy is less than about 60 percent of the matrix fracture energy [15]. Otherwise, the crack propagates across the interface, without deflection. For both the SiC and the MgF_2 specimens included in this study, the indentation cracks did deflect at the interface, indicating that the relative interfacial fracture energy was less than 60 percent of the matrix fracture energy in both cases.

SUMMARY

Two nonoxide materials, SiC and MgF_2 were joined using a spin-on interlayer. The bond phases produced were relatively thin and dense, but the interfacial fracture energy was low.

ACKNOWLEDGMENTS

The authors acknowledge financial support of the Composite Materials and Structures Center of Michigan State University and the use of the electron microscope facilities at the Center for Electron Optics, Michigan State University.

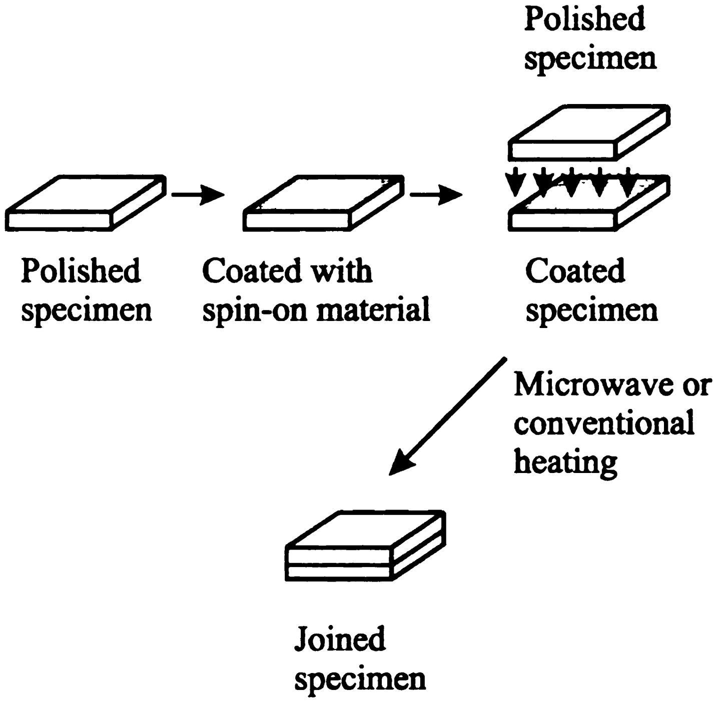

Figure 56. Schematic of the coating and joining technique.

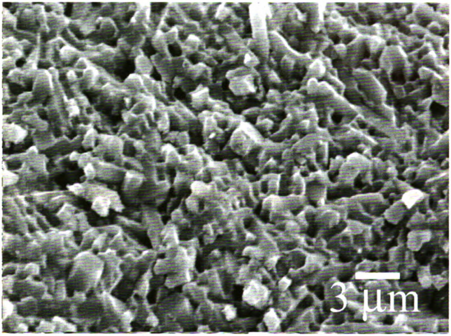

Figure 57. Fracture surface of SiC used in this study.

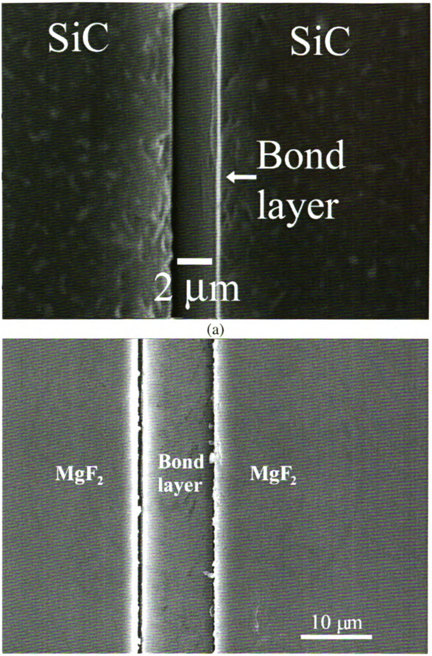

(a)

(b)

Figure 58. (a) SiC joined at 900°C for 20 minutes in flowing N_2 with a 20 gram deadweight applied during joining and (b) MgF_2 specimens joined at 700°C for 20 minutes in air with a 60 gram deadweight applied during joining.

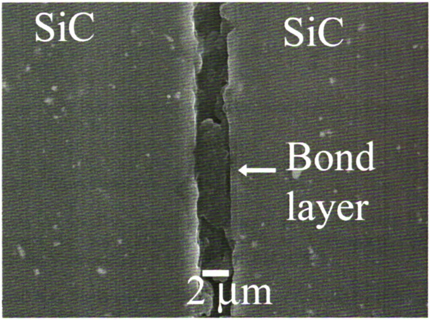

(a)

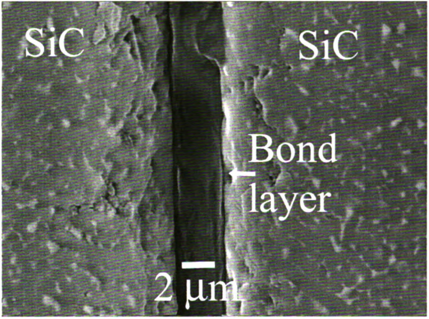

(a)

Figure 59. SEM images of the SiC specimens that had been first heated conventionally at 900^0C (Figure 58a), followed by (a) microwave heating at 1200^0C for 20 minutes or by (b) conventional heating at 1200^0C for 20 minutes.

REFERENCES

1. M. W. Barsoum, pp. 618 - 635 in *Fundamentals of Ceramics*, McGraw-Hill, New York, NY, 1997.

2. C. Kittel, pp. 107-116 in *Introduction to Solid State Physics*, 5th ed., John Wiley and Sons, New York, 1976.

3. L. L. Hench and J. K. West, *Principles of Electronic Ceramics*, pp 351-360, John Wiley & Sons, New York, NY, 1990.

4. C.D. Young and J.G. Duh, "Bonding Mechanism of Electrodes Ni-P Film with AlN substrate and Cu Foil," *IEEE Transactions on Components Packaging and Manufacturing Technology Part A,* **21** [2] 330-344 (1998).

5. C.G. Wang, H.P. Xiong and Z.F. Zhou, "Joining of Si_3N_4/Si_3N_4 with CuNiTib Paste Brazing Filler Metals and Interfacial Reactions of the Joints," *Journal of Materials Science*, **34** [12] 3013-3019 (1999).

6. R.J. Xie, L.P. Huang, Y. Chen and X.R. Fu, "Evaluation of Si_3N_4 Joints: Bond Strength and Microstructure," *J. Mat. Sci.*, **34** [8] 1783-1790 (1999).

7. H.L. Lee, S.W. Nam, B.S. Hahn, B.H. Park and D. Han, "Joining of Silicon Carbide Using MgO-Al_2O_3-SiO_2 Filler," *J. Mat.Sci.*, **33** [20] 5007-5014 (1998).

8. R. Silberglitt, D. Palaith, H.S. Sa'alaldin, W.M. Black, J.D. Katz, and R.D. Blake, "Microwave Theory and Application in Materials Processing," pp. 487 - 495 in *Ceramic Transactions* Vol 21, D. E. Clark, F. D. Gac, and W. H. Sutton, editors, American Ceramic Soc., Westerville, OH (1991).

9. J.G.P. Binner, J.A. Fernie, and P.A. Whitaker, "An Investigation into Microwave Bonding Mechanisms via a Study of Silicon Carbide and Zirconia," *Journal of Materials Science*, **33** [12] 3009-3015 (1998).

10. K.Y. Lee, E.D. Case, D. Reinhard, "Microwave Joining and Repair of Ceramics and Ceramic Composites," *Ceramic Eng.Sci. Proc.*, **18** 543-550 (1997).

11. E.D. Case, J.G. Lee, and K.Y. Lee, "Joining Optical and Infrared Materials Using Spin-On Layers",pp.17-26 in *Joining of Advanced and Specialty Materials*, M. Singh, J.E. Indacochea, and D.Hauser,eds.,ASM International, Materials Park, OH, 1998.

12. K.N. Seiber, K.Y. Lee, and E.D. Case, "Microwave and Conventional Joining of Ceramics using Spin-on Materials," pp. 941-949 in *Proc. 12th Annual Advanced Composites Conference*, Technomic Pub. Co., Lancaster, PA, 1997.

13. E.D. Case, K.Y. Lee, J.G. Lee, and T. Hoepfner, "Geometrical Stability of Holes and Channels During Joining of Ceramics and Ceramic Composites," pp. 27 - 34 in *Joining of Advanced and Specialty Materials*, M. Singh, J.E. Indacochea, and D. Hauser, eds., ASM International, Materials Park, OH., 1998.

14. E.D. Case, K.Y. Lee, and J.G. Lee, "Joining of Polycrystalline Ceramics and Ceramic Composites Using Microwave Heating," pp. 17 - 20 in *Proc 33rd Int. Microwave Power Symp.*, International Power Institute, Manassas, VA., 1998.

15. W. Lee, S. J. Howard, and W. J. Clegg, *Acta Mater.* **44** 3905-3922 (1996).

3.6 Protective Coatings for Infrared Materials

PROTECTIVE COATINGS FOR INFRARED MATERIALS

Jong-Gi Lee, E. D. Case and M. A. Crimp
Materials Science and Mechanics Department
J. Malik and D. K. Reinhard,
Electrical Engineering Department
Michigan State University
East Lansing, MI 48824

ABSTRACT

Solutions of polycarbosilane and hexane have been spun onto magnesium fluoride substrates, producing continuous and adherent coatings upon curing in flowing nitrogen. The study focused on the infrared properties of the films, which were maintained upon coating.

INTRODUCTION

The interaction of electromagnetic waves with ceramic materials involves reflectance, absorptance, transmittance and scattering, such that [1]

$$S + R + A + T = 1 \qquad (1)$$

where S, R, A, and T are coefficients associated with scattering, reflectance, absorptance and transmittance, respectively. Each quantity in equation 1 is a function of a number of

---

E. D. Case, J. G. Lee, M. A. Crimp, D. K. Reinhard, and J. Malik, "Protective Coatings for Infrared Materials", Ceramic Eng. and Sci. Proc., Volume 20, American Ceramic Society, Inc., Westerville, OH, pp. 145-152 (1999)

variables, including the incident wavelength. In addition to the wavelength dependence, the scattering, S, is a function of the number density and dimensions of scattering centers, such as pores, rough surfaces, etc. Reflectance is a function of the index of refraction of the material and the angle of incidence. For the absorptance, A, in the infrared-visible-ultraviolet regime, there are two major absorption mechanisms that produce wavelength-dependent "cutoffs". In the ultraviolet, the cutoff is due to electronic processes [1], while in the infrared, the cutoff is due to coupling of the infrared photons with the lattice normal modes of vibration [1,2]. The frequency of the lattice modes in turn depends on the bond strength and the atomic mass of the atoms that make up the lattice [3]. High atomic mass and weak bonds tend to increase the effective cutoff wavelength. For example, in oxide materials, the metal-oxygen bond tends to strongly absorb infrared wavelengths longer than about 5 to 8 microns [1,2], but if one selects ceramics with weaker bonds, such as magnesium fluoride, zinc sulfide, and zinc selenide, then one enhances the infrared transmission by pushing the IR cutoff to higher wavelengths. However, the weaker bonds tend to give fluorides, sulfides, and selenides relatively poor mechanical properties, such as low strength and hardness, which in turn makes infrared transmitting materials susceptible to abrasion and erosion damage. To reduce abrasion, erosion, and handling damage, one can add a protective coating to the surface of these materials. In this paper we discuss a method for fabricating a thin, adherent silicon-based coating on polycrystalline magnesium fluoride.

EXPERIMENTAL PROCEDURE

A commercial hot-pressed polycrystalline magnesium fluoride (Irtran 1, Eastman Kodak) was used as the infrared transmitting substrate for this study. The magnesium fluoride had an equiaxed microstructure with a mean grain size of approximately 3 microns. The polycarbosilane (PCS) solution used as a spin-on coating in this study was either applied in a undiluted form to the MgF_2 or it was diluted with hexane, using 1 gram of polycarbosilane to n grams of hexane, where the values of n used in this study were 4 grams, 6 grams, and 10 grams.

Using a low-speed diamond saw, magnesium fluoride specimens roughly 1.0 cm X 1.0 X 0.2 cm were sectioned from as-received billets. Both of the 1.0 cm X 1.0 cm specimen faces were polished for each specimen, using an automated polishing machine (Leco Corporation, St. Joseph, MI) and a series of diamond grit sizes ranging from 17 microns to one micron. Using a pipette, several drops of the PCS solution were placed near the center of a 1 cm X 1 cm specimen face. The PCS coated specimens were then spun at rates between 500 and 6000 rpm for 20 seconds using a commercial substrate spinner (Figure 60).

Curing of the coated specimens was done in both air and flowing nitrogen. For the curing in air, the coatings were heated at about $10^{O}C$ per minute to maximum temperatures of up to $265^{O}C$ with hold times of 20 minutes in a laboratory oven. The nitrogen-atmosphere annealing was done with a nitrogen flow rate of approximately 120 sccm to 130 sccm, with a maximum temperature ranging from $400^{O}C$ to $600^{O}C$ and a hold time of 20 minutes. For the nitrogen anneals, both the heating and cooling rate was approximately $20^{O}C$ per minute.

The infrared transmittance for both the coated and uncoated specimens was determined using a Beckman Spectraphotometer IR 4420, over the wavelength range from 2.5 microns to 9 microns (a wavenumber range from 4000 cm^{-1} to 1100 cm^{-1}). A scan speed of 150 cm^{-1} per minute was used for all of the transmittance measurements reported in this paper. The coated specimens were indented using a Vickers indenter with a 49 N load, a load time of 10 seconds, and a loading speed of 70 microns/second.

RESULTS AND DISCUSSION

The varying dilution of PCS (Starfire Systems, Watervliet, NY) with hexane produced coatings with differing thickness. Undiluted PCS spun at a 3000 rpm for 20 seconds produced a continuous coating about 11 microns thick upon curing in air at $100^{O}C$ for 20 minutes (Figure 61). Dilution of 1 gram PCS to 4 grams hexane (Figure 62a) and 1 gram PCS to 6 grams hexane (Figure 62b), both produced coatings about 2 to 3 microns thick when cured in flowing N_2 at $400^{O}C$ and $500^{O}C$, respectively. Specimens sectioned with a low speed diamond saw were mounted in thermosetting plastic, sputter coated with gold, and observed in an environmental scanning electron microscope (Figures 62a and 62b). A dilution of 1 gram PCS to 10 grams hexane produced films roughly 1 micron thick upon curing in flowing N_2. The coatings annealed in air showed numerous strong and very broad IR absorptions, so the air-annealing of the specimens was not pursued past an initial measurement of the IR transmittance for several specimens.

The polished, uncoated MgF_2 (Figure 63) has transmittance comparable to that of the PCS coated specimens cured in flowing N_2 (Figures 64 and 65). MgF_2's sharp absorption at a 2.763 micron wavelength is consistent with the literature for Irtran 1 [4]. Nitrogen atmosphere annealing at $400^{O}C$ gave a broad absorption at about 4.737 microns or 2112 cm^{-1} which corresponds well to a Si-H group absorption reported at 2120 cm^{-1} for PCS [5]. For N_2 anneals at $500^{O}C$ and $600^{O}C$ (Figures 64 and 65) this absorption was absent, which is consistent with temperature-induced changes in PCS chemistry, since anneals at 400^{O}C in Ar yield considerable weight loss due to the evolution of C_6H_5 (phenyl) groups from PCS [6], but by 500^{O}C the weight is stable to above 1200^{O}C [5]. Other volatile species including H_2 and CH_4 may be evolved during annealing.

In general, a coating on a substrate can either increase or decrease the transmittance relative to the uncoated substrate, depending on the optical indices of refraction of the two media and the coating thickness [6]. An increase in transmission is favored if the index of refraction of the coating is lower than that of the substrate and the coating thickness is on the order of 1/4 the wavelength of the incident radiation [6]. Thus, slight increases or decreases in the transmittance with respect to the uncoated specimens may be due to reflectance effects [6], and decreases in transmittance may be due to scattering or absorption effects.

For the thicker (11 micron) coatings, 49N indentations produced coating delaminations about 300 - 400 microns across, in addition to the associated radial cracks, while the 1 to 3 micron-thick films showed a similar extent of delamination. Spalling of both the thick and the thinner films occurred relatively infrequently upon Vickers indentation at 49 N. However, spalling radial coating cracks, and delamination for ceramic coatings is a function of coating thickness, indentor load, as well as the elastic and fracture properties of the coating and substrate [7]. Additional indentation work is underway for the coatings included in this study.

SUMMARY

Thin, adherent coatings were successfully applied to polished MgF_2 substrates using spin-on PCS and hexane solutions. Curing in flowing nitrogen at $500^{O}C$ and $600^{O}C$ produced continuous films about 1 to 3 microns thick, with IR transmittances that very similar to polished and uncoated MgF_2 specimens. Thus, such coatings do not disminish the original IR transmittance of the MgF_2 substrates. The coating thickness decreased as the hexane dilution increased, and as the coating thickness decreased from about 11 microns to about 1 micron, the tendency for coating delamination remained essentially unchanged. The indentation work done to date in this study is only a preliminary indication of the response of the coatings to point contact loading. Future work will include addition characterization of the mechanical integrity of the coatings.

ACKNOWLEDGMENTS

The authors acknowledge financial support of Composite Materials and Structures Center, Michigan State University, East Lansing, MI. The authors also thank W. Sherwood of Starfire Systems, Watervliet, NY for the PCS.

Figure 60. Schematic showing the high-speed substrate spinner used in applying the coatings to the MgF_2 substrates.

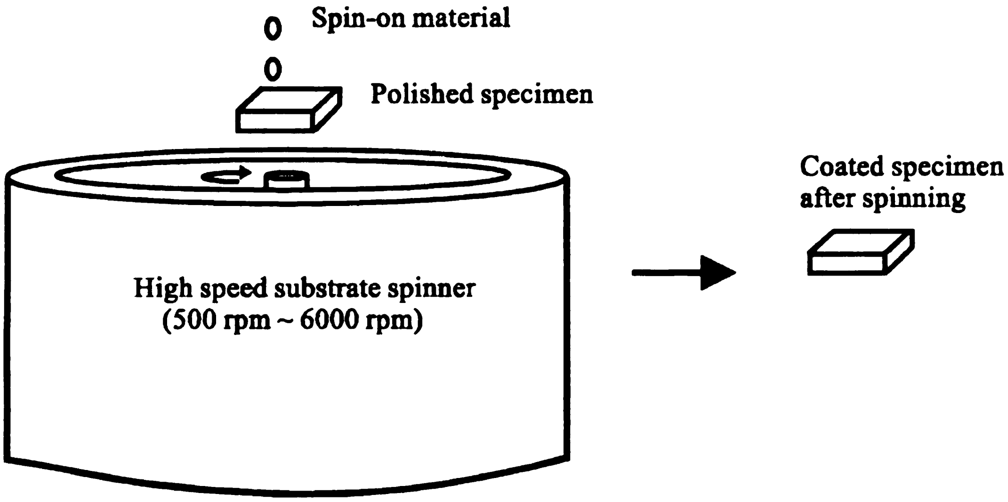

Figure 61. ESEM examined polycarbosilane film which is not added hexane after coating spun at 3000 rpm for 20 seconds and cured at 100°C for 20 minutes in air.

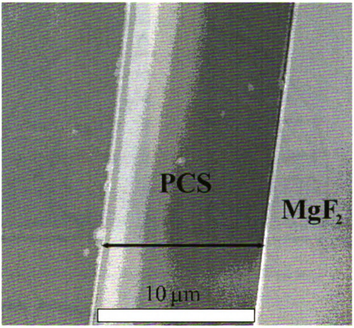

Figure 62. The polycabosilane film thickness using ESEM after coating and transmittance of coated specimens. (a) the film solution of coated specimen was 1 gram PCS and 4 gram hexane mixed solution. The coated MgF_2 was spun at 3000 rpm and cured at 400°C in N_2. (b) the film solution of coated specimen was 1 gram PCS and 6 gram hexane mixed solution. The coated MgF_2 was spun at 5000 rpm and cured at 600°C in N_2. (c) Transmittance for (a), and (d) Transmittance for (b)

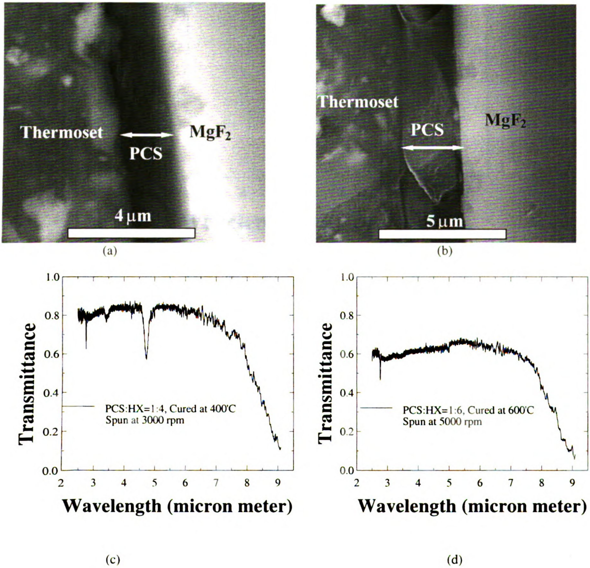

Figure 63. Transmittance of both sides polished MgF_2 specimen.

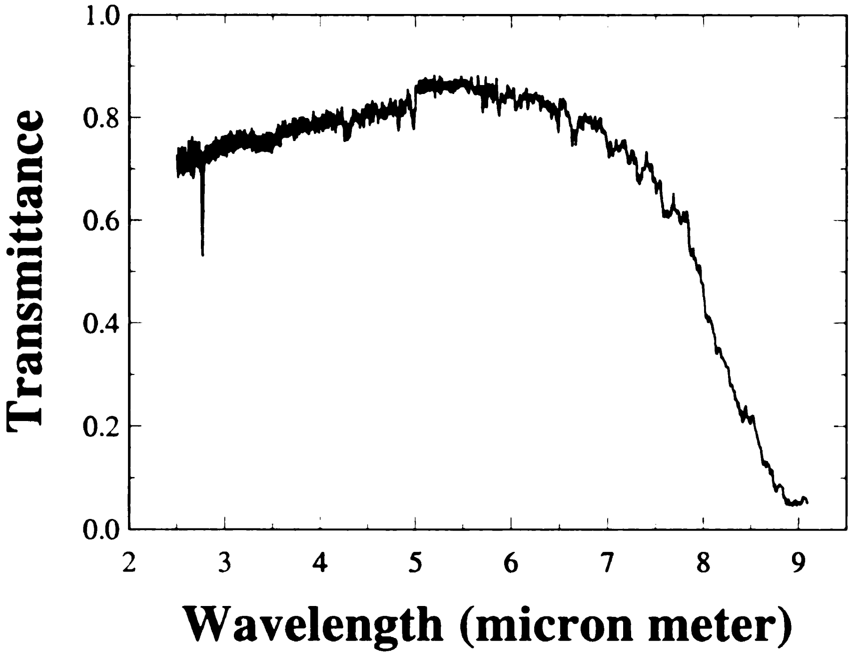

Figure 64. Transmittance of MgF_2 coated with polycarbosilane at 500°C with different spin rate.

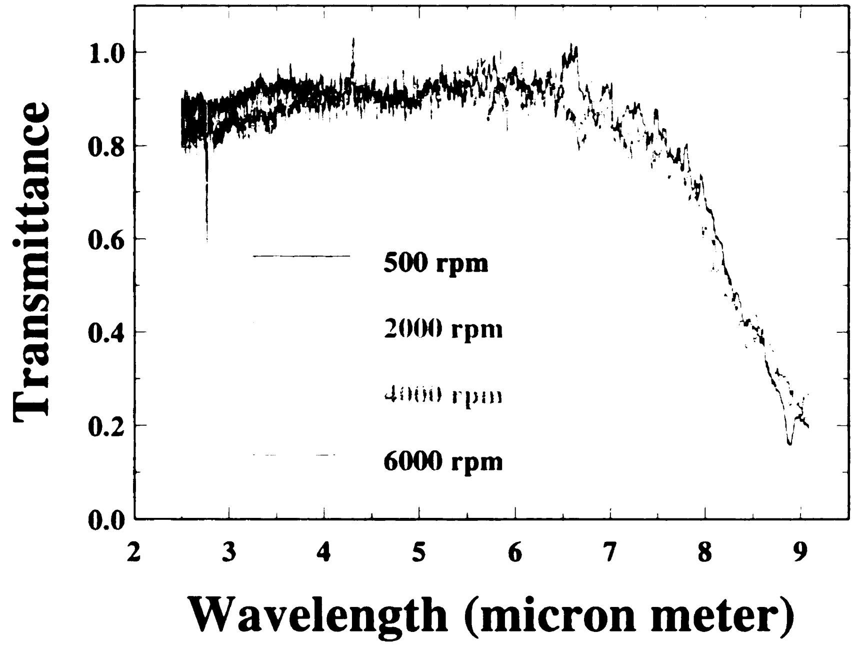

Figure 65. Transmittance of MgF_2 coated with polycarbosilane at 600°C with different spin rate.

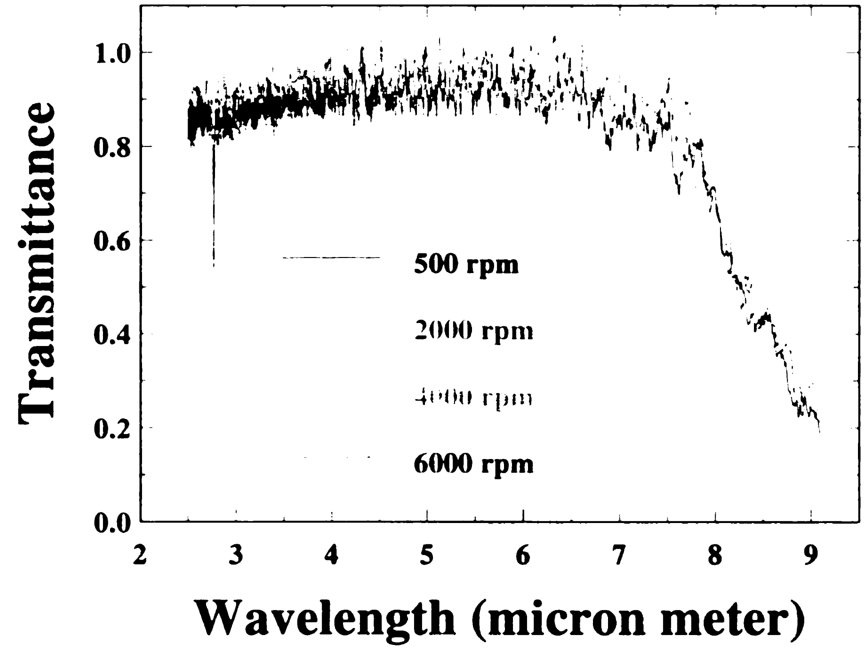

REFERENCES

1. L. L. Hench and J. K. West, *Principles of Electronic Ceramics*, pp 351-360, John Wiley & Sons, New York, NY (1990).

2. M. W. Barsoum, pp. 618 - 635 in *Fundamentals of Ceramics*, McGraw-Hill, New York, NY (1997).

3. C. Kittel, pp. 107-116 in *Introduction to Solid State Physics*, 5th ed., John Wiley and Sons, New York (1976).

4. D. W. Gray, page 6-62 in *American Institute of Physics Handbook*, Second Edition, McGraw-Hill Book Co., Inc., New York, NY (1963).

5. M. Eber and L. E. Jones, pp. 485 - 492 in *Ceramic Eng. and Sci. Proc.*, Volume 19[3], American Ceramic Society, Westerville, OH (1998).

6. M. V. Klein, pp. 201 - 209, *Optics*, Wiley and Sons, New York, NY (1970).

7. D. F. Diao, K. Kato, and K. Hokkirigawa, "Fracture Mechanics of Ceramics Coatings in Indentation", J. of Tribology, 116: 860 - 869 (1994).

3.7 Joining of Polycrystalline Ceramics And Ceramic Composites Using Microwave Heating

JOINING OF POLYCRYSTALLINE CERAMICS AND CERAMIC COMPOSITES USING MICROWAVE HEATING

ELDON D. CASE, KI-YONG LEE, AND JONG-GI LEE
Materials Science and Mechanics Department
Michigan State University, East Lansing, MI 48824

ABSTRACT

Microwave energy can be used to join a variety of ceramics, including both structural ceramics and optical (infrared) transmitting ceramics. A thin, spin-on interlayer can be successful in joining such materials. For optical materials such as MgF_2, microwave joining can produce joins that do not appreciably degrade the optical quality of the material.

INTRODUCTION

Microwave processing offers the potential for the rapid fabrication of ceramic/ceramic composite components of complex geometry. Spin-on layers are widely used for low-cost fabrication of electronic devices including integrated circuits and solar cells. Such layers provide protective layers, dielectric layers, and dopant sources. The

---

E. D. Case, K. Y. Lee, and J. G. Lee, "Joining of Polycrystalline Ceramics and Ceramic Composites Using Microwave Heating," Proceedings of the 33rd International Microwave Power Symposium, International Power Institute, Manassas, VA, pp. 17-20 (1998) spin-on material in liquid form is dispensed onto the surface to be coated. The substrate is then spun at high speeds, leaving a thin layer of the spin-on material.

Techniques for ceramic joining can generally be divided among methods employing a high externally-applied stress (such as diffusion bonding) and methods involving low external stress (such as brazing). Diffusion bonding joins materials at high temperatures and pressures, where solid state diffusion across the joined interface may be assisted by fluxes that enhance the mass diffusion rates (Sandhage, Schmutzler, Wheeler, and. Fraser, 1996; Santella, 1992). Diffusion bonding (and creep) can be a sensitive function of grain size, with the tendency for both creep and successful bonding increasing as the grain size decreases. For example, Elssner et al. showed that alumina plates with a mean grain size of 18 microns did not join, while similar alumina plates with a one micron average grain size did join when processed under nominally identical conditions (Elssner, Diem, and Wallace, 1981). In addition to structural materials such as alumina, optical ceramics, such as magnesium fluoride, have been joined using diffusion bonding (Yen ,. Chang Yu, Yen, Tsai, and Lin, 1991; Yen,. Chang, Tsai., Duh., and Yang, 1992).

Brazing is another method that has been used to join ceramics. In general, "brazing" may be defined as "a joining process in which a filler metal and a flux are sandwiched between the workpieces" (Schaffer, Saxena, Antolovich,. Sanders, and. Waner 1995). At elevated temperatures, the filler /flux system wets the surfaces to be joined. For ceramics, brazing has utilized oxide glasses, oxynitride glasses, metal particles slurries, and metal layers to join ceramic components (Sandhage, Schmutzler, Wheeler, and. Fraser, 1996). In this study, joining is done via thin, spin-on interlayers of silica or sodium silicate.

MATERIALS AND SPECIMEN PREPARATION

A number of polycrystalline ceramic materials have been joined by the authors and co-workers, including structural ceramics such as alumina and zirconia, electronic ceramics, such as alumina and MaCoR^{TM} and optical ceramics, such as magnesium fluoride (Lee, Case, Reinhard , 1997; Seiber, Lee and Case, 1997). The magnesium fluoride specimens were a polycrystalline commercial, hot-pressed material (Irtran-1, Eastman Kodak Company) with a mean grain size of approximately 3 microns. MaCoR^{TM} is a machineable glass ceramic (Corning Code 9658) that is reinforced with randomly-oriented platelets of fluromica. Rectangular specimens of the both MaCoR^{TM} and the magnesium fluoride were cut from as-received billets using a low-speed diamond saw.

For the polycrystalline alumina, disk-shaped specimens were pressed from as-received Sumitomo AKP50 powders having an average particle size of 0.23 microns. The smaller of the alumina specimens approximately 22 mm in diameter and two mm thick, when pressed uniaxially at pressures of approximately 32 MPa. Larger disks, having masses of up to 20 grams and as-pressed diameters of approximately 50 mm also were pressed and sintered. The polycrystalline zirconia specimens pressed in a similar manner to the alumina specimens, using Tsoh zirconia, 3-mol-percent yttria powders with an initial particle size of roughly 0.1 micron.

The bonding agents (that were used as spin-on materials in this study) include a sodium silicate solution (Columbus Chemical Company) and Silicafilm (Emulsitone Company, Whippany, NJ). "Silicafilm" is an organic liquid, which when pyrolyzed produces a film of amorphous silica.

Using an automated polishing system, all specimens were polished using a series of diamond abrasive grit sizes ranging from about 25 microns to 1 micron. For the magnesium fluoride specimens for which optical and infrared transmittance was measured, the specimens were polished on both faces, while the remaining specimens were polished on only one face. The silica film and the sodium silicate solution were applied to the polished specimen using a pipette, then the specimens were spun at speeds between about 500 rpm to 5000 rpm for approximately 20 seconds. For the silica film, the coatings were typically cured in air at 200°C for 20 minutes. After coating and curing, selected alumina, zirconia and MaCor^{TM} specimens, submillimeter-width notches were cut into the specimen surface using a stationary sonic mill (Sonic-Mill, Albuquerque, NM).

SINTERING AND JOINING

The microwave sintering of the alumina and zirconia powders, along with the subsequent joining of all of the specimens, was performed in a cylindrical single-mode microwave cavity, 17.78 cm in diameter (Model CMPR-250, Wavemat Inc., Plymouth, MI). The microwave power was generated by a 0 - 2000 Watt, 2.45 GHz continuous-wave power supply (Sairem Model MWPS 2000, Wavemat Inc., Plymouth, MI). The microwave system is equipped with automated sliding short and launch probe position controls (Figure 66). Details of the microwave cavity and power supply are given detail elsewhere (Lee, Case., Asmussen, and Siegel 1996).

Prior to heating in the microwave, the specimens to be sintered or to be joined were placed in a cylindrical refractory enclosure, which was in turn centered along the axis of the microwave cavity. The refractory enclosure (typically called a "casket") consisted of a hollow cylinder made from a partially-stabilized zirconia (ZYC, Zircar, Inc) with disc-shaped end plates made of an aluminosilicate refractory board (SALI, Zircar, Inc). The zirconia cylinder was 7 cm high with an outer diameter of 10.2 cm and the two aluminosilicate end plates were each 10.2 cm in diameter and 2 cm thick (Figure 67). Processing temperatures ranged from about 1050^0C for the Marcor^{TM} to about 1625^0C for the alumina. The specimen temperatures were measured using an optical pyrometer (Acufiber Optical Fiber Themometer, Model 10, Luxtron Co., Beaverton, OR), which was aligned with a viewport in the microwave cavity and a 5 mm diameter circular hole in the casket wall (Figure 67).

CHARACTERIZATION OF THE JOINED CERAMICS

Using the silica film interlayer, fifteen pairs of MaCor^{TM} specimens were successfully joined at temperatures between 1050^0C and 1075^0C. Five of the 15 specimens were joined with no externally-applied loading, while the 10 remaining specimens were joined using a 20 gram dead-weight load applied during joining using a sintered alumina disk placed on top to the specimen to be joined. Notches cut normal to the joined surfaces (using the Sonic-Mill) retained their shape very well during the joining process. For example, for a notch 331 microns depth and 228 microns wide prior to joining, the notch dimensions after joining decreased by only about 5-percent, to a width of 314 microns and a depth of 215 microns.

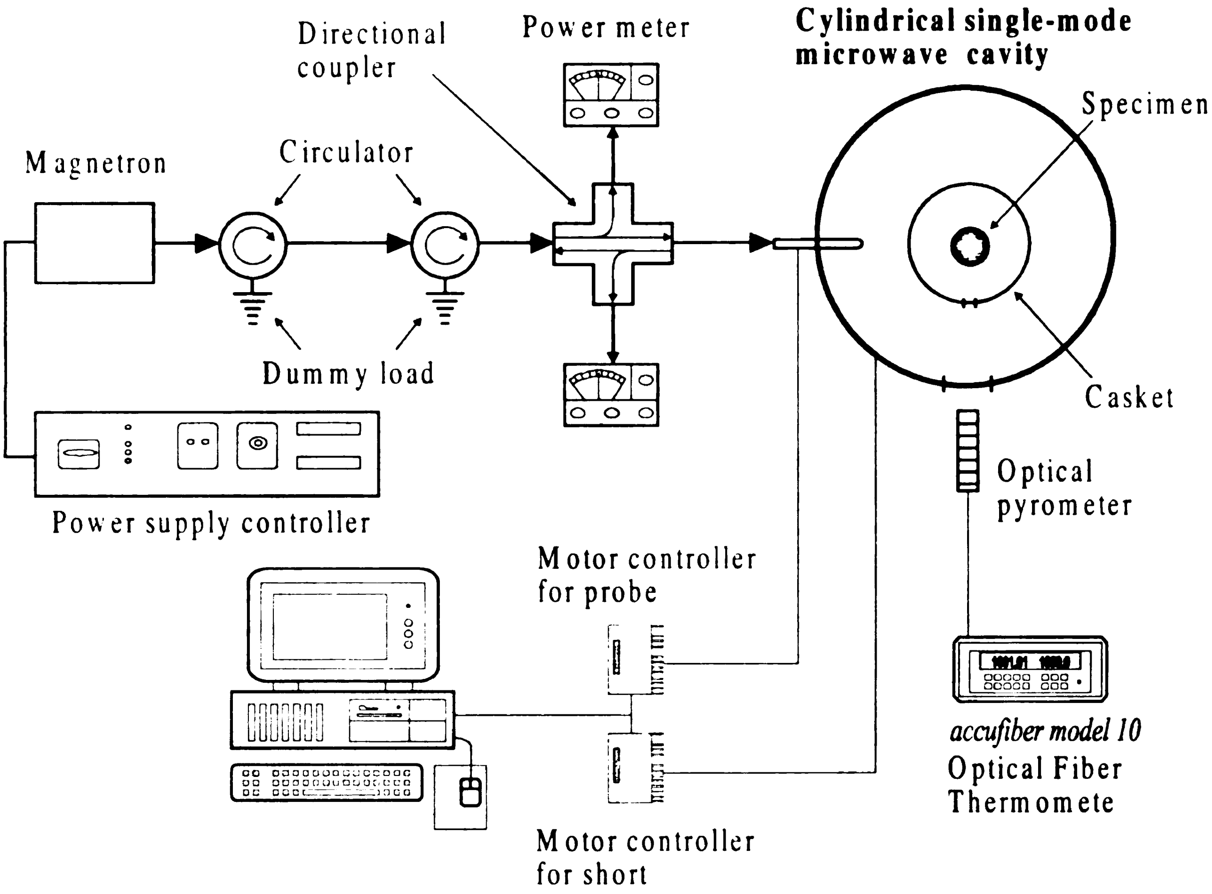

Figure 66. Schematic diagram of the microwave apparatus used to sinter and to join the ceramic specimens (after Lee, Case, and Asmussen, 1997).

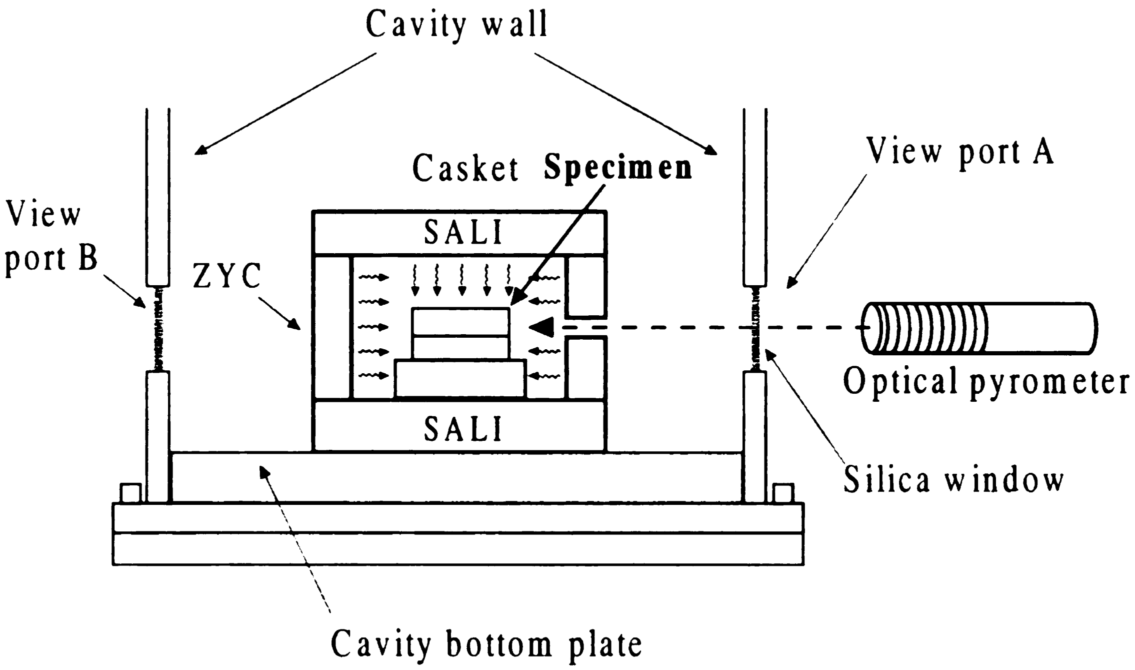

Figure 67. Schematic showing cross-sectional view of the microwave cavity, with the refractory casket centered along the cavity axis. The casket, composed of a hollow zirconia (ZYC) cylinder and disc-shaped aluminosilicate (SALI) endplates, encloses a ceramic specimen. The specimen temperature is measured by an optical pyrometer.

The microwave-sintered alumina specimens also were joined using a spin-on silica layer. Joining was accomplished at temperatures between about 1550^{0}C and 1640^{0}C. Microstructural examination in both a conventional Scanning Electron Microscope (SEM) and a Environmental Scaning Electron Microscope (ESEM) showed no apparent "bonding layer", the microstructure seemed quite continuous across what was the plane of the join. (Unlike the SEM, no conductive metal specimen coating is required to examine ceramic specimens in the ESEM, thus the joint region in the specimens could be examined in the ESEM without possible interference from an applied conductive surface coating. The joined alumina specimens were fractured in bend, and the fracture plane did not deviate at the join. In addition, Vickers indentation cracks were induced into the joined alumina specimens (near the interface), and the subsequent Vickers cracks propagated undeflected across the interface. The macrocrack behavior and the indentation crack behavior both suggest that the alumina/alumina bond has very high mechanical integrity. In addition to the alumina specimens, zirconia specimens were joined at temperatures from about 1450^{0}C to 1520^{0}C, but the mechanical properties of the bonds have not yet been fully evaluated.

The MgF_2 specimens did not join using the spin-on silica film, but the MgF_2 specimens did join upon heating at 700^{0}C for 20 minutes, using the sodium silicate solution as a bonding agent. The IR transmittance of the microwave-joined MgF_2 specimens was measured over the wavelength range of 880 nm to 1600 nm using a spectraphotometer. For specimens of equivalent thickness, the transmittance of the microwave-joined specimens was nearly identical to the transmittance for unjoined specimens over the measured wavelength range. MgF_2 specimens also were joined at under the same conditions (sodium silicate solution bonding agent, heated to 700^{0}C for 20 minutes), but using the conventional radiant heating rather than microwave heating. Due to scattering at second phases observed only in the bonded region of the conventionally-heated MgF_2, the transmittance of the conventionally-heated MgF_2 was considerably lower than the microwave-joined MgF_2 for specimens of equal thickness. At 1600 nm the transmittance of the microwave-joined specimens were about a factor of two higher than that for the conventionally-joined material.

CONCLUSIONS

Joins made using microwave heating of spin-on interlayers can be made both quite thin and quite strong. For the joined alumina specimens, the bond layer after joining could not be detected using a Scanning Electron Microscope. In addition, a Vickers indentation crack placed near the interface propagated across the interface without deflection.

The transmittance of optical and infrared materials can be a function of the joining technique, as was observed for magnesium fluoride. Presumably, the degradation of optical properties is due to optical scattering by second phases that form in the bond region during firing. The genesis of the differences in microstructure between the conventionally-fired and the microwave heated specimens needs further study.

Using spin-on interlayers and microwave joining, ceramic specimens can be joined without significantly perturbing either the dimensions or the geometry of submillimeter notches cut into the specimen (for the MaCor™, alumina, and zirconia specimens).

ACKNOWLEDGMENTS

The author acknowledges the financial support of the Michigan Research Excellence Fund provided through the Electronic and Surface Properties of Materials Center, Michigan State University

REFERENCES

1. Elssner, G., Diem, W. and Wallace, J. S., 1981, pp. 629-639 in "Surfaces and Interfaces in Ceramic and Ceramic-Metal Systems", Edited by J. Pask and A. G. Evans, Plenum Press, New York.

2. Lee K. Y, Case E. D., Asmussen, J. Jr., and Siegel M., 1996, "Binder Burnout in a Controlled Single-Mode Microwave Cavity," Scripta Materialia, 35[1]:107-111.

3. Lee K. Y, Case E. D., and Reinhard D., 1997, "Microwave Joining and Repair of Ceramics and Ceramic Composites," Ceramic Eng. and Sci. Proc., 18: 543-550.

4. Lee K. Y, Case E. D. and Asmussen, J. Jr., 1997, "The Steady-State Temperature as a Function of Casket Geometry for Microwave-Heated Refractory Caskets," Materials Research Innovations, 1[2]: 101-116.

5. Sandhage K. H., Schmutzler H. J., Wheeler R., and. Fraser H. L, , 1996, "Mullite Joining by Oxidation of Malleable, Alkaline-Earth-Bearing Bonding Agents", J. Am. Ceram. Soc., 79[7]: 1839-1850.

6. Santella M. L., "A Review of Techniques for Joining Advanced Ceramics", 1992, Amer. Ceram. Soc. Bull., 71: 947-954.

7. Schaffer J. P., Saxena A., Antolovich S. D.,. Sanders T. H, Jr., and. Waner S. B, 1995, pp. 718 - 720 in The Science and Design of Engineering Materials, Irwin Press, Chicago.

8. Seiber K. N., Lee K. Y and Case E. D., 1997, "Microwave and Conventional Joining of Ceramics using Spin-on Materials," pp. 941-949 in Proceedings of the 12th Annual Advanced Composites Conference, Technomic Publishing Co., Lancaster, PA.

9. Yen T. F.,. Chang Y. H, Yu D. L., Yen F. S., Tsai D. S., and Lin I-Nan, 1991, "Diffusion bonding of MgF_2 optical ceramics," Mat. Sci. and Engineering, A147 121-128.

10. Yen T. F.,. Chang Y. H, Tsai D. S., Duh S. L., and Yang S. J., 1992, “LiF-film-assisted diffusion bonding of MgF$_2$ ceramics,” Mat. Sci. and Engineering, A154, 215-221.

3.8 Joining Dissimilar Ceramic Materials

JOINING DISSIMILAR CERAMIC MATERIALS

J. G. Lee, E. D. Case, L. Zeng, and M. A. Crimp
Materials Science and Mechanics Department
Michigan State University
East Lansing, MI 48824

Abstract

Bi-material ceramic joins will be discussed, where the joining was accomplished by heating in a single-mode microwave resonant cavity. The joined ceramics include the following combinations of polycrystalline ceramics: (1) alumina and a partially stabilized zirconia (2) SiC platelet reinforced alumina and a glass ceramic, (3) hydroxyapatite and a glass ceramic, (4) zirconia - 3 mol% yttria and a glass ceramic and (5) an 85wt% alumina – 15 wt% partially stabilized zirconia particle composite and partially stabilized zirconia. The glass ceramic used was a commercial glass ceramic reinforced by mica platelets.

Introduction

The past few years, researchers have bonded ceramics with a variety of metals, other ceramics and with polymeric materials [1 -13]. A number of researchers have used brazing techniques to join metals with ceramics such as silicon nitride [1], sialon [2], molybdenum disilicide [3], and aluminum nitride [4]. In addition, ceramics have been joined to ceramics using brazing, where a metallic interlayer is used to join the ceramic components. However, the final bond thickness can be 40 to 50 microns thick or more [5].

E. D. Case, J. G. Lee, L. Zeng, and M. A. Crimp, "Joining of Dissimilar Ceramic Materials", Joining of Advanced and Speciality Materials II, ASM International, Materials Park, OH. pp. 10-17 (2000)

In contrast with the studies that join ceramics using thick bond layers, work done by the current authors and co-workers [6 - 10] has focused on minimizing the bond thickness. While we have joined like materials (such as alumina to alumina, or silicon carbide to silicon carbide), dissimilar ceramics have been joined, including: (1) alumina/zirconia- 3 mol% yttria, (2) SiC platelet reinforced alumina/glass ceramic, (3) hydroxyapatite/glass ceramic, and (4) zirconia - 3 mol% yttria/glass ceramic, where the glass ceramic used was MaCor^{TM}, a commercial glass ceramic reinforced by mica platelets and (5) an 85wt% alumina – 15 wt% partially stabilized zirconia particle composite and partially stabilized zirconia.

As used in this paper, the term "dissimilar" refers to a number of material properties. For example, among the ceramic materials included in this study (alumina, zirconia- 3 mol% yttria, SiC platelet reinforced alumina, hydroxyapatite, and a mica reinforced glass ceramic, MaCo^{rTM}) the linear coefficient of thermal expansion ranges from a 9 X 10^{-6} K^{-1} for zirconia to 17.5 X 10^{-6} K^{-1} for HAP (Table 21). In addition, the thermal conductivites and the Young's modulus for the materials included in this study also span a broad range of values (Tables 22 and 23).

Experimental Procedure

Materials

Two of the materials used in this study were commercially obtained as densified billets, while the remaining materials were microwave sintered from commercially available powders. One of the commercial materials included in this study was MaCor^{TM} (Corning Code 9658), which is a flurophlogopite mica platelet reinforced glass ceramic

in the system SiO_2-Al_2O_3-MgO-K_2O-F. In addition to MaCor™ , the other commercial material included was an Al_2O_3/SiC platelet composite material having 80 volume % alumina and 20 volume % SiC platelets (Max Tech, Inc, Lansing MI).

The three commercial ceramic powders used in this study include a partially stabilized zirconia powder, an alumina powder, and a hydroxyapatite (HAP) powder (Table 24). The partially stabilized zirconia powder was a 3 mol % yttria-zirconia powder (TZ-3YS, Tosoh Ceramic Division, Bound Brook, New Jersey) powder having a vendor-specified initial particle size of 350 nm and 7 m^2/g specific surface area, as determined by BET measurements [14]. A 99.99 % pure alumina power (TMDAR, Taimi Chemicals Co. LTD) was also used, which has a vendor-specified specific surface area of 13.6 m^2/g specific surface area and a 0.21 micron average initial particle size, and 2.32 g/cm^3 green density. The calcium hydroxyapatite (HAP, $Ca_{10}(OH)_2(PO_4)_6$) specimens were prepared using a nominally 99% pure powder (Cerac™ Incorporated Specialty Inorganics) having an initial particle size of roughly one micron as determined by direct SEM measurements on the HAP powders.

Specimen preparation

The alumina, zirconia, and the alumina/zirconia composite powder specimens were first made into powder compacts using uniaxial pressing in a hard die at approximately 32 MPa. The as-pressed dimensions of the disk-shaped powder compacts were approximately 2 cm in diameter and 2 mm in thickness. All of the specimens sintered in this study were processed inside an aluminosilicate casket (Figure 68) using a microwave cavity (Figure 69).

For the alumina and zirconia powders, four to seven compact powder specimens were then sintered in a 2.45 GHz single mode microwave cavity (Model CMPR-250, Wavemat, Inc., Plymouth, MI, Figure 69). The microwave power supply was a Sairem, Model MWPS 2000, which generates from zero to 2000 Watts of microwave power. During sintering, the sintering temperature was controlled by adjusting an input power with automatic sliding short and probe [6 - 10].

Before sintering, the specimens were placed in a ceramic specimen enclosure (casket) composed of a hollow, porous partially stabilized zirconia cylinder capped on the top and bottom with disk-shaped aluminosilicate end plates (Figure 69). The casket was then placed in the microwave cavity, which the center of the casket aligned coaxially with the microwave cavity. The specimen temperature was monitored using an optical pyrometer system (Accufiber Optical Fiber Thermometer, Model 10, Luxtron Co., Beaverton, OR), which was sighted through a 0.5 mm circular hole that was drilled through the porous zirconia cylinder that comprised the body of the casket.

In contrast to the microwave sintering of the alumina and zirconia compacts, all the HAP specimens included in this study were sintered in air in a conventional furnace at 1300°C for 11 hours, giving relative densities of up to approximately 95 percent of theoretical.

For the commercially densified materials, the as-received billets of both the MaCor^{TM} and the Al_2O_3/SiC platelet composites (Max Tech, Inc, Lansing MI) were cut into specimens approximately 1 cm × 1cm using a low speed diamond saw.

All of the ceramic materials included in this study were polished using a series of diamond paste, with grit sizes from 35 microns to 1 micron. After polishing, the specimens were cleaned for 20 minutes in an ultrasonic cleaner using de-ionize water and detergent.

After polishing and cleaning, the specimens were coated with the organic silica precursor liquid (Emulsitone Company, Whippany, New Jersey). In order to coat the specimens with a thin, uniform film of silica, the specimens were placed on a commercial high speed substrate spinner. Four to five drops of the silica precursor were pipetted onto the specimen surface. The specimens were spun at 3000 rpm for 20 seconds, followed by curing in air in an electrically heated furnace for 20 minutes at 200^{0}C.

Joining Procedure

Joining was performed via microwave heating. The coated specimens were placed in the same 2.45 GHz single-mode microwave cavity (Model CMPR-250, Wavemat Inc., Plymouth, MI) used in sintering the powder compacts. Also, the same cylindrical zirconia refractory casket insulated the specimens during joining. Alumina dead weights ranging from 20 to 50 grams were placed on the specimens prior to joining. The joining was performed at temperatures between 1020°C to 1500°C (Table 25). A summary of the joining conditions is given in Table 25.

The joined specimens were then sectioned using a low speed diamond saw. The cut sections of the specimens were mounted with in a thermal setting polymer. The cut surfaces were polished with a series of diamond paste. The joined specimens were then examined in a Scanning Electron Microscope (SEM).

TEM specimens were prepared by sectioning joined specimens in a low speed diamond saw. Disks 3 mm in diameter were then cut from the sections using an ultrasonic disk cutter. The disks were glued into Molybdenum rings and dimpled using a VCR

Model D500I dimpler. The final thinning was done using a Gatan PIPS with single-sided milling at an angle of 4 degrees. TEM observations were made at 200 kV using a Hitachi H-800 microscope.

Results and Discussion

Dissimilar ceramics may also be taken to mean dissimilar in terms of their use. The ceramics included in this study represent a broad spectrum of current and potential uses, as will be briefly discussed here.

MaCor^{TM} is used as electrical and/or thermal insulators and structural components, as well as in electrical and opto-electronic devices [15]. MaCor^{TM} is a very interesting material since it is machinable using ordinary metal working tools. The physical basis for the machinability of MaCor^{TM} is the mica platelets that are randomly distributed in its glass ceramic matrix. Cracks that form during the machining of MaCor^{TM} interact with the mica platelets such that when the MaCor^{TM} is machined, cracks deflect around the platelets rather than propagating long cracks. Ceramic – ceramic joining that provides a machinable ceramic base for a component or component assembly has many potential advantages. For example, such machinable bases may aid in interfacing ceramic components in a variety of environments, such as allowing convenient attachments for engine or biological applications.

HAP is a bioacitve ceramic material, in that when it is in contact with either blood or simulated biological fluid, bone grows on its surface. In fact, the major mineral constituent of both bones and teeth is HAP, although living bones and teeth have a significant non-mineral content. Consequently, HAP is used for hard tissue implants because of its close resemblance to human bone and teeth.

Alumina and zirconia have widespread use as ceramic materials. The 3 mol% yttria-partially stabilized zirconia included in this material has excellent fracture toughness. Both alumina and zirconia have important uses as bioinert ceramics [19], ceramics that unlike HAP do not induce bone growth and their surfaces when subjected to biological fluids, and hence are use materials for replacement joint surfaces, where one does not wish to induce bone growth [19].

The alumina – zirconia joins (Figures 70 and 71) were quite interesting. The SEM micrograph (Figure 70) shows are very interface that lacks a discernable interface. In fact, the interface is slightly uneven (on the scale of the grain size within the specimen). In greater detail, the TEM micrograph (Figure 71) shows that after joining, the interface between the two materials lack an apparent interface layer, although a silica layer (approximately 150 nm thick) had been applied to both the alumina and the zirconia prior to joining. These types of microstructures are similar to those observed during Transient Liquid Metal Phase bonding in alloy materials [21].

Figure 72 shows a channel, approximately 400 microns wide at the "top" of the channel and about 175 microns deep that was formed in a 85 wt% alumina – 15 wt% zirconia specimen. Figure 72 depicts the channel following sintering of the 1350^0 C for one hour in the microwave cavity described in the experimental procedure section. The specimen was then polished and joined with a sintered and polished zirconia disk (Figure 73), where the joining was done at 1450^0C, with a hold time of 20 minutes and a dead weight loading of 20 grams (Table 26). As was the case with the other joins, a silica interlayer was used, where the silica film was applied to only the zirconia before joining. Such channels could be of interest in to distribute fluids (such as cooling fluids, fuels, or biological fluids) in a component.

For the MaCor^{TM} – 3 mol% yttria-zirconia bonds, SEM and TEM micrographs are shown in Figures 74 and 75, respectively. Figure 75 shows considerable grooving of grains at the MaCor^{TM} – zirconia interface, which may be indicative of considerable local dissolution of the zirconia.

It should be emphasized that although silica interlayers were applied to all specimens prior to bonding, preliminary TEM observations of the joints has revealed direct bonding of the base materials, with no evidence of interfacial bond layers. For example, Figure 75 shows the interface between MaCor^{TM} and 3-mole% Y stabilized ZrO_2, which shows extensive wetting of the ZrO_2 by the glassy matrix of the MaCor^{TM}. This results in significant interlocking along the interface. In comparison, the TEM micrographs of the Al_2O_3-ZrO_2 bonds (Figure 71), show some wetting, but the wetting that is observed is more limited than in the MaCor^{TM}-ZrO_2 case. The Al_2O_3 and ZrO_2 appear to have bonded directly and possesses sharp interfaces. These results indicate that there may be a number of joining mechanisms operative in this specimens as one spans the spectrum of materials with a considerable glassy phase (such as MaCor^{TM}) to those materials with very limited grain boundary phases, such as the alumina and zirconia materials included in this study.

Acknowledgments

The authors acknowledge the financial support of the Composite Materials and Structures Center and the Electronic Surface and Properties of Materials Center, College of Engineering, Michigan State University.

Table 21. Thermal expansion coefficients for the Materials Included in this Study

Materials	Temp. Interval	Thermal expansion (10^{-6} K^{-1})	References
MaCor™	25°C-300°C	9.3	15
Al_2O_3	25°C-1000°C	8.8	17
ZrO_2	Room Temp	9	14
ZrO_2	25°C-1000°C	11	14
HAP	25°C-400°C	14.5	16
HAP	400°C-800°C	17.5	16

Table 22. Thermal Conductivites of the Materials Included in this Study

Materials	Thermal conductivity	References
MaCor™	1.46 W/m ·°C	15
Al_2O_3	30.0-35.0 W/m ·K	18
ZrO_2	N/A	
HAP	0.013 J s^{-1} cm^{-1} K^{-1}	20

Table 23. Young's moduli for the Materials Included in this Study

Materials	Young's moduli	References
MaCor™	64 GPa	15
Al_2O_3	390 GPa	18
ZrO_2	190 GPa	18
HAP	80 –100 GPa	19

Table 24. Sintering conditions for materials used in this study.

Materials	Initial particle size	Mass	Sintering Temp	Sintering Time	Final Density
Alumina	0.21 μm	2 grams	1300°C	1 hour	96 %
Zirconia	0.59 μm	3 grams	1375°C	1 hour	97 %
HAP		10 grams	1300°C	11 hours	2.974 g/cm^3

Table 25. Processing conditions for dissimilar materials using microwave power.

Materials Joined	Spin-on interlayer	Joining Temp(°C)	Hold Time (min)	Dead Weight (gm)
ZrO_2 with Al_2O_3	Silica film	1500	20	50
HAP with MaCor^{TM}	Silica film	1020	20	20
ZrO_2 with MaCor^{TM}	Silica film	1020	20	20
SiC/Al_2O_3 with MaCor^{TM}	Silica film	1020	20	20

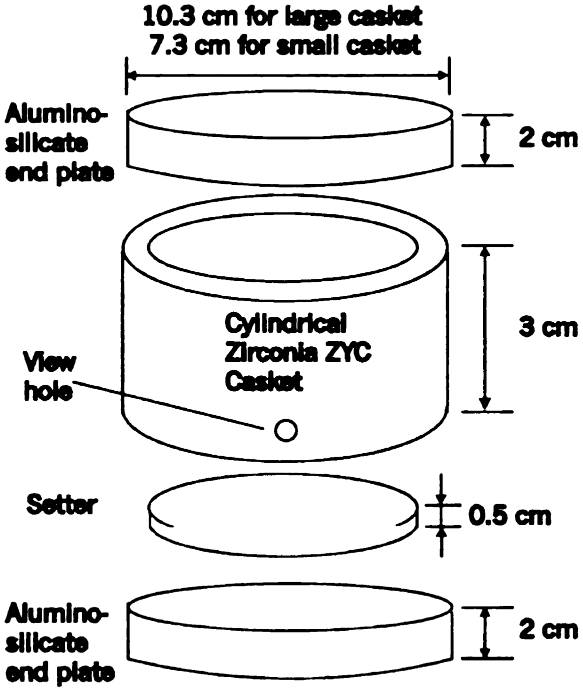

Figure 68. Schematic of the insulating casket used in this study for both microwave sintering and microwave joining.

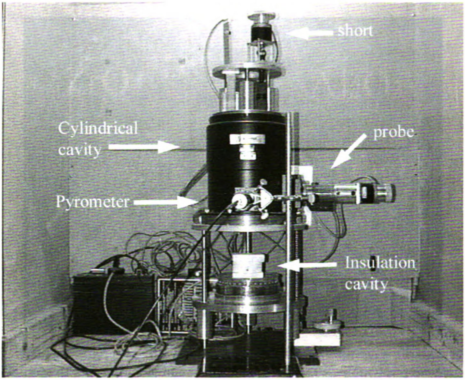

Figure 69.Photograph of the single-mode, 2.45 GHz microwave cavity used both to sinter the alumina, zirconia, alumina/zirconia powders and to join all specimens included in this study. The pyrometer and the insulating cavity (casket) also are shown.

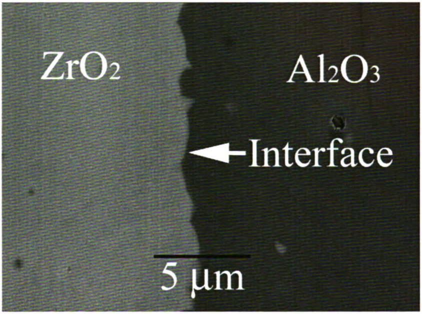

Figure 70. SEM micrograph of the bond region of a joined alumina – zirconia specimen. Note the absence of a discernable bond layer between the two joined specimens.

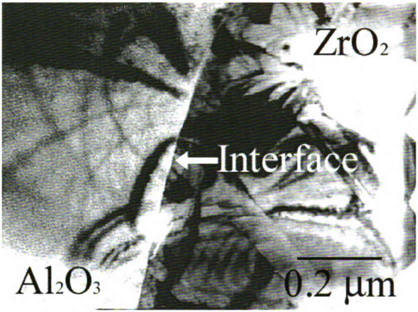

Figure 71. A TEM micrograph of the bond region of the same alumina – zirconia specimen depicted by an SEM micrograph in Figure 70. In the TEM micrograph, no significant bond layer is visible.

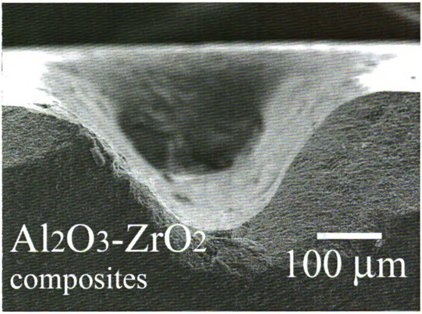

Figure 72. A SEM micrograph of a microwave-sintered 85 wt % alumina – 15 % zirconia specimen containing a "pressed-in" channel.

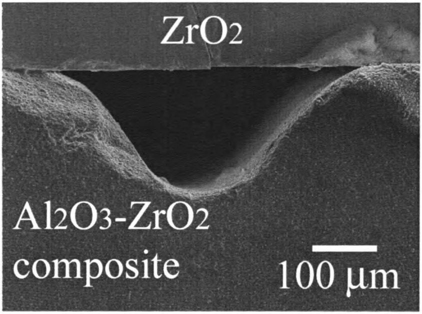

Figure 73. The notched 85 wt % alumina – 15 wt% zirconia specimen depicted in Figure 72, joined with a partially stabilized zirconia (3 mol% yttria – zirconia) specimen.

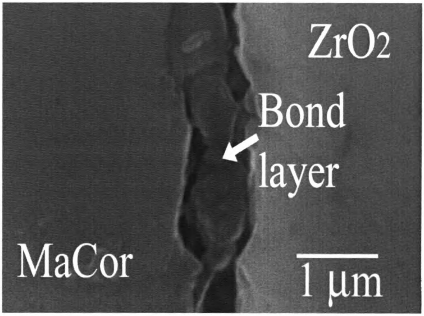

Figure 74. A SEM micrograph of the join between zirconia and MaCor^{TM}.

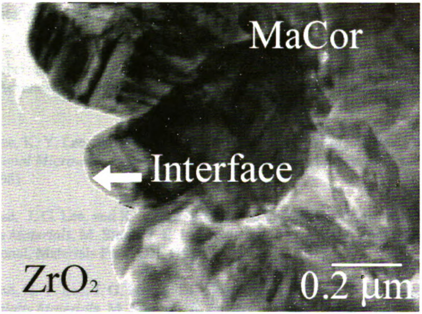

Figure 75. A TEM micrograph of the MaCor^{TM} – zirconia join, for which there appears to be extensive wetting of the interface by the glassy matrix phase of MaCor^{TM}.

References

1. G. Chaumat, B. Drevet, and L. Vernier, *J. European Ceram Society*, 17 [15-16], 1925-27 (1997).

2. A. P. Xian, *J. Materials Science*, 32 [23], 6387-93 (1997)

3. S. D. Conzonne, D. P. Butt, A. H. Bartlett, *J. Mater. Sci*, 32 [13], 3369-74 (1997)

4. D. Huh and D. H. Kim, *J. Materials Res.*, 12 [4], 1048-55 (1997)

5. L. Esposito, A. Bellosi, S. Guicciardi, G. de Portu, *J. Mater. Sci.*, 33 [7] 1827- 36 (1998)

6. K. N. Seiber, K. Y. Lee, and E. D. Case, pp. 941-949 in *Proceedings of the 12th Annual Advanced Composites Conference*, Technomic Publishing Co., Lancaster, PA. (1997)

7. E. D. Case, K. Y. Lee, and J. G. Lee, pp. 17 - 20 in *Proceedings of the 33rd International Microwave Power Symposium*, International Power Institute, Manassas, VA. (1998)

8. E. D. Case, J. G. Lee, and K. Y. Lee, pp. 17 - 26 in *Joining of Advanced and Specialty Materials*, M. Singh, J. E. Indacochea, and D. Hauser, eds., ASM International, Materials Park, OH. (1998)

9. E. D. Case, K. Y. Lee, J. G. Lee, and T. Hoepfner, pp. 27 - 34 in *Joining of Advanced and Specialty Materials*, M. Singh, J. E. Indacochea, and D. Hauser, eds., ASM International, Materials Park, OH. (1998)

10. J. G. Lee, K. Y. Lee and E. D. Case, pp. 509 - 520 in *Ceramic Transactions*, Volume 94, American Ceramic Society, Inc., Westerville, OH. (1998)

11. C. Mukherjee and Eldon D. Case, submitted, *J. European Ceram. Soc.* (1999)

12. C. Mukherjee, E. D. Case, K. Y. Lee, and A. Lee, accepted for publication, *J. of Mat. Sci.* (1999)

13. C. Mukherjee, E. D. Case and A. Y. Lee, Accepted for publication, *Ceramic Eng. and Sci. Proc.*, Volume 20. (1999)

14. For Tosoh TZ-3YS partially stabilized zirconia powders, data from vender web site (www.tosoh.com)

15. MaCor^{TM} data from vender (Corning) web site

16. Je-Won Choi, Young-Min Kong, and Hyoun- Ee Kim, *J. Am. Ceram. Soc.*, 81 [7] 1743-48 (1998)

17. W.D. Kingery, H.K. Bowen, and D.R.U. Uhlmann, p 595, *Introduction to Ceramics*, Second Edition, New York, N.Y. (1976)

18. M. Barsoum *Fundamental of Ceramics*, p 401 and 505, First edition, McGraw-Hill, New York, N.Y. (1997)

19. L. L. Hench, *J. of Am. Cer. Soc.*, 81, [7] 1711 (1998)

20. Kijima T, Tsutsumi M, *J. of Am. Cer. Soc.*, 62, 455-60 (1979)

21. W. F. Gale, *JOM*, 51[2], 49 – 52, (1999).

Discussion and Conclusion

4.1 Thermal Stress in the Dissimilar Ceramics Joined in This Thesis

In this thesis, the dissimilar ceramics were joined using a silica spin-on interlayer (section 3.8 in this thesis). The different thermal expansion between two dissimilar ceramics caused thermal stress in the joint. We shall use research of Ning et al. [61] and Lee et al. [57] to help in our analysis of stresses developed in the materials joined in this thesis.

Ning et al. [61] reported joining of Si_3N_4 (13 mm square and 20 mm long) with a 99.992 % pure aluminum foil (no dimension was reported) to produce a 6 mm thick braze. The bond layer formed a silica –alumina noncrystalline layer after the specimen was heated at 800°C between the Si_3N_4 and Al braze. The thermal expansion mismatch caused thermal stress in the joint upon cooling. According to Ning et al. [61], "If two dissimilar materials can deform only elastically with stress and the stresses developing on both sides of the bond layer do not interfere with each other" [59]. Ceramic materials used in this thesis deform elastically to fracture. Ning et al. [61] evaluated the thermal stress of dissimilar joined specimens using the mismatch in coefficient of thermal expansion by [57, 61]

$$\sigma_i = -\sigma_j = \frac{E_i E_j}{E_i + E_j}(\alpha_i - \alpha_j)\Delta T \qquad (1)$$

where E is Young's modulus, α is the thermal expansion coefficient, ΔT is (T_{final}-$T_{initial}$) and *i* and *j* are the materials being joined. Assuming elastic deformation, $\sigma_i = E_i \varepsilon_i$ and $\sigma_j = E_j \varepsilon_j$, where the thermal strain is given by $\varepsilon_i = \alpha_i \Delta T$ and $\varepsilon_j = \alpha_j \Delta T$. In figure 76, material *i*, which has a lower thermal expansion coefficient, experiences a compressive stress and material *j*, which has a higher thermal expansion coefficient, experience a

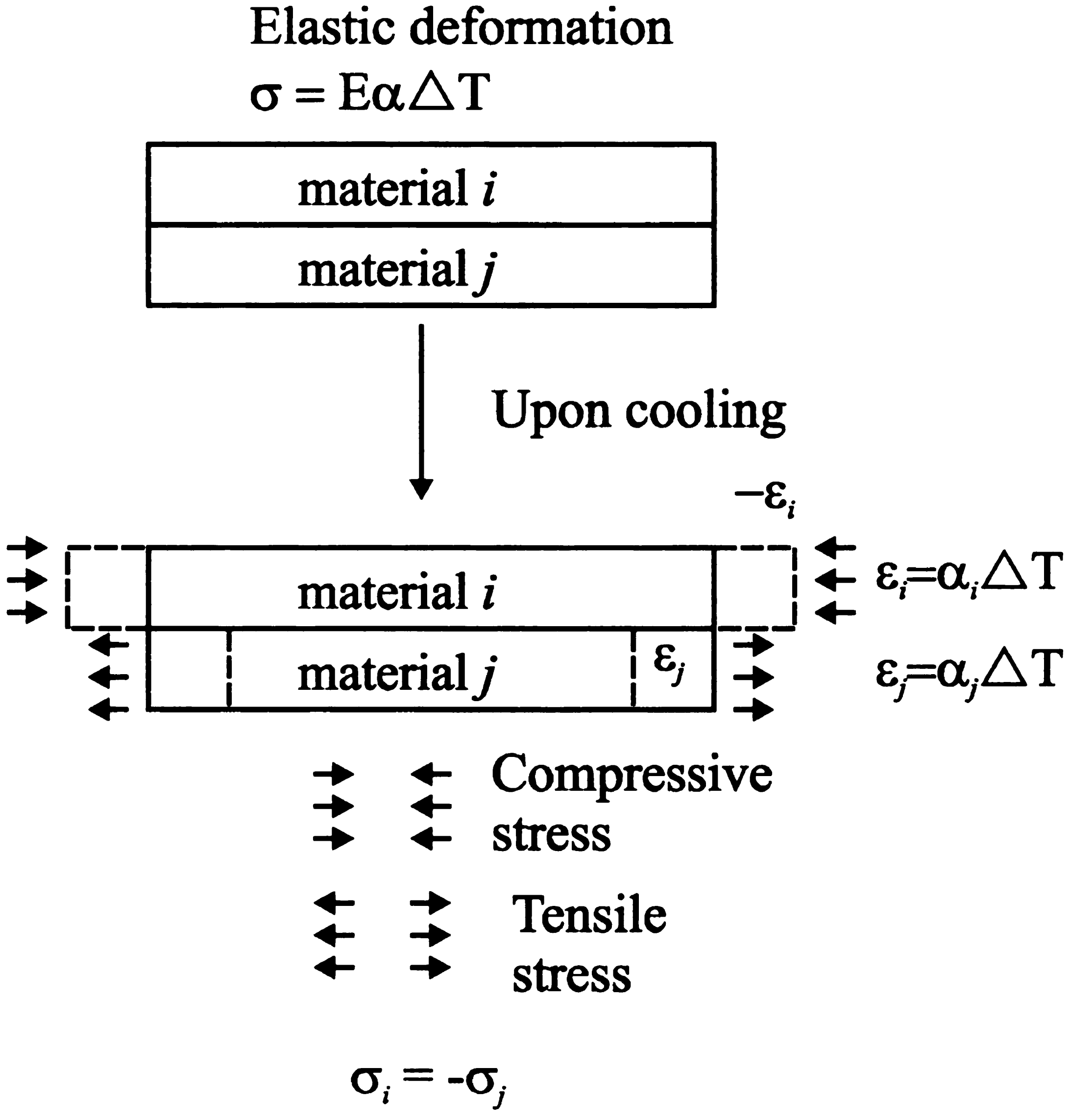

Figure 76. A schematic of the thermal stress induced in two different joined materials upon cooling.

tensile stress. The tensile and compressive stresses are equal in magnitude, thus, $\sigma_i = -\sigma_j$.

Equation (1) may be derived as follows:

$$\sigma_i = E_i\varepsilon_i = -\sigma_j = E_j\varepsilon_j \tag{2}$$

$$\varepsilon_{total} = \varepsilon_i - \varepsilon_j \tag{3}$$

$$\varepsilon_i = \frac{\sigma_i}{E_i} \text{ and } \varepsilon_j = \frac{\sigma_j}{E_j} \tag{4}$$

$$\varepsilon_{total} = \frac{\sigma_i}{E_i} - \frac{\sigma_j}{E_j} = \frac{\sigma_i}{E_i} + \frac{\sigma_i}{E_j}(\sigma_i = -\sigma_j) \tag{5}$$

$$\varepsilon_{total} = \sigma_i\left(\frac{1}{E_i} + \frac{1}{E_j}\right) \tag{6}$$

solving for σ_i gives

$$\sigma_i = \frac{E_i E_j}{E_i + E_j}\varepsilon_{total} \tag{7}$$

since $\varepsilon_{total} = \varepsilon_i - \varepsilon_j$ and $\varepsilon_{total} = \alpha_i\Delta T - \alpha_j\Delta T = (\alpha_i - \alpha_j)\Delta T$ (8)

since ΔT the same in both cases. Substituting equation (8) into (7) yields

$$\sigma_i = \frac{E_i E_j}{E_i + E_j}(\alpha_i - \alpha_j)\Delta T = -\sigma_j$$

Figure 77 showed different thermal stress distribution between two materials being joined. Compressive stress (lower thermal expansion) was denoted with minus sign while tensile stress was denoted with plus sign.

Ning et al. [61] assumed the silica –alumina noncrystalline layer to be mullite. The thermal stresses calculated according to equation (1) were (for the following dissimilar

Table 26. Thermal properties of materials used in reference [61].

Materials	Thermal expansion (10^{-6} K^{-1})	Young's moduli
Al	23	70 GPa
Si_3N_4	2	300 GPa
Mullite	5	100 GPa

Table 27. Thermal properties of materials used in reference [57].

Materials	Thermal expansion (10^{-6} $^oC^{-1}$)	Young's moduli
Al_2O_3	7.8	330 GPa
Inconel 600	12.1	214 GPa
Ti braze	8.9	106 GPa

material combinations) Si_3N_4/Al = 476 MPa, Si_3N_4/mullite = 114 MPa, and mullite/Al = 296 MPa, the data from Table 26. Ning et al. [61] explained that the lower thermal stress in the Si_3N_4 and silica-alumina noncrystalline layer due to smaller CTE difference between the Si_3N_4 and silica-alumina noncrystalline layer than that of CTE difference between the Si_3N_4 and Al. However, no cracks were reported for Si_3N_4/Si_3N_4 joint using the Al braze with a joint strength of 146 MPa. Thus, the strength of the joint was not strong enough to overcome the thermal stress. Following Ning et al. [61], Lee et al. [57] joined 10 mm x 10 mm x 5 mm bar of 99 % alumina that was joined with a 10 mm diameter and 5 mm height Inconel 600 disk. The Inconel 600/alumina specimen showed a crack in the alumina joint. Using table 27 and $\triangle T = 1000^oC$, the thermal stress was about 560 MPa. Due to the thermal stress, a crack was produced continuously at the alumina joint (Figure 78). As expected from Ning et al's work [61], the joint strength was poor due to high thermal stress. Lower thermal stress was calculated 90 MPa (using table 27). When a Ti braze was used as a bond agent, no cracks were found.

Table 31 shows calculated thermal stress values of joined alumina with zirconia (3 mol % yttria), zirconia (3 mol % yttria) and MaCor^{TM} with HAP used data from table 28 and 29. These thermal stresses may exceed the strength of materials being joined and thus could produce a crack in the bond layer. However, unlike the results from Ning and Lee, no cracks were observed despite the difference in CTE (Coefficient of Thermal Expansion) between two substrates. Silica-film after coating and curing was about 130 nm (very thin), thus, the bond layer was ignored to calculate thermal stresses of joined Al_2O_3 with ZrO_2 (Figure 70), HAP with MaCor^{TM} (Figure 38), and ZrO_2 with MaCor^{TM} (Figure 74).

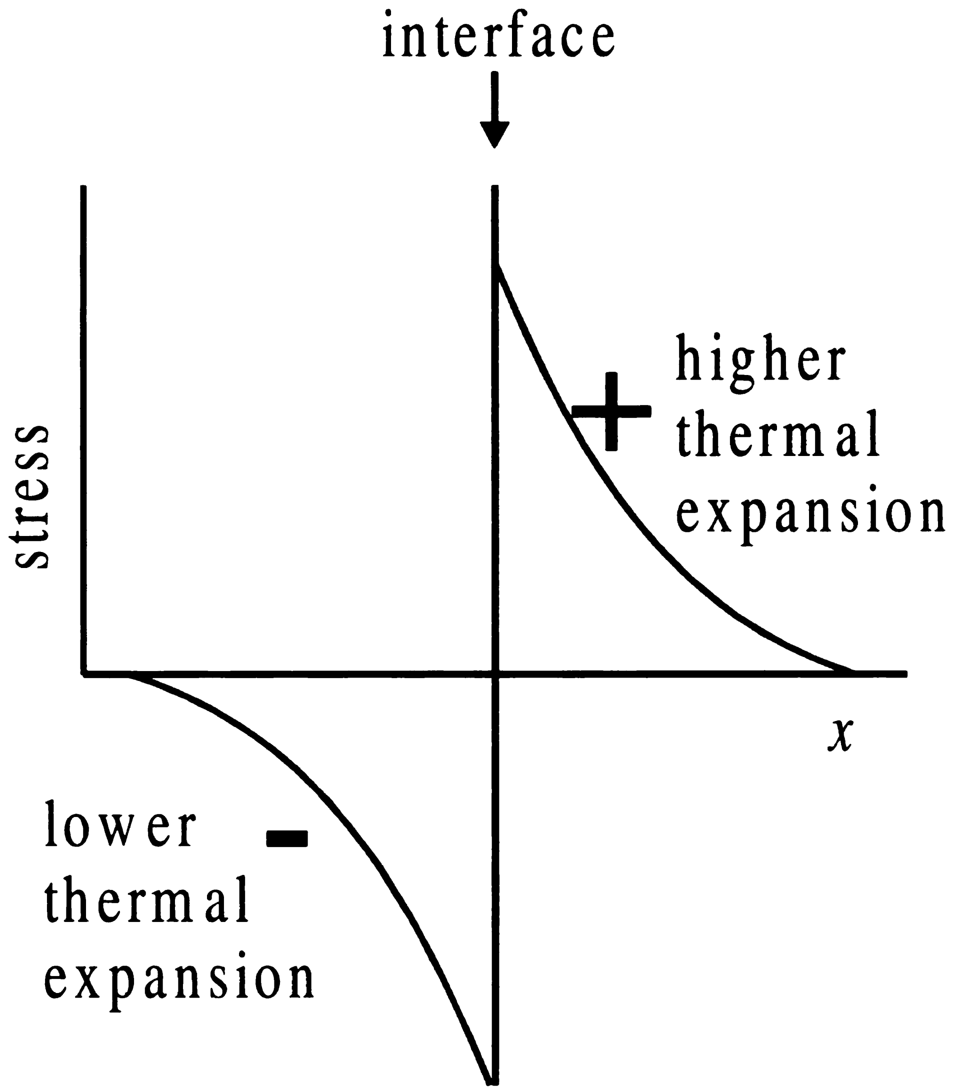

Figure 77. A schematic of different thermal stress distribution between two materials that have been joined along a planar interface [61].

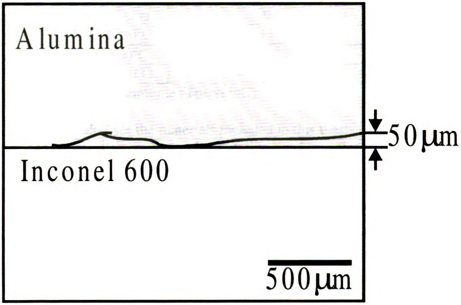

Figure 78. A continuous crack occurred in alumina due to compressive thermal stress. The spacing between alumina and interface was about 500 µm and the crack started from the interface [57]

Table 28. Thermal expansion coefficients for the materials included in this thesis.

Materials	Temp. Interval	Thermal expansion (10^{-6} K^{-1})	References
MaCor™	25°C-300°C	9.4	58
	25°C-600°C	11.4	
	25°C-800°C	12.6	
Al_2O_3	25°C-1000°C	8.8	38
ZrO_2^*	Room Temp	9	60
ZrO_2*	25°C-1000°C	11	59
HAP	25°C-400°C	14.5	41
HAP	400°C-800°C	17.5	

ZrO_2* : 3 mol % ytrri – zirconia (Tosoh InC)

Table 29. Young's moduli for the materials included in this thesis.

Materials	Young's moduli	References
MaCor™	64 GPa	43
Al_2O_3	390 GPa	39
ZrO_2*	200 GPa	60
HAP	80 – 100 GPa	36

ZrO_2* : 3 mol % ytrri – zirconia (Tosoh InC)

Table 30. Poisson's ratio for the materials included in this thesis.

Materials	Poisson's ratio	References
MaCor™	0.29	58
Al_2O_3	0.25	39
ZrO_2	0.30	60
HAP	0.28	62

Table 31. Calculated thermal stress values of joined specimens

Joined Materials	Calculated Thermal stress
Al_2O_3/ZrO_2	501 MPa
ZrO_2/MaCor™	100 MPa
HAP/MaCor™	247 MPa

Alumina with zirconia joined specimen showed an almost invisible bond layer and no cracks although occassional quasi-elliptical pores were observed in the bond layer. Alumina has a lower thermal expansion coefficient. From equation (1), the calculated thermal stress was 501 MPa which is a compressive in the alumina. The partially stabilized zirconia tensile strength was 520 MPa [63]. The calculated thermal stress in the partially stabilized zirconia was 501 MPa. Thus, the partially stabilized zirconia tensile strength was higher than the thermal stress induced due to joining PSZ with alumina. The MaCor^{TM} tensile strength was 90 MPa [64] and the calculated thermal stress in joined HAP with MaCor^{TM} was 247 MPa. Due to the thermal expansion coefficients (equation 1) the stress in the MaCor^{TM} should be tensile. Since the tensile stresses in MaCor^{TM} far exceed its tensile strength, the MACor^{TM} should fracture according to equation (1). However, no cracks were found with MaCor^{TM}.

4.2 Summary of Results

Thin and strong bond layers can be produced using spin-on interlayers as bonding agents in ceramic/ceramic joining. Using various spin-on interlayers, ceramic/ceramic joining was successfully done in this thesis. The joined ceramics include MgF_2/MgF_2 ([49], section 3.1 of this thesis), alumina/zirconia composites with alumina/zirconia composites, a mica platelet reinforced glass ceramic (MaCor^{TM}) with zirconia -3mol % yttria, MaCor^{TM} with polycrystalline hydroxyapatite and SiC platelet reinforced alumina with MaCor^{TM} ([50], section 3.2 in this thesis), alumina with zirconia –3 mol % yttria ([56], section 3.8 in this thesis), and SiC with SiC ([53], section 3.5 in this thesis).

The optical transmittance of joined MgF_2 [49] was higher for the microwave joined specimens than for the conventionally joined specimens. Microwave joined infrared material (MgF_2) showed optical absorption factor α (0.156) which was similar to the α value measured for a polished MgF_2 specimen (0.149). Conventionally joined MgF_2 showed higher α (0.342) due to second phases in the bond-layer caused by optical scattering, where the higher α value indicates the conventionally joined specimens transmitted much less of the IR radiation than did the microwave joined specimens.

Bond-layers of joined dissimilar ceramics were in range of 0 to 3 microns thick except SiC platelet reinforced alumina with MaCor^{TM} joined specimen bond layer (10 microns, Figure 40) due to a reaction bond-layer. The "zero" thickness bond layer refers to those cases in which a bond layer was not observed by either SEM or TEM observation. Observation by TEM (work done by L. Zeng and M. A. Crimp in section 3.8 in this thesis) showed no apparent bond layers in joined alumina with partially stabilized zirconia.

Ceramic/ceramic joining was successfully done without significantly changing the dimensions in alumina/zirconia composites, fully stabilized zirconia, partially stabilized zirconia, MaCor^{TM}, and hydroxyapatite using a silica spin-on interlayer. The averaged notch dimension of about 400 microns depth and 350 microns width were measured and calculated from table 17, 18, 19, and 20 in this thesis. Table 32 shows each averaged notch dimension in depth and width. Each measured notch depth and width produced in one specimen was added, then divided by the number of notches. The dimension change notch was calculated by the following equation.

$$\frac{\text{Averaged notch depth before joining - Averaged width after joining}}{\text{Averaged depth before joining}} \text{X } 100$$

Table 32. Averaged notch stability before and after joining in this thesis.

Material Notched	# of notch -es	Notch Width, before joining	Notch Width, after joining	Difference (%)	Notch depth, before joining	Notch depth, after joining	Difference (%)
Al_2O_3/ZrO_2	3	317μm	311 μm	2 %	329 μm	327 μm	1 %
$^{**}ZrO_2$	4	318 μm	315 μm	1 %	419 μm	415 μm	1 %
$^{*}ZrO_2$	5	372 μm	375 μm	1 %	264 μm	247 μm	3 %
MaCor^{TM}	3	340 μm	346 μm	2 %	431 μm	444 μm	3 %
HAP	3	335 μm	330 μm	2 %	431 μm	444 μm	3 %

*ZrO_2: 3 mol % yttria-zirconia

**ZrO_2: 8 mol % yttria-zirconia

*ZrO_2 was joined with MaCor^{TM} (no notches were made in MaCor^{TM})

The differences of the notch dimension before and after joining were 3 % in depth and 2 % in width after average difference of each single notch from table 17, 18, 19, and 20 ([52], 3.4 in this thesis).

Using Blackglas™ spin-on interlayer, one conventionally joined SiC (Hexoloy) with SiC (Hexoloy) at 900°C showed smooth and thin (in range of 2 to 3 microns thick) bond layer ([53], section 3.5 in this thesis).

4.3 Future Studies

Conventionally joined SiC with SiC followed heat-treatment by the microwave at 1200°C for 20 minutes showed a decreasing bond layer. Additional heating made a thinner bond layer. However, the nature of additional heating should be studied further.

Appendices

APPENDIX A

Literature surveyed joining techniques cited in introduction section. The number was set via references number.

Table A1. Joining materials, dimension, adhesive, thickness of adhesive, heating method, heating rate cooling rate, T_{max}, hold time, bonding pressure, mechanical test, span length, dimension, loading rate, cross speed, micrograph, thickness of bondlayer, strength of material, bonding or shear strength, and atmosphere were written. Reference number 1 to 18 used bonding agent during joining.

References	Materials	Dimension	Adhesive	Thickness of adhesive	Heating method
1	Si_3N_4 with Zirconia	10 mm in diameter 5 mm thick	Pure nickel foil	0.2-0.8 mm	Diffusion bonding furnace
2	Hot pressed sialon	15x15x5mm bar or hot pressed dic of 20 mm diameter and 5 mm thickness	Y-sialon	Slurry	Unknown
	Hot pressed sialon		Y-sialon		
	Hot pressed sialon		Y-sialon		
	Pressureless sintered sialon		Y-sialo		
	Pressureless sintered sialon		Y-sialon		
3	Si_3N_4 with Si_3N_4	20x20x8 mm	glass slurry	Slurry	Not reported
4	AlN with copper or tungsten	Not reported	Ag-Cu-Ti	No	Conventional furnace
			Ag-Cu-Ti-Co	No	
			Ag-Cu-Ti-Nb	No	
5	Si_3N_4 with Si_3N_4	20x20x8 mm	Y_2O_3-SiO_2-Al_2O_3-Si_3N_4	Slurry	Furnace
6	Sialon with sialon	25x20x5 mm	Y_2O_3-SiO_2-Al_2O_3-Si_3N_4	Slurry	Furnace
7	RBSiC with RBSiC	76x7x6 mm^3	methyl-hydroxyl-siloxane	18±4μm	Furnace
8	ZrO_2/Ti/ZrO	10 mm in diameter 5 mm height for TZP 10x10x1 mm for Ti	Ti-6wt%Al-4wt%-V	10x10x1 mm	Conventional furnace
	ZrO_2/Pt/Ti/ZrO_2				
	ZrO_2/Pt/ Ti-6wt%Al-4wt%-V				

References	Heating rate	Cooling rate	T_{max}	Hold time	Bonding pressure	Mechanical test
1	5-25°C/min	10°C/min	1000-1100^{oC}	90 min	20-37 MPa	Shear strength
2	Not reported	Not reported	1130°C	1 hour	5 MPa	Microhardness test (Hv)
			1400°C	1 hour	5 MPa	
			1600°C	1 hour	5 MPa	
			1600°C	1 hour	0 MPa	
			1600°C	1 hour	0 MPa	
3	10°C/min	Not reported	1450-1750°C	10-20 min	No pressure	Three point bend
4	0.43 K/sec	0.2 K/sec	820-920°C	0-30min	Not reported	Shear strength
			820-920°C	0-30min		
			820-920°C	0-30min		
5	Not reported	Not reported	1600°C	30 min	5 MPa	Three point bend
6	100°C/min	100°C/min	1600°C	10 min	2 MPa	no
7	1°C/min	1°C/min	800-1200°C	1 hour	No pressure	no
8	Not reported	Not reported	1328°C and 1494°C	1-180 min	5 MPa	Vickers indentation
			1162°C and 1245°C	15-180 min	5 MPa	Not reported
			1162°C and 1245°C	90 min	5 MPa	Not reported

Refere-nces	Span length	Dimension	loading rate	cross speed	Micrograph	Thickness of bond layer
1	no	no	no	no	Yes	No
2	no	no	no	no	Yes Yes Yes Yes Yes	5-10 μm 1-2 μm less than 0.5 μm less than 0.5 μm almost invisible
3	no	3x4x36mm	no	no	Yes	20-35 μm
4	no	no	no	no	Yes	~3-10 μm
					Yes	~ 1–10 μm
					Yes	~ 0.8–3.5 μm
5	no	no	no	0.5mm/min	Yes	12 μm
6	no	no	no	no	Yes	1.5 ±0.5 μm
7	inner 6mm outer 12 mm	1.5x3x15mm^3	no	0.2mm/min	Yes	6.5, 4.5, and 2.5μm
8	no no no	no no no	no no no	no no no	Yes Yes Yes	Unknown Unknown Unknown

References	Strength of materials	Bonding or shear strength	Atmosphere
1	No	No	$4x10^{-4}$ Pa (Vacuum)
2	1549 Hv	1371 Hv	Flowing Nitrogen
	1572 Hv	1550 Hv	
	1535 Hv	1553 Hv	
	1440 Hv	1431 Hv	
	1440 Hv	No	
3	700 MPa	400 MPa	Flowing argon
4	Not reported	118 MPa	Not reported
		116 MPa	
		147 MPa	
5	700 MPa (?)	550 MPa	Flowing Nitrogen
6	No	No	Flowing Nitrogen
7	250±10 MPa	70-220 MPa	Flowing argon
8	736 ± 71 Hv	Just annealed metal 60 Hv	Flowing argon
	Not reported	Not reported	
	Not reported	Not reported	

References	Materials	Dimension	Adhesive	Thickness of adhesive	Heating method
9	Pressurelessly sintered Si_3N_4 with Si_3N_4	20x20x8 mm^3	slurry in the system of Y-Si-Al-O-N	Slurry	furnace
10	Sintered Sialon	Bar (3x4x20mm)	Sn-5at% Ti alloy	0.15 mm	Cold wall type of Vacuum furnace
11	Si_3N_4 with Si_3N_4	bar (3x4x20mm)	CuNiTiB paste Brazing filler metal	No	Vacuum furnace
12	Pressureless Sintered SiC	15x25x20 min	MgO-Al_2O_3-SiO_2 (MAS) filler	1 mm	Graphite vacuum furnace and Alumina tube furnace
13	Al_2O_3-ZrO_2 (30%) composites	Block (15x4x4 mm)	sodium silicate glass powder	Slurry (powder mixed with glycerol)	Microwave (2.45 GHz, 700 W)
14	Al_2O_3	3 mm diameter 10 mm long	Sintered ceramic 92 % to 96 % Al_2O_3	0.6 mm	Microw-ave
	Al_2O_3		No	No	
	SN220		Sheet of SN501	0.6 mm	
	SN501		No	No	
15	Al_2O_3 (99%)	disc(10 mm x 6 mm)	sodium silicate glass powder	Slurry (powder mixed with glycerol)	Microw-ave
15	Refractory alumina (low purity	Not reported	sodium silicate glass powder	Slurry (powder mixed with glycerol)	Microw-ave

Refere-nces	Heating rate	Cooling rate	T_{max}	Hold time	Bonding pressure
9	10°C/min	Not reported	1450-1650°C	10-20 min	0-5 MPa
10	Not reported	Not reported	827°C	20 min	8mPa (vacuum)
11	15 K/min	15 K/min	1007-1127°C	10 min	Vacuum
12	15°C/min	100°C/min	1500-1600°C	30 min	No load
13	within 2 min at 1000°C	Not reported	1000^{oC}	9 min	No
14	40°C/min	15°C/min	1601°C and 1720°C	3 min	0-2.4MPa
			1750°C or above	3 min	0.6MPa
	No	No	1720°C	3 min	6.2 MPa
			No		
15	reached at about 1000°C within about 10 min	cool down fast after de coupling	~1000°C	~ 5 min	Not reported
	reached at about 1000°C within about 10 min	cool down fast after de coupling			

References	Mechanical test	Span length	Dimension	loading rate	cross speed
9	Three point bend	No	$3x4x36mm^3$	0.5mm/mim	no
10	Four Point	27 mm	No	0.2 mm/min	18 mm
11	Three Point	No	No	0.5 mm/min	No
12	Three point	No	3x4x35mm	No	0.5 mm/min
13	Three point and Hv Hardness	30 mm	no	no	no
14	Four point	No	No	No	No
15	Hv Hardness	No	No	No	No

Refere-nces	Microgr-aph	Thickness of bond layer	Strength of materials	Bonding or shear strength	Atmosphere
9	Yes	~10 µm	700 MPa	650 MPa	Flowing Nitrogen
10	Yes	~0.1 mm	400 MPa	~100 MPa (Sn-5Ti-Ag active solder)	Vacuum
11	Yes	Vary with braze (about 48 – 58 microns)	Not reported	224.8 (highest joint) at 1353K	Vacuum $(3.0\text{-}6.5\times10^{-3})$ Pa
12	Yes	10 µm at 1500°C 5 µm at 1600°C	370 MPa	380 MPa Up to 800°C and 80 MPa at 900°C	Ar flowing
13	Yes	about 500 µm	No (but joint strength was stronger than glass phase)	28MPa	Not reported
14	No	No	from reference	370 MPa	Air
	Yes	?		420 MPa	
	No	No	525 MPa	~390MPa	N_2
	No	No	344 MPa	~520 MPa	
15	Yes	About 300 µm	Glass: 515 kg/mm^2)	582-1100 Hv	Air

Refere-nces	Materials	Dimension	Adhesive	Thickness of adhesive	Heating method
16	Al_2O_3 with Al_2O_3	15 mm square face 20 mm length	99.5 wt% pure alumina	Not reported	Conventional brazing
	Al_2O_3 with Al_2O_3				Conventional brazing
	Al_2O_3 with Al_2O_3				SQ Brazing (tightly fixed)
	Al_2O_3 with Al_2O_3				SQ brazing (loosely contact)
	As received Si_3N_4	15x10x10 min			SQ brazing
	Pre-Oxidation (900°C) treated Si_3N_4				SQ brazing
17	Invar-alumium-silicon nitride-alumium-Invar	disc 1mm high and 13 mm in diameter (SiC) Invar Rod (7mm in diameter and 7 mm height)	Aluminum (99.9 wt%) sheet	0.5 mm thick and 7 mm in diameter	furnace
18	Ti-6Al-4V alloy sheets with alumina thin plates	1mmx0.63 mm for both alumina and Ti alloy (7 layers)	63 wt%Ag, 1.75 Ti , bal brazing alloy	50 microns (840°C eutectic T)	Furnace (brazing)

Refere-nces	Heating rate	Cooling rate	T_{max}	Hold time	Bonding pressure	Mechanical test	Span length	loading rate
16	Not reported	No	800°C	10min	0.01 MPa	Three-point	30 mm	No
			800°C		0.01 MPa			
			600 & 800°C		50 MPa			
			600 & 800°C		50 MPa			
			600°C		50 MPa		25 mm	
			600°C		50 MPa			
17	Not reported	no	700°C-950°C	2 to 30min	0 to 0.15 MPa	Four point	10 mm	No
18	15°C/min	~15°C/min	850°C	10 min	0.15 MPa	Three point bending test	40 mm	

References	Dimension	cross speed	Micrograph	Thickness of bond layer	Strength of materials	Bonding or shear strength	Atmosphere
16	3x3x40 mm	0.5 mm/ min	Yes	0	350 MPa	Not joined	Air
				10 microns		49 MPa	Flowing Argon
				10 microns		325 MPa	Air
				300 microns		228 MPa	Air
	3x3x30 mm		No	200 microns	900 MPa	57 MPa	Air
				200 microns		404 MPa	Air
17	2x2x15 mm^3	No	Yes	10 to 20 microns		400 to 500 MPa	Ar, air, and N_2
18	50 mm long, 5 mm wide and 4.4 and 5.75 mm thick for mutilayers	0.3 mm/ min	Yes	Not reported	Al_2O_3 :280 MPa Ti alloy : 1100 MPa	263 MPa	Vacuum (10^{-5}torr)

Table A2. Joining materials, dimension, adhesive, thickness of adhesive, heating method, heating rate cooling rate, T_{max}, hold time, bonding pressure, mechanical test, span length, dimension, loading rate, cross speed, micrograph, thickness of bondlayer, strength of material, bonding or shear strength, and atmosphere were written. The number was set via references number. Reference number 24 to 29 used no bonding agent during joining.

References	Materials	Dimension	Adhesive	Thickness of adhesive	Heating method	Heating rate	Cooling rate
24	HPSC	rod (5x5x50mm)	no	no	Microwave 300W, 2.45 GHz, TE_{102}	$0.6\ ^{\circ}Cs^{-1}$	$4.6\ ^{\circ}Cs^{-1}$
	RBSC	disc (15x9mm)				$2.0\ ^{\circ}Cs^{-1}$	$3.0\ ^{\circ}Cs^{-1}$
	Y-PSZ	rod (7x40 mm)				$0.5\ ^{\circ}Cs^{-1}$	$3.5\ ^{\circ}Cs^{-1}$
	Y-PSZ	tube (1.8x6.4x45)				$2.8\ ^{\circ}Cs^{-1}$	$4.0\ ^{\circ}Cs^{-1}$
25	Clay-bonded SiC	Tube (1/2" & 1")			SALD (Selective Area Laser Deposition)		
	HiNicalon Fiber in SiC	No					
	Hexoloy	Tube (1/2" & 3/8")					
26	Al_2O_3 with MgO	5 mm X 5 mm X 25 mm	No	No	Microwave	120°C/min	120°C/min
27	Si_3N_4 with Si_3N_4 (Al_2O_3 and Y_2O_3 additives for sintering)	15x15x20mm	No (but heated in powder bed)	No	Diffusion bonding and then heat treated at 1950°C for 3.6Ks	No	No

Refere-nces	Materials	Dimension	Adhesive	Thickness of adhesive	Heating method	Heating rate	Cooling rate
28	Zirconia with zirconia/ Hydroxy apatite composites	Not reported	No	No	First CIP at 300 MPa and then HIP	Not reported	Not reported
	Alumina with alumina/ Hydroxy apatite composites						
29	Si_3N_4 with Si_3N_4	15x15x20 mm^3	No	No	Diffusion bonding	Not reported	Not reported

References	T_{max}	Hold time	Bonding pressure	Mechanical test
24	1310°C	-	0.5 MPa	No
	1190-1375°C	up to 2	0.5-2.0 MPa	No
	1400-1565°C	10 min	2.7 ± 2.0 MPa	Viker's indent
	1230°C	10 min	3.2 ± 2.0 MPa	No
25	Using Laser Beam (?)			Vicker indenter (500g load)
26	1577°C to 1877°C	2- 10min	0.03-0.5 MPa	Three point
27	1500°C	3.6Ks	20 MPa	Bending test
28	1225°C	1 hr	200 MPa	Three bending
	Fractured during CIP			
29	1500°C	3.6Ks	21 MPa	Three bending

References	Span length	Dimension	loading rate	cross speed
24	No	No	No	No
25	No	No	No	No
26	30 mm	no	no	0.5 mm/min
27	outer 30 mm inner 10 mm	3x4x40mm	No	No
28	No	30x3.5x3.5 mm^3	No	No
29	No	3x4x40 mm^3	No	No

References	Micro graph	Thickness of bond layer	Strength of materials	Bonding or shear strength	Atmosphere
24	No	No	No	No	Not reported
	Yes	from (10-20 microns at 1190°C, 0.5 MPa) to (3-5 microns at 1375°C, 2 MPa)			
	Yes	Invisible			
	No	No			
25	Yes	Hard to see	Not reported		Vacuum
26	Yes	Almost impossible to fine out	MgO: 150, Al_2O_3:340	70MPa	Air
27	Yes	Almost invisible	about 0.8 GPa	Joined :~0.3GPa Joined and annealed :~0.5GPa	N_2
28	Yes	Not identical	Zirconia : 916 MPa Z/HAP composites : 860MPa	845 MPa	Not reported
	No	Fractured	Al_2O_3: 577 MPa Al/HAP composites: 601 MPa	Fractured	
29	Yes	occasionally porous interface	about 0.8 GPa	148 MPa	N_2 gas (0.1 and 1 MPa pressure)

APEPPENDIX B

Sintering and joining heating rate using the Microwave energy in this thesis.

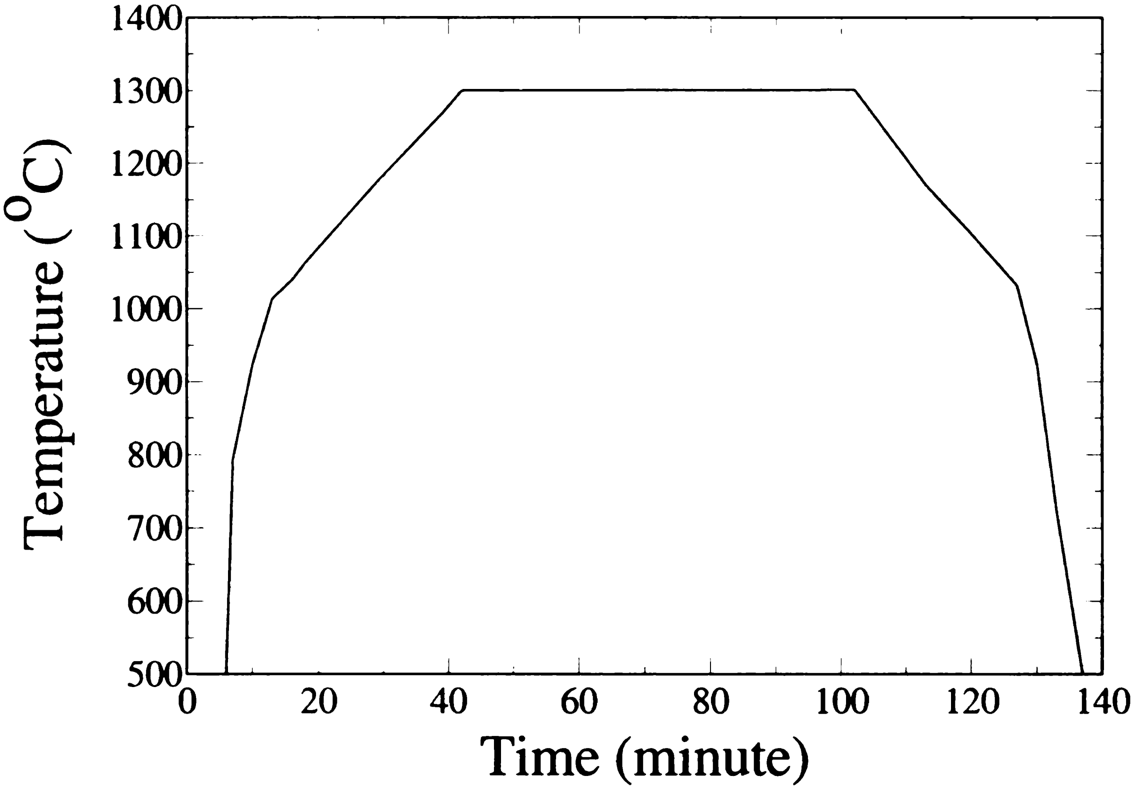

Figure B1. A graph of sintering TM-DAR (Alumina). TM-DAR was sintered at 1300°C for 60 minutes with heating rate 10°C/min.

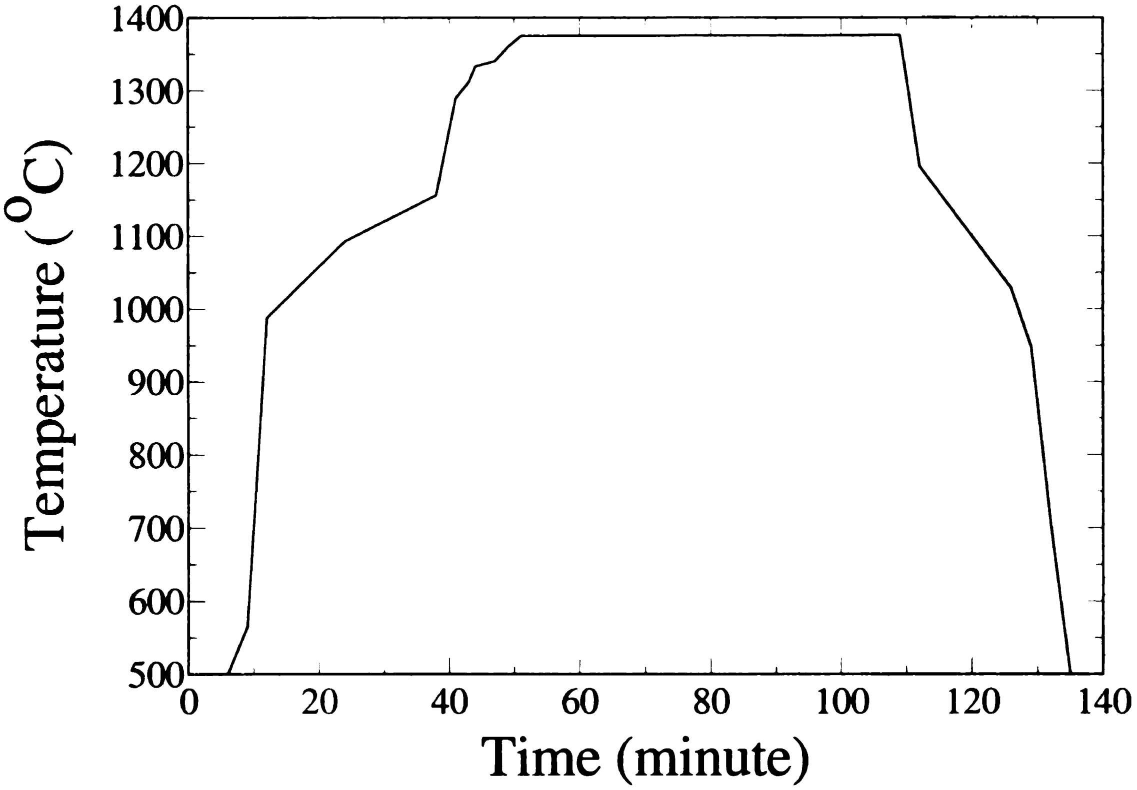

Figure B2. A graph of sintering partially stabilized zirconia. Partially stabilized zirconia was sintered at 1375°C for 60 minutes with heating rate 10°C/min.

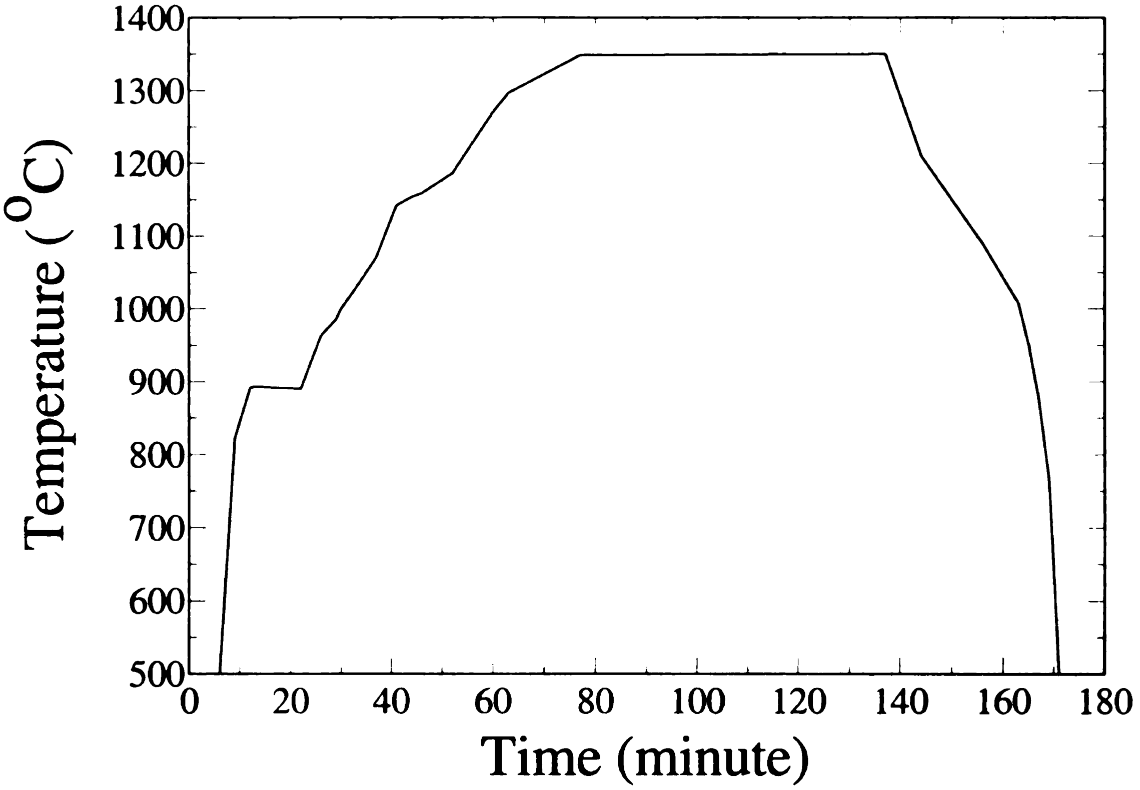

Figure B3. A graph of sintering fully stabilized zirconia. Fully stabilized zirconia was sintered at 1350°C for 60 minutes with heating rate 10°C/min.

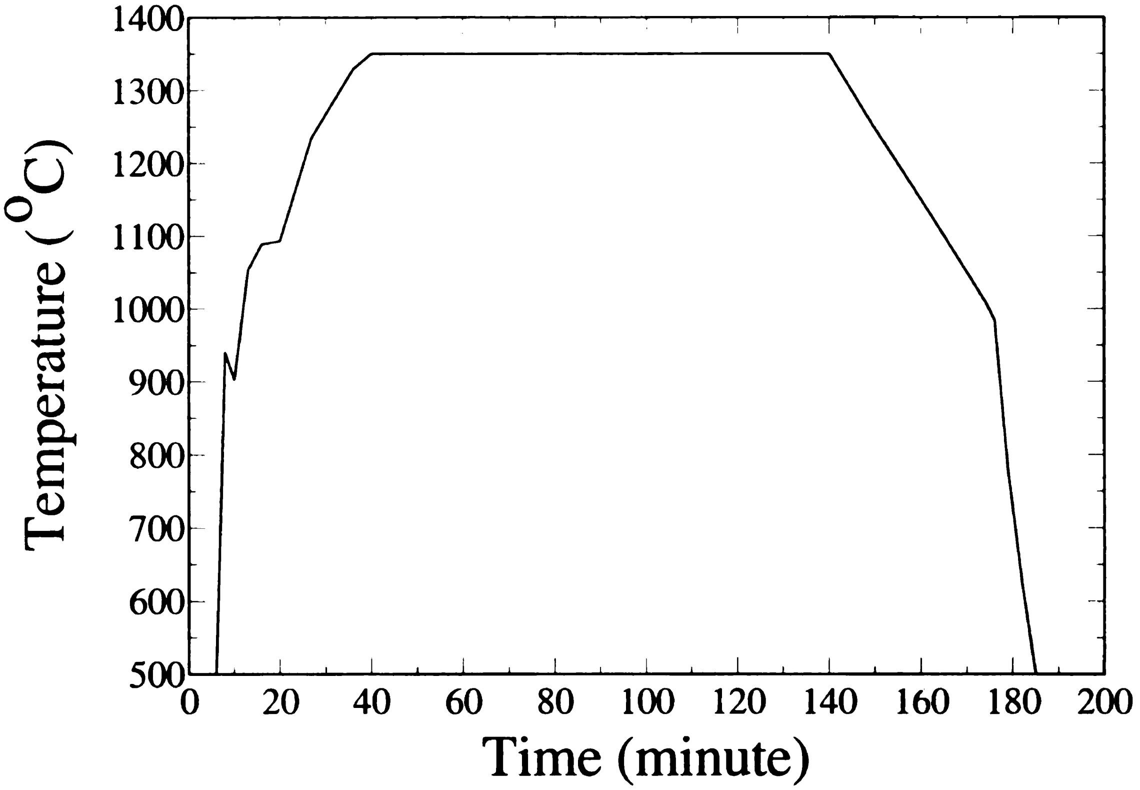

Figure B4. A graph of sintering alumina (85 wt %)-zirconia (15 wt %) composites. Alumin/zirconia composites was sintered at 1350°C for 60 minutes with heating rate 10°C/min.

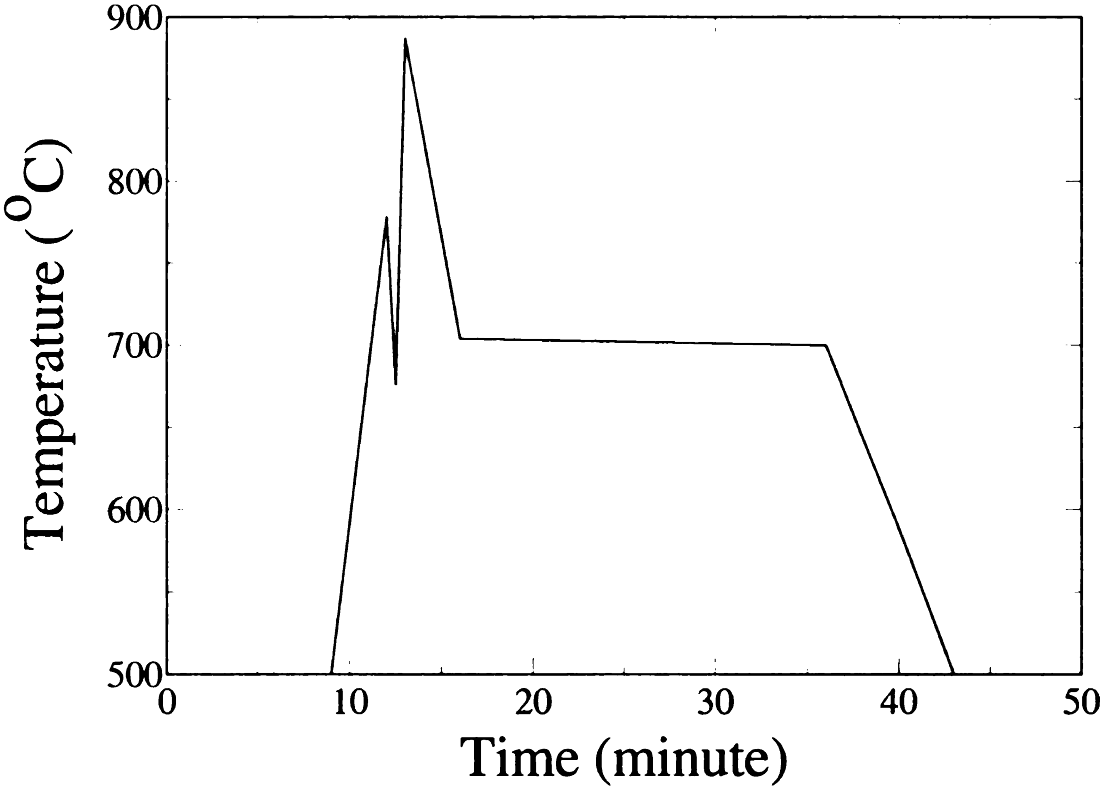

Figure B5. A graph of heating rate of microwave joined MgF_2/MgF_2 joined at 700°C for 20 minutes using sodium silicate solution spin-on interlayer.

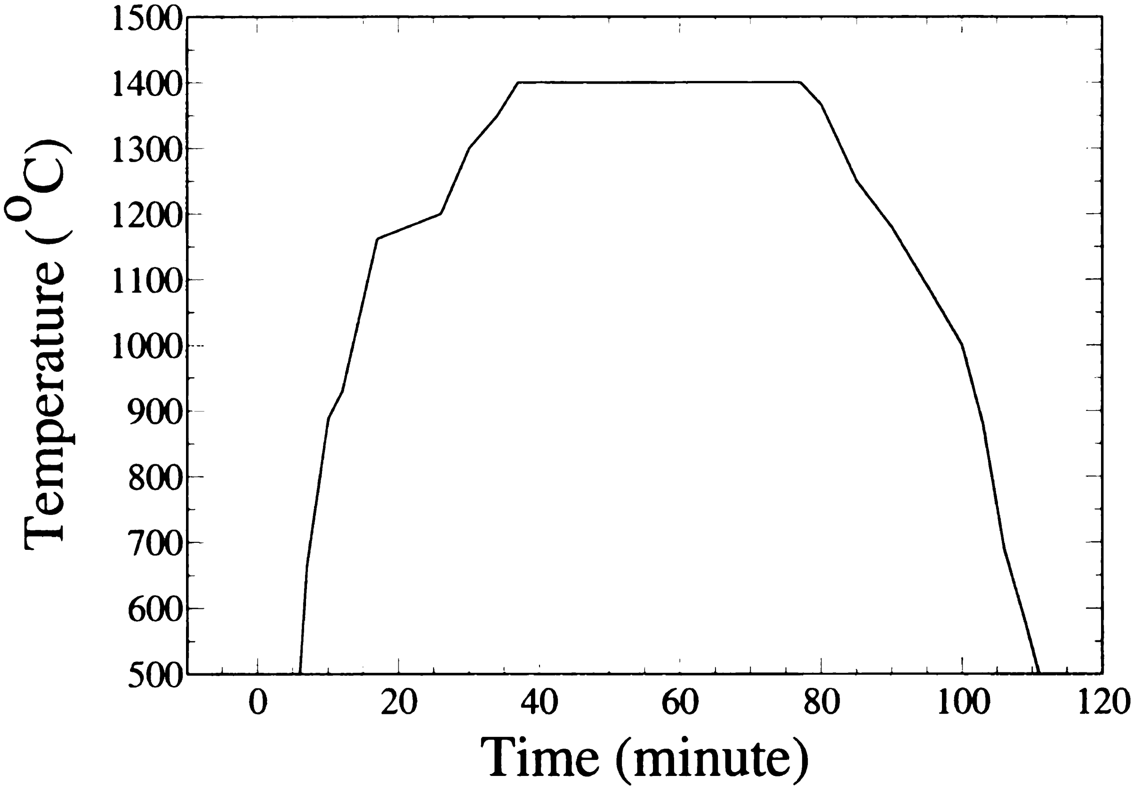

Figure B6. A graph of heating rate of microwave joined AKP 30/AKP 30 joined at 1400°C for 20 minutes using sodium alginate spin-on interlayer.

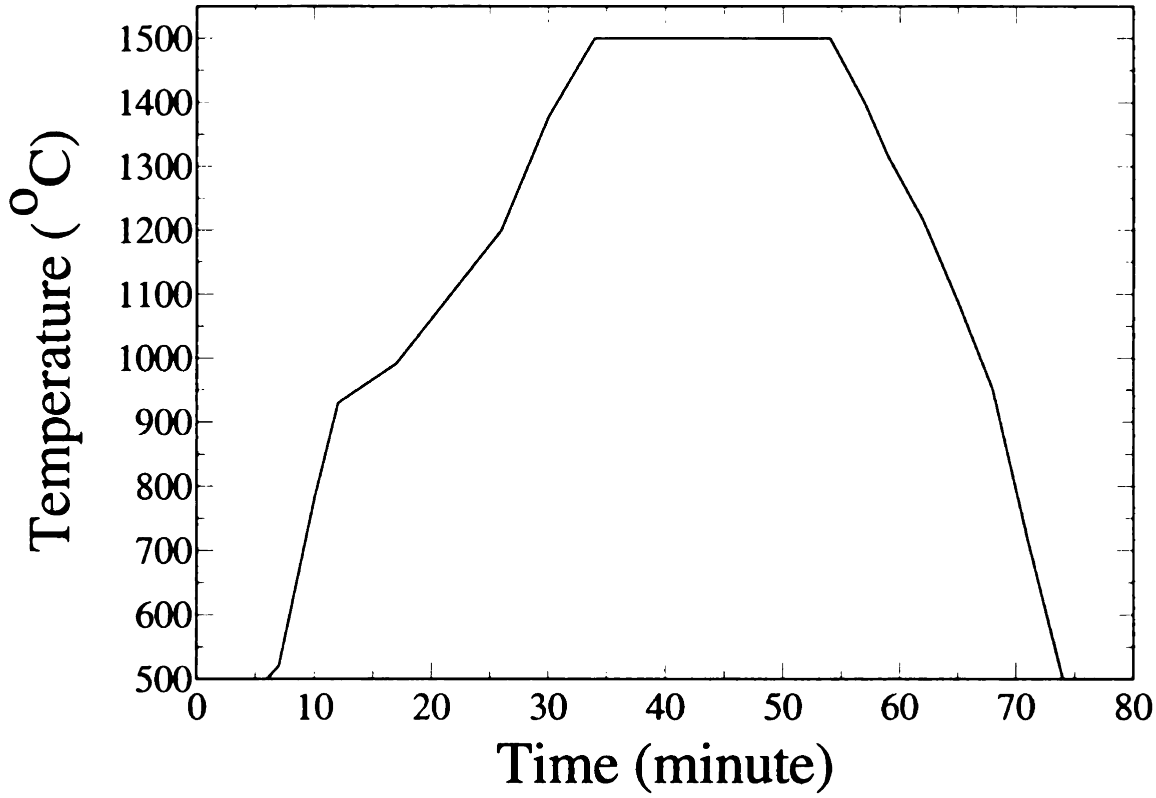

Figure B7. A graph of heating rate of microwave joined partially stabilized zirconia/partially stabilized zirconia joined at 1500°C for 20 minutes using silica film spin-on interlayer.

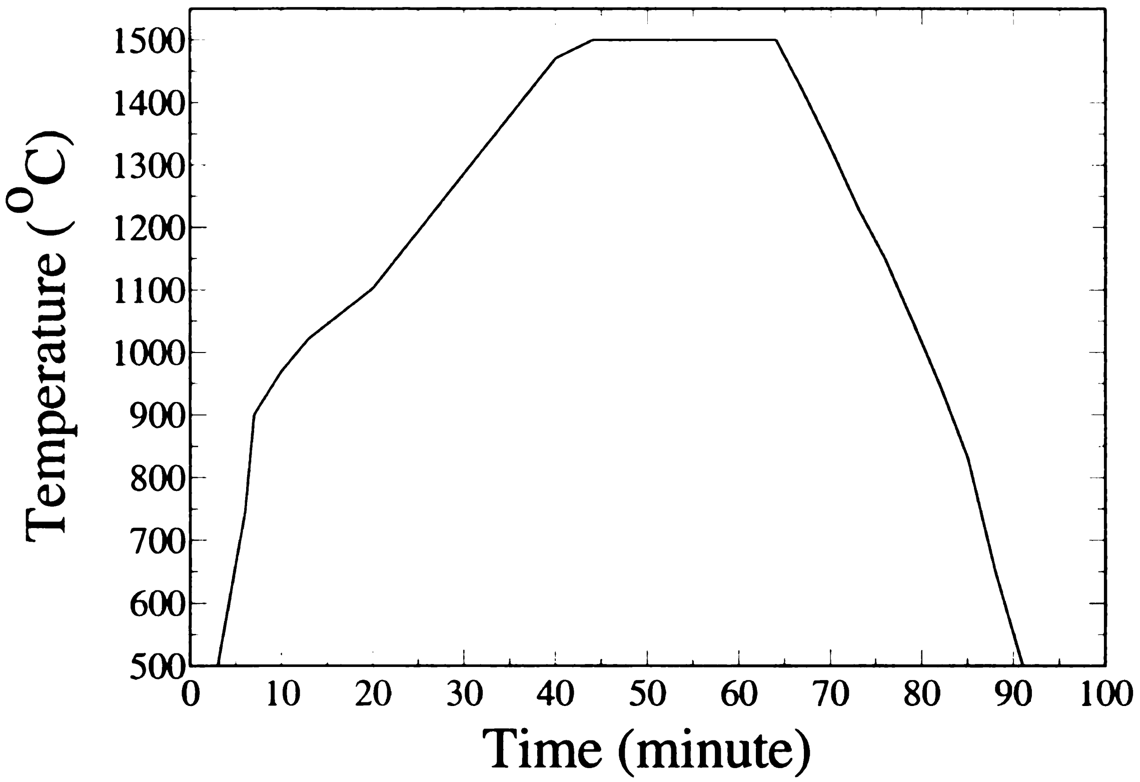

Figure B8. A graph of heating rate of microwave joined partially stabilized zirconia with alumina joined at 1500°C for 20 minutes using silica film spin-on interlayer.

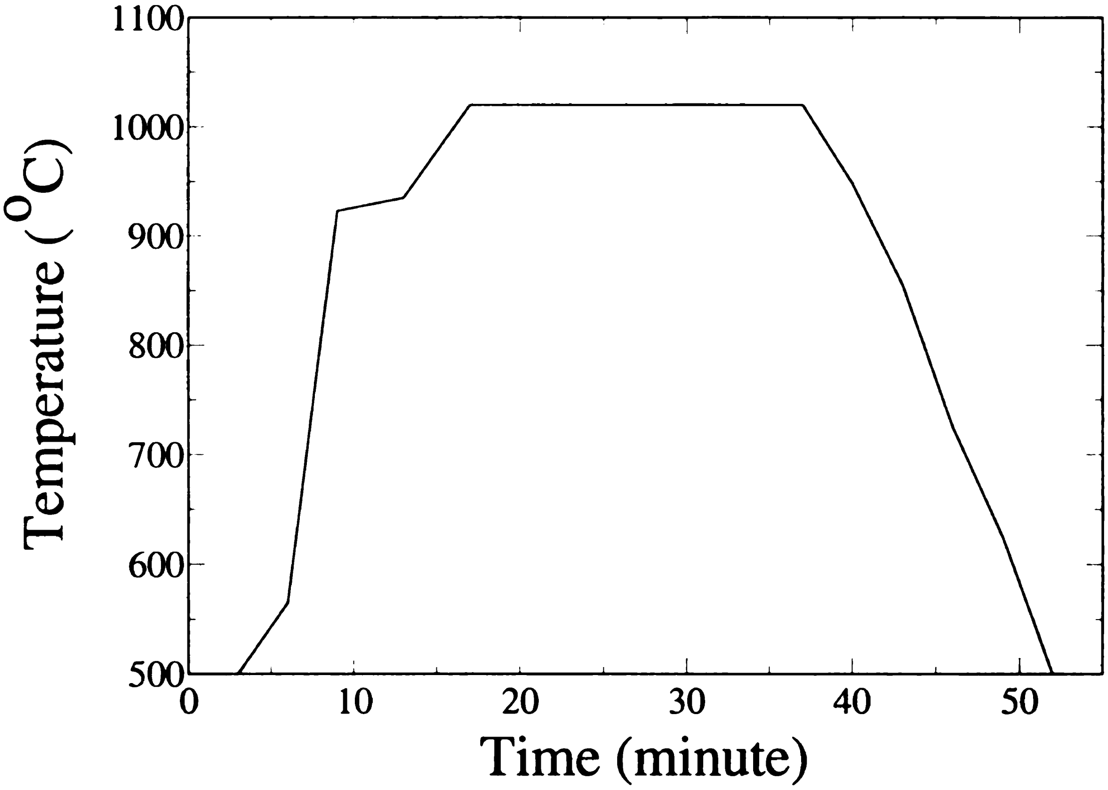

Figure B9. A graph of heating rate of microwave joined HAP with MaCor™ joined at 1020°C for 20 minutes using silica film spin-on interlayer.

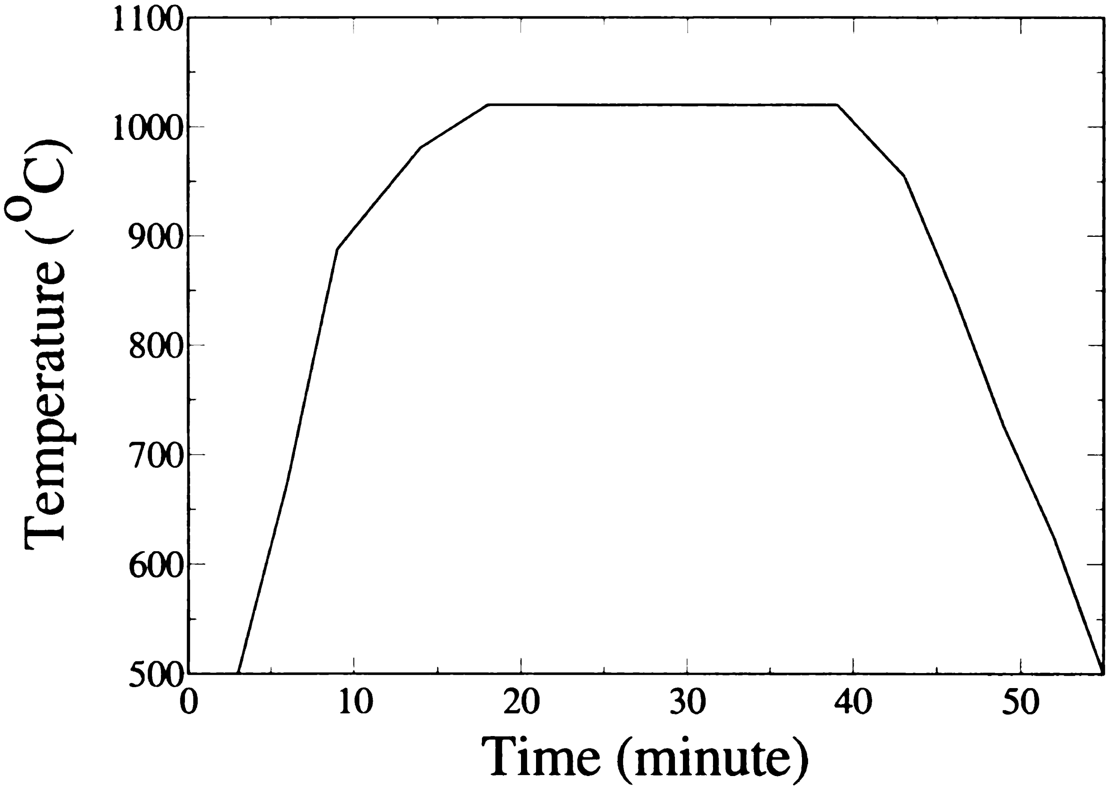

Figure B10. A graph of heating rate of microwave joined partially stabilized zirconia with MaCor^{TM} joined at 1020°C for 20 minutes using silica film spin-on interlayer.

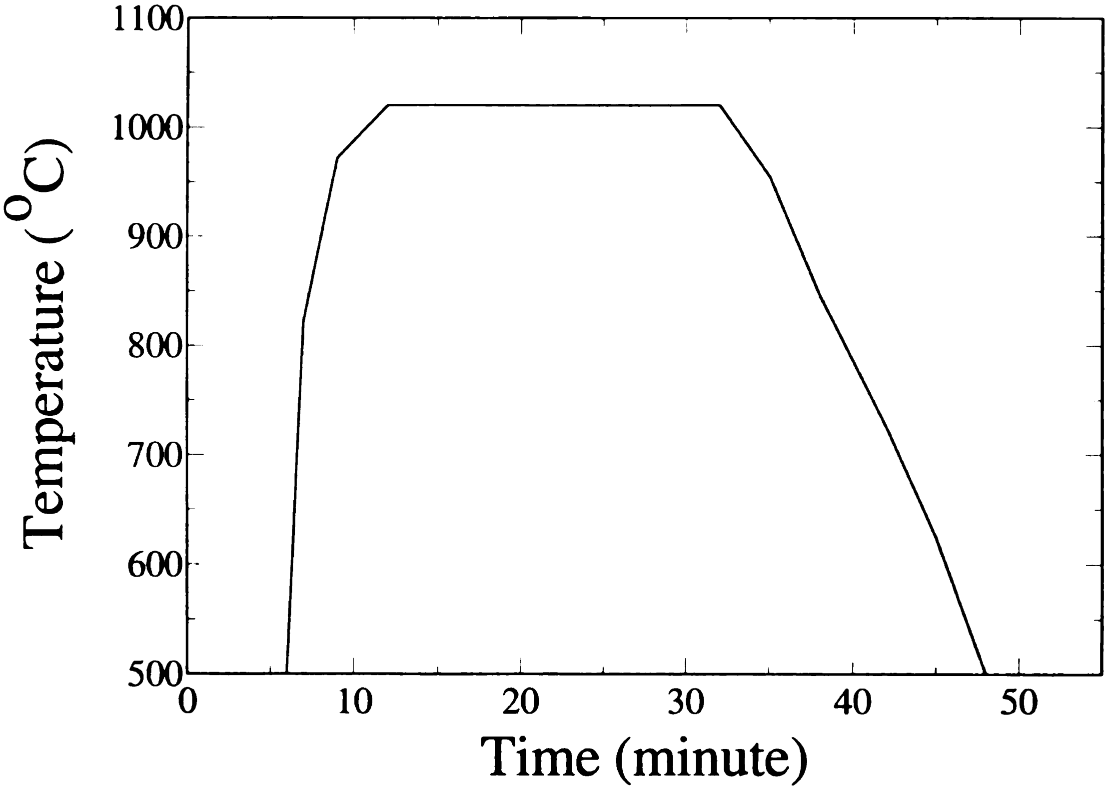

Figure B11. A graph of heating rate of microwave joined SiC platelet reinforced alumina with /MaCor™ joined at 1020°C for 20 minutes using silica film spin-on interlayer.

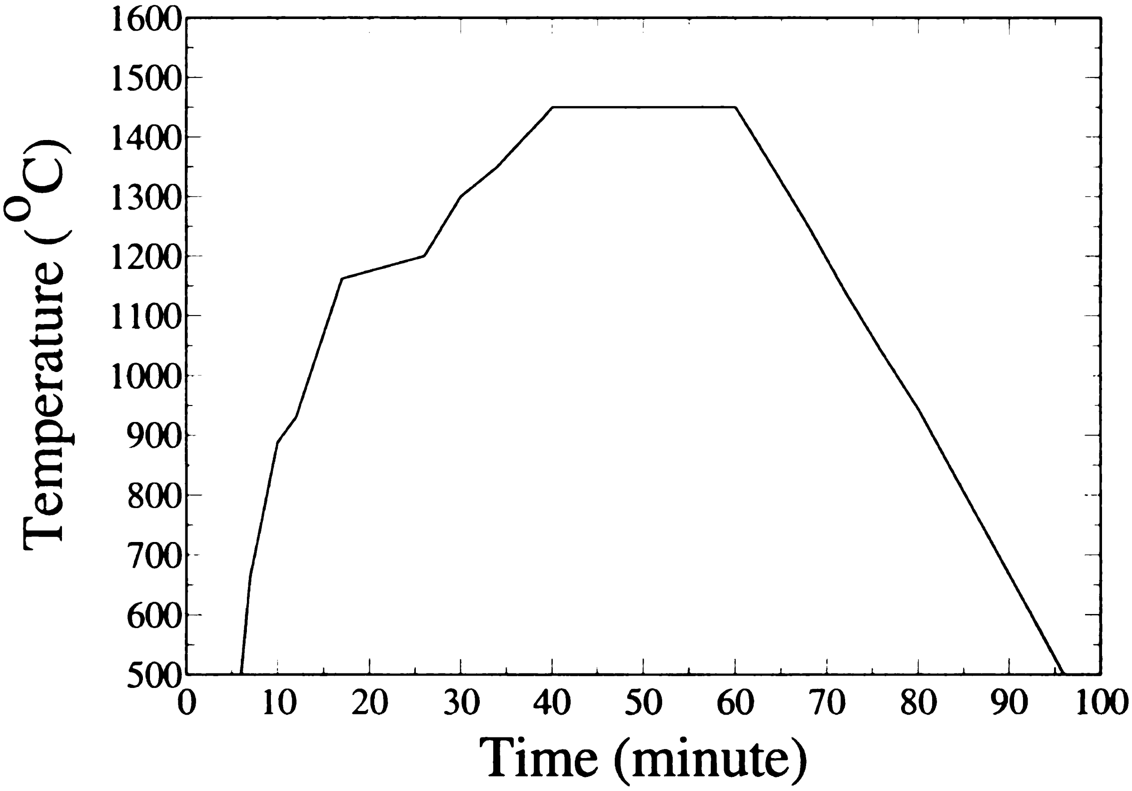

Figure B12. A graph of heating rate of microwave joined alumina/zirconia composites with alumina/zirconia composites joined at 1450°C for 20 minutes using silica film spin-on interlayer.

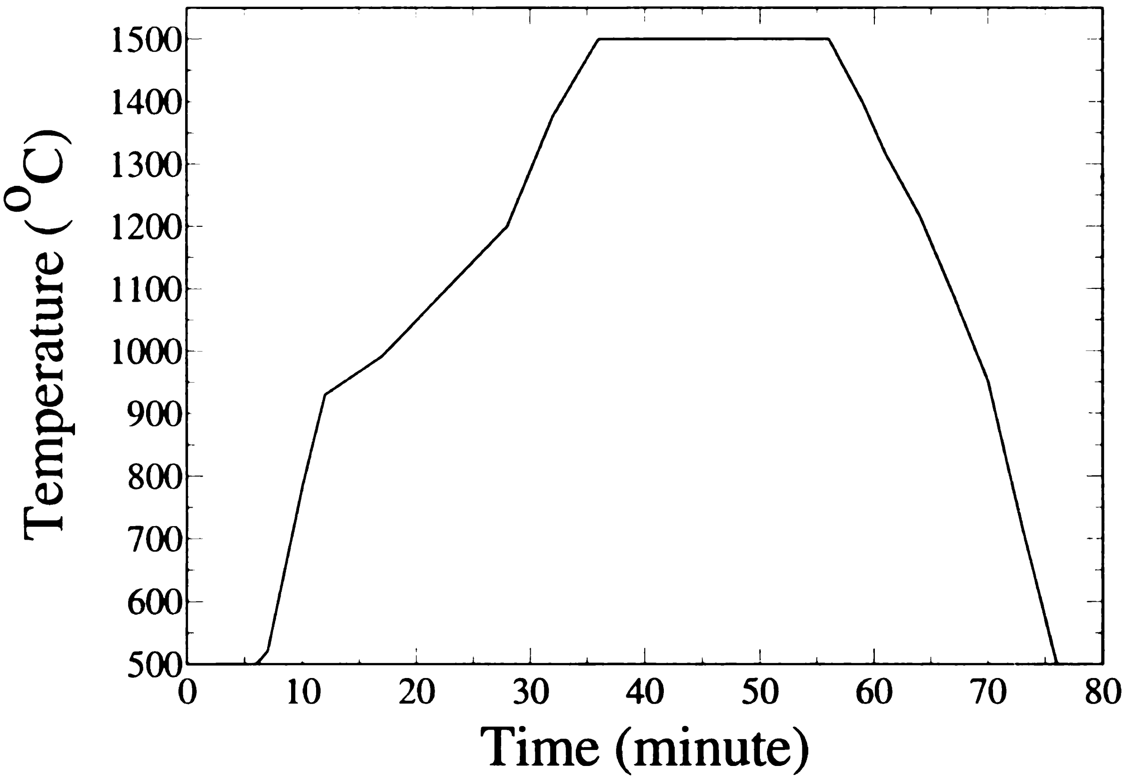

Figure B13. A graph of heating rate of microwave joined fully stabilized zirconia with fully stabilized zirconia joined at 1450°C for 20 minutes using silica film spin-on interlayer.

APPENDIX C

Micrographs of joined ceramic/ceramic not included in results section.

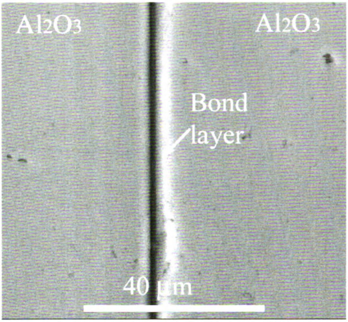

(a)

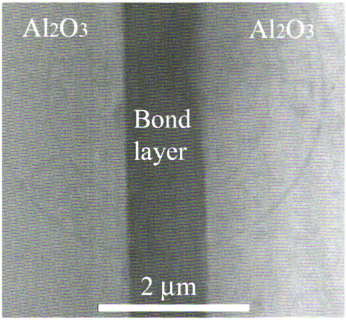

(b)

Figure C1. ESEM micrographs of conventionally-joined AKP 30 (alumina) joined at 1400°C for 20 minutes using sodium alginate spin-on interlayer (a) lower magnification of joined Al_2O_3 and (b) higher magnification of joined Al_2O_3.

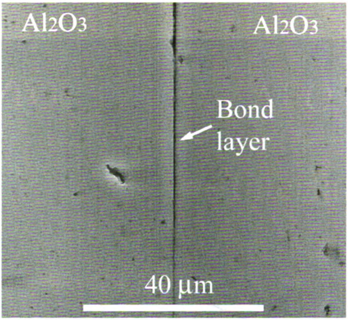

(a)

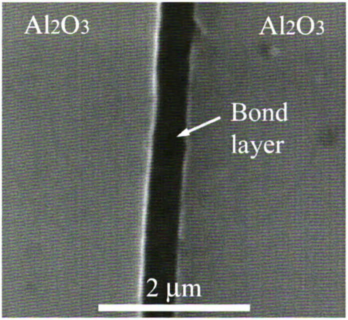

(b)

Figure C2. ESEM micrographs of microwave-joined AKP 30 (alumina) joined at 1400°C for 20 minutes using sodium alginate spin-on interlayer (a) lower magnification of joined Al_2O_3 and (b) higher magnification of joined Al_2O_3.

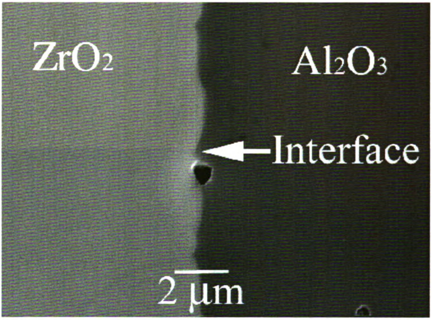

(a)

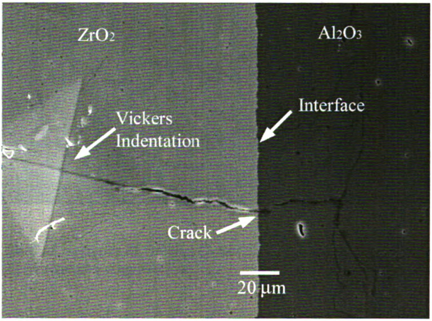

(b)

Figure C3. (a) A micrograph of microwave-joined alumina with zirconia (3 mol % Y_2O_3) at 1500°C for 20 minutes using silica spin-on interlayer showing interface and (b) a crack induced byVikers indentation was deflected from ZrO_2 to Al_2O_3 through interface.

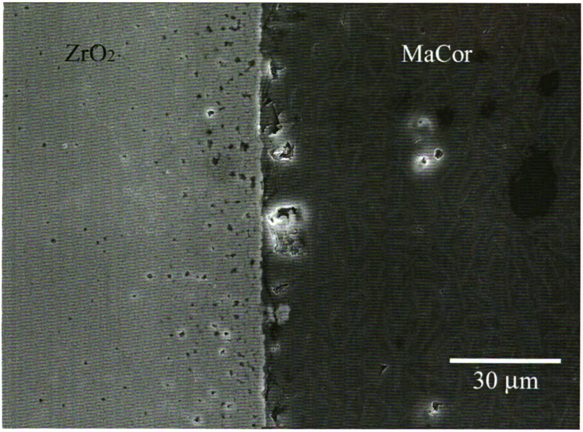

Figure C4. SEM micrographs of zirconia (3 mol % Y_2O_3) with MaCor™ joined at 1020°C for 20 minutes showing interface.

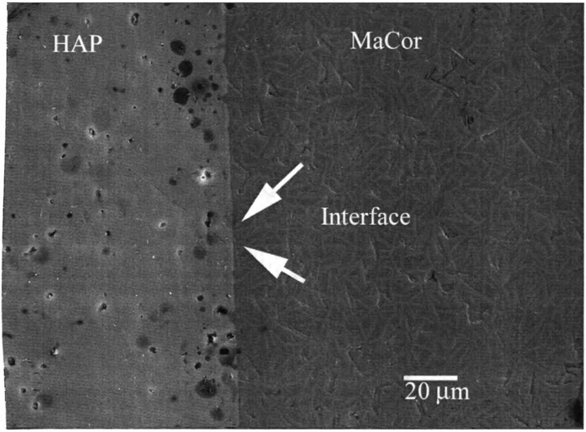

Figure C5. SEM micrograph of HAP with MaCor™ joined at 1020°C for 10 minutes. The mica platelet rainforcement in the MaCor™ is evident in the micrograph.

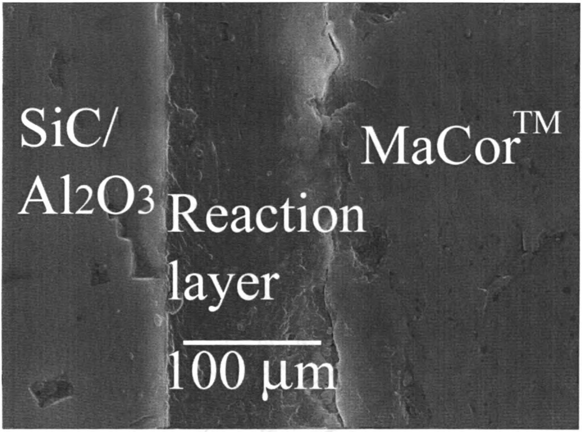

Figure C6. SEM micrograph of SiC platelet reinforced alumina with MaCor™ joined at 1020°C for 10 minutes.

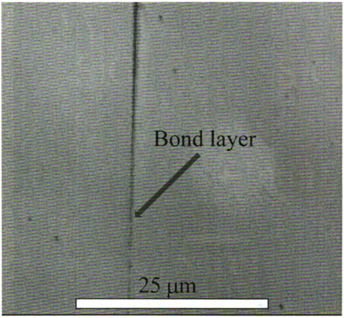

(a)

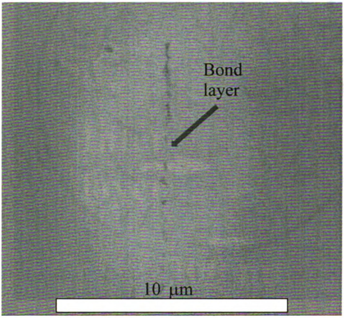

(b)

Figure C7. ESEM micrographs of microwave-joined ZrO_2 (3 mol % Y_2O_3) joined at 1500°C for 20 minutes using silica spin-on interlayer (a) lower magnification of joined ZrO_2 and (b) higher magnification of joined Al_2O_3.

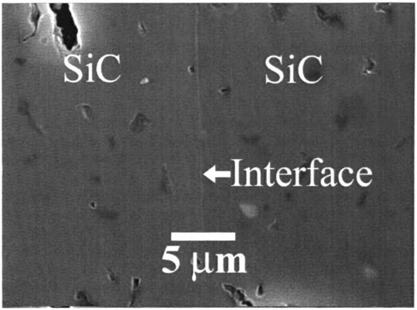

(a)

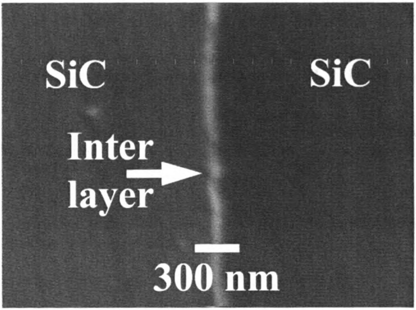

(b)

Figure C8. SEM micrographs of conventionally-joined SiC joined at 1000°C for 20 minutes using Blackglass spin-on interlayer (a) lower magnification of joined SiC and (b) higher magnification of joined SiC.

References

1. R. H. Vegter and G.D Ouden, "Diffusion Bonding of Zirconia to Silicon Nitride Using NiKel Interlayers", Journal of materials Science, Vol. 33. pp. 4525-4530 (1998)

2. L. M. Weldon, S. Hampshire and M. J. Pomeroy, "Joining of Ceramic Using Oxide and Oxynitride Glasses in the Y-Sialon System", Jouranl of the European Ceramic Society, Vol. 17, pp. 1941-1947 (1997)

3. R. Xie, L.Huang, Y. Chen, X. Fu, "Effect of Chemical Compositions of adhesive and Joining Processes on Bond Strength of Si_3N_4/Si_3N_4 joints", Ceramic Internatioanl, Vol. 25, pp. 101-105 (1999)

4. T. Kuzumaki, T.Ariga and Y.Miyamoto, "Effect of Additional Elements in Ag-Cu Based Filler Metal on Brazing of Aluminum Nitride to Metal", ISIJ International, Vol. 30, No. 12, pp. 1135-1141 (1990)

5. R.Xie, L.Huang, and X.Fu, "Bond Strength and Microstructual investigation on Si_3N_4/Si_3N_4 Joint bonded with Glass-Ceramic", Journal of Materials Science Letters, Vol. 17, pp. 761-763 (1998)

6. P.A.Walls and M.Ueki, "Joining of SiAlON Ceramics Using Composite β-SiAlON-Glass Adhesives", Journal of American Ceramic Society, Vol. 75, No. 5, pp. 2491-2497 (1992)

7. P.Colombo, V.Sglavo, and E. Pippel, and J. Woltersdorf, "Joining of Reaction-Bonded Silicon Carbide Using A Preceramic Polymer", Journal of Materials Science, Vol. 33, pp. 2405-2412 (1998)

8. R. N. Corriea, J. V. Emiliano, and P. Moretto, "Microstructure of Diffusional Zirconia-titanium and zirconia-(Ti-6wt% Al-4 wt% V) Ally Joints", Jouranl of Materials Science, Vol. 33, pp. 215-221 (1998)

9. R.Xie, L.Huang, Y.Chen, X.Fu, "Evaluation of Si_3N_4 Joints: Bond Strength and Microstructure", Journal of Materials Science, Vol. 34, PP. 1783-1790 (1999)

10. A.Xian, "Joining of Sialon Ceramics by Sn-5 at % Ti Based Ternary Active Solders", Journal of Materials Science, Vol. 32, PP. 6387-6393 (1997)

11. C.G.Wang, H.P.Xiong, Z.F.Zhou, "Joining of Si_3N_4/Si_3N_4 with CuNiTiB Paste Brazing Filler Metals and Interfacial Reactions of the Joints", Journal of Materials Science, Vol. 34 [12], PP. 3013-3019 (1999)

12. H.L.Lee, S.W.Nam, B.S.Hahn, B.H.Park, and D.Han, "Joining of Silicon Carbide Using MgO-Al_2O_3-SiO_2 Filler", Journal of Materials Science, Vol. 33, pp. 5007-5014 (1998)

13. S. Aravindan and R. Krishnamurthy, "Joining of Ceramic Composites by Microwave Heating", Materials Letters, Vol. 38, PP. 245-249 (1999)

14. H. Fukushima, T. Yamanka, and M. Matsui, "Microwave Heating of Ceramics and Its Application to Joining", Microwave Processing of Materials, vol. 124, Edited by W.H. Sutton, M. H. Brooks, and I. J. Chabinsky. Materials Research Society, Pittsburgh, PA, pp 267-272 (1988)

15. S. Aravindan and R. Krishnamurthy, "Microwave Joining of Alumina Using Sodium Silicate Glass As a Bonding Agent", Industrial Ceramic, Vol. 15[3], PP. 173-176 (1998)

16. K.Suganuma, "New Process for Brazing Ceramics Utilizing Squeeze Casting", Journal of Materials Science, Vol. 26, pp. 6144-6150 (1991)

17. K.Suganuma, T.Okamoto, and M.Koizumi, "Joining of Silicon Nitride to Silicon Nitride and to Invar Alloy Using An Aluminum Interlayer", Journal of Materials Science, Vol. 22, pp. 1359-1364 (1987)

18. D.Sherman, "The mechanical Behavior of Layered Brazed Metal/Ceramic Composites', Materials Letters, Vol. 33, pp. 255-260 (1998)

19. K.Y. Lee, E.D. Case, and D. Reinhard, "Microwave Joining and Repair of Ceramics and Ceramic Composites," Ceramic Engineering and Science Proceedings, vol. 18, pp. 543-550 (1997).

20. K.N. Seiber, K.Y. Lee, and E.D. Case, "Microwave and Conventional Joining of Ceramic Composites Using Spin-On Materials," Proceedings of the 12th Annual ASC Technical Conference on Composite Materials, Dearborn, MI, pp. 941-949 (1997).

21. O.M. Akselsen, "Review Advances in Brazing of Ceramics," Journal of Materials Science, vol. 27, pp. 1989-2000 (1992)

22. M.G. Nicholas in "Joining of Ceramics", edited by M.G. Nicholas, (Chapman and Hall, London, 1990) pp. 15-18 and 71-93

23. J.D.Cawley, "Joining of Ceramic-Matrix Composites," Journal of American Ceramic Bulletin, vol. 68, no. 9, pp. 1619-1623 (1989)

24. J.G.P.Binner, J.A.Fernie, and P.A.Whitaker, "An Investigation into Microwave Bonding Mechanisms Via A Study Of Silicon Carbide And Zirconia", Journal of Materials Science, Vol. 33, PP. 3009-3015 (1998)

25. S.Harrison and H.L. Marcus, "Gas-Phase Selective Area Laser Deposition (SALD) Joining of SiC", Materials and Design, Vol.20, pp. 147-152 (1999)

26. T.Sato, N.Takahashi and K.Shimakage, "Microwave Joining of Alumina to Magnegia", Journal of Ceramic Society of Japan, vol. 104, no. 10, pp. 905-907 (1996)

27. M. Nakamura, I. Shigematatsu, M. Nakanishi, K, Shimojima, Y. Yamada, and Y. Shigegaki, "Microstructure of Joining Interfaces of Si_3N_4 Ceramics Formed by Diffusion Bonding", Journal of Materials Science Letter, vol.16, no. 20, pp. 1654-1655 (1997)

28. J.Li, L.Hermansson, and R.Soremark, "Joining of Ceramics of Different Biofuction by Hot Isostatic Pressing", Journal of American Ceramic Society, Vol. 76, pp. 2685-2686 (1993)

29. M.Nakamura, I.Shigematsu, "Diffusion Joining of Si_3N_4 Ceramics by Hot pressing Under High Nitrogen Gas Pressure", Journal of Materials Science Letters, Vol. 16, pp. 1030-1032 (1997)

30. J.G.PBinner, J.A.Fernie, P.A.Whitaker, and T.E. Cross, "The effect of composition on the Microwave Bonding of Alumina Ceramics", Journal of Materials Science, Vol. 33, pp. 3017-3029 (1998)

31. W.H. Sutton, "Microwave Processing of Ceramic Materials," Journal of American. Ceramic Society Bulltin. 68[2], pp. 376-386 (1989).

32. D.E.Clark and W.H.Sutton, "Microwave Processing of Materials", Annual Review of Materials Science, vol. 26, pp. 299-331 (1996)

33. H. Fukushima, T. Yamanka, and M. Matsui, "Microwave Heating of Ceramics and Its Application to Joining", Microwave Processing of Materials, vol. 124, Edited by W.H. Sutton, M. H. Brooks, and I. J. Chabinsky. Materials Research Society, Pittsburgh, PA, pp 267-272 (1988)

34. I.Ahmad, R.Silberglitt, Y.L.Tian, and J.D.Katz, "Microwave Joining of SiC Ceramics And Composites", Ceramic Transactions, Microwaves: Theory and Application in Materials Processing IV, vol. 80, pp. 455-463 (1997)

35. R.Silberglitt, W.M.Black, and J. D.Katz, "Recent Developments in Microwave Joining", MRS Bulletin, vol. 18, pp 47-50 (1993)

36. L.L. Hench, "Bioceramics," Journal of American Ceramic Soceity, vol. 81 [7], pp 1705-1728 (1998)

37. TM-DAR material data sheet from Taimi Co

38. W.D. Kingery, H.K. Bowen, and D.R.U. Uhlmann "Introduction to Ceramics," Second Edition, New York, N.Y. pp 595 (1976))

39. M.Barsoum"Fundamental of Ceramics" First edition, McGRAW-HILL, New York, N.Y. pp. 401 and 505 (1997))

40. HAP material data sheet from Cerac INC, Milwaukee, WI.

41. J.W.Choi, Y.M.Kong, and H.E.Kim, Reinforcement of Hydroxyapatite Bioceramic by addition of Ni3Al and Al2O3, J. Am. Ceram. Soc 81: [7] pp1743-1748 (1998)

42. Two kinds of zirconia data sheet from Tosoh Ceramics Division, Bound Brook, NJ materials data sheet)

43. http://www.corning.com/search_main.html

44. http://www.vidrine.com/vidrine/iropmat.htm

45. S.Rangarajan, R.Belardinelli, and P.B.Aswath, "Processing, Physical and Thermal properties of Blackglas™ matrix composites reinforced with Nextel™ Fabric", Journal of Materials Science 34: (3) 515-133 (1999)

46. http://www.glassonline.com/dictionary/375.html

47. http://members.rediff.com/manuagarwal/RAM2.html

48. K.Y.Lee, "Microwave Processing of Ceramics and Ceramic Composites Using a Single-Mode Microwave Cavity," Ph. D Thesis, Michigan State University (1998)

49. J. G. Lee, K. Y. Lee and E. D. Case, "Joining of Diamond Thin Films to Optical and IR Materials," Ceramic Transactions, Volume 94, American Ceramic Society, Inc., Westerville, OH. pp. 509 – 520 (1998)

50. J. G. Lee and E. D. Case, "Microwave Joining of Particulate Composites", Advances in Ceramic Matrix Composites V, Ceramic Transactions Volume 103, American Ceramic Society, Inc., Westerville, OH, pp. 571-581 (2000)

51. E. D. Case, K. Y. Lee, J. G. Lee, and T. Hoepfner, "Geometrical Stability of Holes and Channels During Joining of Ceramics and Ceramic Composites," in Joining of Advanced and Specialty Materials, M. Singh, J. E. Indacochea, and D. Hauser, eds., ASM International, Materials Park, OH, pp 27-34 (1998)

52. J. G. Lee and E. D. Case, "Joining Ceramics to Produce Components with Precise Internal Channels", in Innovative Processing and Synthesis of Glass, Composite, and Ceramic Materials III, Volume 108, Ceramic Transactions, American Ceramic Society. pp. 433 – 442 (2000).

53. J. G. Lee and E. D. Case, "Joining of Non-Oxide Ceramics Using Conventional and Microwave Heating", Ceramic Engineering and Science Proceedings 21[4], American Ceramic Society. pp. 589-597 (2000)

54. E. D. Case, J. G. Lee, M. A. Crimp, D. K. Reinhard, and J. Malik, "Protective Coatings for Infrared Materials", 23rd Cocoa Beach International Conference on Engineering Ceramics and Structures, American Ceramic Society, Cocoa Beach, FL, January, pp. 145-152 (1999)

55. E. D. Case, K. Y. Lee, and J. G. Lee, "Joining of Polycrystalline Ceramics and Ceramic Composites Using Microwave Heating," in Proceedings of the 33rd International Microwave Power Symposium, International Power Institute, Manassas, VA, pp. 17-20 (1998)

56. E. D. Case, J. G. Lee, L. Zeng, and M. A. Crimp, "Joining of Dissimilar Ceramic Materials", Joining of Advanced and Speciality Materials II, ASM International, Materials Park, OH. pp. 10-17 (2000)

57. H.R.Hwang, R.Y.Lee, "The Effect of Metal Coating on the Diffusion Bonding in Al_2O_3/Inconel 600 and the Modulus of Rupture Strength of Alumina," Journal of Materials Science, vol. 31, pp. 2429-2435 (1996)

58. http://www.accuratus.com/MACOR.htm

59. http://www.tosoh.com

60. N.Yoshikawa, A.Kikuchi, S.Taniguchi, and T.Takahashi, "Tetragonal to Monoclinic Transformation in Y-TZP Joined with Metallic Materials," Journal of Materials Science, vol. 34, pp. 5586 (1999)

61. X.S.Ning, T.Okamoto, Y.Miyamoto, A.Koreeda, and K. Suganuma, "Effect of Oxide Additive in Silicon Nitride on Interfacial Structure and Strength of Silicon nitride Joints Brazed with Alumina," Journal of Materials Science, vol. 24, pp. 2865-2870 (1989)

62. D.E.Grenoble, J.L.Katz, K.L. Dunn, R.S.Gilmore, and K.L.Murty, "The Elastic Properties of Hard Tissues and Patites," Journal of. Biomed Materials. Research, vol. 6 (3), pp. 221-223(1972)

63. K.Noguchi, M.Fujita, and T.Makaki, and M.Mizushina, "Tensile Strength of Yttria-Stabilized Tetragonal Zirconia Polycrystals," Journal of American Ceramic Society, vol. 72 [7], pp. 130-1307 (1989)

64. www.ferroceramic.com/tables/t_07.htm